Modulation of the Neuroinflammatory Response Following Genetic and Environmental Manipulations in the Zebrafish (*Danio rerio*)

A THESIS SUBMITTED TO

THE GRADUATE SCHOOL OF ENGINEERING AND SCIENCE

OF BILKENT UNIVERSITY

IN PARTIAL FULFILLMENT OF THE REQUIREMENTS FOR

THE DEGREE OF

MASTER OF SCIENCE

IN

NEUROSCIENCE

By Beyza Özen

May 2022

Modulation of the Neuroinflammatory Response Following Genetic and Environmental Manipulations in the Zebrafish (*Danio rerio*)

By Beyza Özen

May 2022

We certify that we have read this thesis and that in our opinion it is fully adequate, in scope and in quality, as a thesis for the degree of Master of Science.

Michelle Marie Adams (Advisor)

Hacı Hulusi Kafalıgönül

Çağdaş Devrim Son

Approved for the Graduate School of Engineering and Science

Ezhan Karaşan

Director of the Graduate School

ABSTRACT

Modulation of the Neuroinflammatory Response Following Genetic and Environmental Manipulations in the Zebrafish (*Danio Rerio*)

Beyza Özen

M.Sc in Neuroscience

Advisor: Michelle Marie Adams

May 2022

Aging is an inevitable process through which organisms experience functional and physical decline. Cellular changes such as mitochondrial dysfunction, telomere attrition, and loss of proteostasis constitute the main components of this process. One of the hallmarks of brain aging is the increased inflammatory status of the brain. This process is named neuroinflammation and is seen both in the development of neurodegenerative disorders and in healthy aging. The over-activation of microglia and astrocytes, increased secretion of pro-inflammatory cytokines and reactive oxygen species, NLRP3/NALP3 inflammasome activation, and the upregulation of NF-κB signaling pathway are among the markers of neuroinflammation. Deregulated nutrient sensing through mammalian target of rapamycin pathway(mTOR), impaired neurogenesis, and synaptic integrity over time are among the common outcomes of this process. Genetic susceptibility is also another factor to contribute the vulnerability to inflammation. Therefore, further studies are necessary to investigate the effects of the inflammation-stimulating agents and the genetic susceptibility.

Thus, this study aimed to develop copper sulfate as an inflammatory stimulating agent for both zebrafish embryos and adults. For this objective, we conducted long-term and short-term copper sulfate embryo treatment studies.

The gene expression results showed that the inflammatory response was quite predictable in embryos by increasing pro-inflammatory markers early on and later increasing anti-inflammatory cytokines. Secondly, we conducted copper sulfate and rapamycin treatment in very old (38 months) zebrafish animals to investigate the impact of the inflammation on mTOR signaling and synaptic integrity. The protein expression results indicated that rapamycin was an effective for mTOR suppression in very old animals but copper sulfate was not able to stimulate a robust inflammatory response. Also, synaptic integrity markers were mostly stable among treatment groups in very old animals. Finally, we used $tsc2^{+/-}$ adult animals and applied rapamycin treatment to very old (33 months) $tsc2^{+/-}$ adults to assess the effect of overactive mTOR signaling and the possibility of reversing this in the progression of inflammation. Comparatively, we wanted to understand the effect of copper sulfate exposure in very old (43 months) $ztor^{+/-}$ animals that have a downregulated mTOR pathway. The results showed that the rapamycin effect was not significant between wild-type and $tsc2^{+/-}$ animals in terms of pro-inflammatory cytokines and autophagy markers. Similarly, the copper sulfate effect was not different between wild type and $ztor^{+/-}$ animals for pro-inflammatory markers. However, autophagy markers decreased significantly in mutants.

In conclusion, this study showed that aging affects the regulation of the inflammatory response within the brain. Also, genetic manipulations on the mTOR pathway would provide crucial insights to investigate the neuroinflammatory profile of the brain in the course of aging.

Keywords: neuroinflammation, mTOR signaling, zebrafish, synaptic integrity

ÖZET

Zebra Balığında (*Danio Rerio*) Genetik ve Çevresel Manipülasyonların Ardından Nöroinflamatuar Yanıtın Modülasyonu

Beyza Özen

Nörobilim Yüksek Lisans Programı

Tez Danışmanı: Michelle Marie Adams

Mayıs 2022

Yaşlanma, organizmaların işlevsel ve fiziksel gerileme yaşadığı kaçınılmaz bir süreçtir. Mitokondriyal disfonksiyon, telomer yıpranması ve proteostaz kaybı gibi hücresel değişiklikler bu sürecin ana bileşenlerini oluşturur. Beyin yaşlanmasının ayırt edici özelliklerinden biri, beynin artan inflamatuar durumudur. Bu sürece nöroinflamasyon adı verilir ve hem nörodejeneratif bozuklukların gelişiminde hem de sağlıklı yaşlanmada görülür. Mikroglia ve astrositlerin aşırı aktivasyonu, proinflamatuar sitokinlerin ve reaktif oksijen türlerinin artan salgılanması, NLRP3/NALP3 inflamatuar aktivasyonu ve NF-κB sinyal yolunun upregülasyonu, nöroinflamasyonun belirteçleri arasındadır. Memeli rapamisin yolu (mTOR) hedefi yoluyla düzensiz besin algılaması, bozulmuş nörojenez ve zamanla sinaptik bütünlük bu sürecin ortak sonuçları arasındadır. Genetik yatkınlık da iltihaplanmaya karşı savunmasızlığa katkıda bulunan başka bir faktördür. Bu nedenle inflamasyonu stimüle eden ajanların etkilerini ve genetik yatkınlığı araştırmak için daha ileri çalışmalara ihtiyaç vardır.

Bu nedenle, bu çalışma, hem zebra balığı embriyoları hem de yetişkinler için inflamatuar uyarıcı bir ajan olarak bakır sülfat geliştirmeyi amaçladı. Bu amaçla uzun süreli ve kısa süreli bakır sülfat embriyo tedavi çalışmaları gerçekleştirdik. Gen ekspresyonu sonuçları, inflamatuar yanıtın, erken dönemde proinflamatuar belirteçleri artırarak ve daha sonra anti-inflamatuar sitokinleri artırarak

embriyolarda oldukça tahmin edilebilir olduğunu gösterdi. İkinci olarak, iltihabın mTOR sinyalizasyonu ve sinaptik bütünlük üzerindeki etkisini araştırmak için çok yaşlı (38 aylık) zebra balığı hayvanlarında bakır sülfat ve rapamisin tedavisi gerçekleştirdik. Protein ekspresyonu sonuçları, rapamisinin çok yaşlı hayvanlarda mTOR supresyonu için etkili olduğunu ancak bakır sülfatın güçlü bir inflamatuar yanıtı uyaramadığını gösterdi. Ayrıca, sinaptik bütünlük belirteçleri, çok yaşlı hayvanlarda tedavi grupları arasında çoğunlukla stabildi. Son olarak, aşırı aktif mTOR sinyalinin etkisini ve inflamasyonun ilerlemesinde bunu tersine çevirme olasılığını değerlendirmek için $tsc2^{+/-}$ yetişkin hayvanları kullandık ve çok yaşlı (33 aylık) $tsc2^{+/-}$ yetişkinlere rapamisin tedavisi uyguladık. Karşılaştırmalı olarak, aşağı regüle edilmiş bir mTOR yoluna sahip çok yaşlı (43 aylık) $ztor^{+/-}$ hayvanlarda bakır sülfat maruziyetinin etkisini anlamak istedik. Sonuçlar, proinflamatuar sitokinler ve otofaji belirteçleri açısından yabanıl tip ve $tsc2^{+/-}$ hayvanlar arasında rapamisin etkisinin önemli olmadığını gösterdi. Benzer şekilde, proinflamatuar belirteçler için bakır sülfat etkisi, yabanıl tip ve $ztor^{+/-}$ hayvanlar arasında farklı değildi. Bununla birlikte, mutantlarda otofaji belirteçleri önemli ölçüde azaldı.

Sonuç olarak, bu çalışma yaşlanmanın beyindeki inflamatuar yanıtın düzenlenmesini etkilediğini göstermiştir. Ayrıca, mTOR yolu üzerindeki genetik manipülasyonlar, yaşlanma sürecinde beynin nöroinflamatuar profilini araştırmak için çok önemli bilgiler sağlayacaktır.

Anahtar Kelimeler: nöroinflamasyon, mTOR sinyalizasyonu, zebrabalığı, sinaptik bütünlük

Acknowledgements

First and foremost, I would like to express my deepest gratitude to my supervisor Professor Michelle Marie Adams. I learned a lot more than I could imagine thanks to her guidance and support. It was a great chance for me to be on her research team.

I would like to thank the members of my thesis committee Associate Professor Çağdaş Devrim Son and Assistant Professor Hulusi Kafalıgönül.

I also want to thank all former and the current members of Adams Lab; Hande Özge Aydoğan, Duygu Macaroğlu, Melek Umay Tüz Şaşik, Begün Erbaba, Büşranur Şeker, Fulya Kızıldağ, Sena Güçer, Seçil Gülden. I would like to give special thanks to Ergül Dilan Çelebi Birand, Narin Ilgım Ardıç Avcı, Elif Tuğçe Karoğlu Eravşar and Naz Mengi for their endless guidance, help and support. Also, I want to thank Duygu Mutlu and Serena Sevdiye Aktürk for their unique support and friendship.

I would like to thank my closest friends Ayşe Kevser Arslan, Fatma Elif Albayrak, Gizem Karakaya, Miray Muratoğlu and Zeynep Camuşcu for their emotional support and guidance. Even though we are physically far away, I know you are there for me whenever I need you.

I would like to express my endless love and deepest gratitude to my family. My parents Emine Özen and Mehmet Özen supported me endlessly in every decision I made. I am thankful for my grandmother Zekiye Gürlen for her unconditional love and my uncle Sinan Gürlen for his encouragement throughout this process. Also, I would like to thank my cousin Elif Özen for her unconditional support and trust in me. Finally, I am profoundly thankful for my amazing sister,

Mısra Özen for her love, endless support, and guidance. You never stopped trusting me, even when I felt my worst. This would not have been possible without you, thank you.

I want to acknowledge the Scientific and Technological Research Council of Turkey (TUBITAK) with grant number 119S660 for the financial support in these experiments.

Contents

List of Figures

List of Tables

Abbreviations

4E-BP1	Eukaryotic translation initiation factor 4E-binding protein
AA	Arachidonic acid
AD	Alzheimer's Disease
ALS	Amyotrophic lateral sclerosis
AP-1	Activator protein-1
APP	Amyloid precursor protein
Aβ	Amyloid beta-peptide
CFA	Freund's adjuvant
COX-2	Cycylooxygenase-2
CSF	Cerebrospinal fluid
CNS	Central nervous system
CPP	Conditioned place preference
CR	Caloric restriction
CVMI	Cerebral ventricular injection
DCAMKL1	Doublecortin-like kinase
E/I	Excitatory/inhibitory
FOXO	Mammalian forkhead members of the class O

GEP	Gephyrin
GFAP	Glial fibrillary acidic protein
GH	Growth hormone
HD	Huntington Disease
Hpf	Hours post fertilization
HSC	Hematopoietic stem cells
IF	Intermittent fasting
IGF-1	Insulin-like growth factor
IKK	Nf-kb essential modulator (NEMO) dependent IKB kinase
IL-1	Interleukin-1
IL-1β	Interleukin-1β
IL-4	Interleukin-4
IL-6	Interleukin-6
IL-8	Interleukin-8
IL-10	Interleukin-10
IL-13	Interleukin-13
LPS	Lipopolysaccharide
LTD	Long-term depression

LTP	Long-term potentiation
MAPKs	Mitogen-activated protein kinases
METH	Methamphetamine
mPFC	Medial prefrontal cortex
MS	Multiple sclerosis
mTOR	Mammalian target of rapamycin
NEMO	Nf-kb essential modulator
NMDA	N-methyl-D-aspartic acid
NO	Nitric oxide
OHSC	Organotypic hippocampal slice cultures
PD	Parkinson’s disease
PFC	Prefrontal cortex
p-S6	Phospho-ribosomal protein S6
PSD-95	Post-synaptic density 95
PTGS	Prostaglandin-endoperoxide synthase
qPCR	Quantitative polymerase chain reaction
ROS	Reactive oxygen species
RT-PCR	Real-time polymerase chain reaction

SIRT	Sirtuin
SYN	Synaptophysin
TBI	Traumatic brain injury
TGF	Transforming growth factor
TNF	Tumor necrosis factor
TSC	Tuberous sclerosis complex
UV	Ultraviolet
VD	Vascular dementia
VM	Ventral mesencephalon

CHAPTER 1

Introduction

1.1 Aging

Aging can be defined as the decreasing physical and biological integrity over time, and functional decline as an outcome of this process [1]. Thanks to the advancements in technology, more people live until 60 years or more. According to the World Health Organization, 2 billion people will be 60 and older by 2050 [2]. The aging population is increasing all over the world and also in Turkey [3]. However, a rapidly aging population is a risk factor for the growth of populations, particularly in terms of created economic value and social security system policies [4]. One important reason is that humans become more vulnerable to various age-associated diseases, as a result, economic efficiency decreases drastically within the society together with accumulated healthcare costs [5]. Cancer, cardiovascular diseases, and neurodegenerative disorders such as Alzheimer's disease(AD), and Parkinson's disease(PD) are among the age-related pathologies in humans due to the change in brain function [1]. As expected, cognitive and behavioral dysfunctionalities are common outcomes of these debilitating disorders [6]. Unfortunately, all of these dysfunctionalities affect both the efficiency of economic development and the integration of the elderly population into society by disrupting a healthy aging process [7]. Despite the accumulated effort of modern science, the causes of aging and possible preventive manipulations to this process have not been analyzed completely, yet [8]. Therefore, it is important to understand the hallmarks of aging and its effects on brain function and health to develop novel therapeutic strategies. This approach would create effective solutions for the aging population while increasing not only their life span but also their contribution and integration into society.

1.2 The Hallmarks of Aging

The comprehensive research on aging has declared some common hallmarks which have the potential to affect many biological systems. These hallmarks can be divided into 3 main categories, depending on their functions: primary hallmarks, antagonistic hallmarks, and integrative hallmarks. Primary hallmarks are responsible for the damage and these can be counted as the DNA damage theory, telomere attrition, epigenetic alterations, and loss of proteostasis. Antagonistic hallmarks occur as a response to deterioration and these are mitochondrial dysfunction, cellular senescence, and deregulated nutrient-sensing. Finally, integrative hallmarks are responsible for the phenotype, and these are stem cell exhaustion together with altered intercellular communication [1].

1.2.1 Primary Hallmarks

1.2.1.1 The DNA Damage Theory

DNA damage theory of aging postulates that genomic instability is one of the major causes of aging [9]. Various factors such as ultraviolet (UV) radiation and environmental toxins cause DNA damage and this leads to genomic instability. Genomic instability reduces the replication capacity of the genome which is followed by decreased tissue regeneration. Decreased regeneration capacity causes aging or premature aging throughout life [10].

1.2.1.2 The Role of Epigenetic Alterations

Epigenetic alterations often refer to histone modifications and DNA methylation [1]. In one study, human diploid fibroblasts (HDF) experience a decrease in heterochromatin-like domains in the course of aging [11]. Also, specific enzymes and effectors that take part in transcription and translation processes are known to cause histone modifications in the aging process [12]. As for DNA methylation, in a longitudinal study, it is demonstrated that DNA methylation is

decreased in Alu elements in aging individuals [13]. However, the relation between DNA methylation and aging is not very clear. Although hypomethylation is detected in some studies like the previous one, DNA hypermethylation is also possible in tumor suppressor genes with increasing age [14]. More research is needed to elucidate this topic further.

1.2.1.3 Telomere Attrition

Telomeres are protective hexamer protein complexes known as shelterin at each end of eukaryotic chromosomes. These are particularly susceptible to aging-associated deterioration since they are shortened with increasing age. Some studies have found that telomere attrition increases in the course of aging by negatively affecting cellular senescence and regeneration [15]. Telomere shortening is also associated with the premature onset of many diseases including aplastic anemia, pulmonary fibrosis, and atherosclerosis which is thought to be related to the aging process [1], [16]. Various environmental factors including smoking, obesity, exposure to harmful toxins, and stress are also known to lead to both excessive telomere shortening and premature aging [17]. When these factors are considered, telomere attrition can be regarded as a cause and/or mediating variable in the progression of age-related disorders.

1.2.1.4 Loss of Proteostasis

Loss of proteostasis is defined as the deficiency of the whole mechanism of protein folding, degradation, and intracellular stabilization of proteins [18]. This deficiency accumulates in different tissues and leads to various pathologies as the organism ages. In one study, it is found that the accumulation of protein aggregates negatively impacts muscle aging and muscle function in Drosophila as a result of loss of proteostasis [19]. Also, misfolded proteins are

known to be one of the causes of age-related neurodegenerative disorders such as AD disease and PD [1]. Therefore, loss of proteostasis should be considered among the important factors for the aging process.

1.2.2 Antagonistic Hallmarks

1.2.2.1 Mitochondrial Dysfunction and Reactive Oxygen Species

The mitochondrial free radical theory of aging states that mitochondrial deterioration accumulates in the course of aging and reactive oxygen species(ROS) activation accelerates as an outcome, which leads to cellular dysfunction [24]. ROS are free radicals, they can be found within the cell, organelles, and mitochondria. They contain at least one unpaired electron that's why they are highly reactive. ROS generation mainly occurs due to the mitochondrial activation as a side-product of the cell metabolism. When ROS production is at its baseline levels, it can be beneficial for cell signaling, growth, and differentiation. However, excessive ROS production leads to several dysfunctions within the cell metabolism. To prevent this outcome, several enzymes constantly take part in regulating ROS levels, and not being able to cope with ROS levels initiates oxidative stress [20].

Mitochondrial dysfunction as a hallmark of aging also occurs independently from ROS generation. Mitophagy is known as the selective elimination of mitochondria by autophagy and altered mitophagy rates, mitochondrial DNA(mtDNA) mutations, and changes in mitochondrial membrane structure cause dysfunctionalities in the course of aging [21].

1.2.2.2 Cellular Senescence

In cellular senescence, the long-lasting cellular arrest is enforced for an unknown duration, due to the various stress factors. Recently, it has emerged as an important factor in age-related

pathologies. The probability of cellular senescence is thought to be increased during aging. However, for aging-associated diseases, cellular senescence can be both a cause and a consequence. Senescent cells can impact the production of various inflammatory markers such as interleukin-6 (IL-6), interleukin-1β (IL-1β), and tumor necrosis factor-α (TNF-α), this could be a signaling mechanism for anti-inflammatory response and/or the expression of cellular damage. Additionally, a complex interaction between cellular senescence and environmental factors is believed to exist, a homeostatic response may be provided for regulation within the system [22].

1.2.2.3 Deregulated Nutrient Sensing

In mammalian species, the anterior pituitary gland produces the growth hormone(GH) which is currently mediated by the insulin-like growth factor(IGF-1). IGF-1 is produced as a response to growth hormone and takes a role in the regulation of insulin signaling together with insulin hormone. Therefore, IGF-1 and insulin signaling is known as the ‘’insulin and IGF-1 signaling’’ (IIS) pathway. They work for the glucose-sensing mechanism of the cells. IIS pathway has downstream targets such as the mammalian forkhead members of the class O (FOXO) transcription factors, PI3K-Akt signaling pathway, and the mammalian target of rapamycin(mTOR) signaling pathway. All of these targets are effective in regulating longevity and metabolism so aging-associated pathologies [1].

Among these pathways, the mTOR pathway has significant effects on cell growth, anabolic reactions, autophagic regulation, and inflammation. mTOR kinase consists of two multiprotein complexes: mTORC1 and mTORC2. The down-regulation of mTOR has been shown to extend longevity in mice, yeast, and fruit flies [23], and mTOR activity increases in mice's hypothalamic neurons in the course of aging [24]. Therefore, down-regulation of mTOR can

be assumed to extend longevity. Two interventions are effective in mTOR down-regulation so far, rapamycin treatment and a dietary regimen which includes caloric restriction(CR). Acute rapamycin treatment is effective in mTORC1 pathway down-regulation but not in the mTORC2 pathway [25] and both rapamycin treatment and CR effects occur an age-dependent manner. In one study using zebrafish, rapamycin has suppressed the mTOR pathway more successfully in young animals than in old animals and intermittent fasting(IF) can activate neural progenitor cell marker, doublecortin-like kinase (DCAMKL1) while showing similar effects with rapamycin. However, two autophagy genes are not influenced by both CR and rapamycin treatments [26]. In another study, CR effects are found to be mediated by telomere lengths again in an age-dependent manner [27]. Therefore, mTOR pathway inhibition depends on many factors including the duration, timing, and density of the intervention whether it is CR or rapamycin treatment. Nevertheless, CR has been a prominent intervention by suppressing the mTOR pathway through decreased nutrient-signaling to extend longevity [1].

1.2.3 Integrative Hallmarks

1.2.3.1 Stem Cell Exhaustion

One of the main hallmarks of aging can be defined as the permanent decline in functions of tissues and stem cell exhaustion comprehensively points to this hallmark. Stem cells are capable of preventing functional decline by providing regenerative capacity to the cells. However, stem cell exhaustion is often seen in the course of aging [1]. Hematopoietic stem cells(HSC) have critical roles in providing blood cell production since they can induce new mature blood cells [28]. Although the number of HSC increases in mice during aging, their regenerative capacity is decreased [29]. Cell-intrinsic mechanisms are believed to cause this phenotype, but aging may be a negatively contributing factor. In one research, long-term hematopoietic stem

cells(LT-HSC) are extracted from both young and old mice and genes that are related to lymphoid specification and transformation and the existence of lymphoid progenitor cells are up-regulated, especially in the old mice. This can be one of the driving factors behind developing leukemia at an advanced age and also explain the aging-associated immune deterioration [30]. Stem cell rejuvenation by preventing stem cell exhaustion has a great capacity to reverse the immune deterioration and related functional decline at the organismal level so it is an important concept to work on.

1.2.3.2 Altered Intercellular Communication

Besides cell-intrinsic mechanisms, intercellular communication is also altered. Changes in the inflammatory response in the course of aging which is known as ‘’inflammaging’’ are one of the prominent examples of altered intercellular communication. The increased secretion of pro-inflammatory cytokines, defective autophagy response, and the up-regulated nuclear factor kappa-B (NF-kB) pathway response subsidize this intercellular communication as a response to aging. It is also known that changes in one tissue for example increased pro-inflammatory response also mediate the aging-related outcomes in other tissues within the organism. Some interventions are proposed to prevent these phenotypes such as the regulation of the gut microbiome to rescue the outcomes of the inflammaging phenotype and the administration of anti-oxidant compounds [1].

1.3 Brain Aging

Aging-associated outcomes within the brain can be detected easily since aging affects cognitive functions robustly for many elderly. However, the underlying mechanism behind brain aging mainly occurs through the changes in cellular and molecular mechanisms during aging.

1.3.1 Changes in Cellular and Molecular Mechanisms In the Course of Aging

The underlying factors behind many cognitive and executive deficits seen in aged individuals are robust changes in cellular and molecular mechanisms within the brain. These changes can be observed in various cell types such as neurons and glial cells. Also, protein accumulation and insufficiency of synaptic plasticity are among common alterations [36].

Neurons are the main information supplier cells of the brain and they are affected heavily by the negative consequences of aging. Neurogenesis is diminished and neuronal morphology is changed in terms of reduced dendritic branching and spine numbers. Particularly, large in size neurons need to maintain energy supply through dendrites but they can be more vulnerable to aging since energy supply may not be maintained. Also, the activity of ions is crucial for the preservation of electrical activity but this can be dysregulated too [37]. As for the number of neurons, the latest agreement states that the reduction in number does not account for the observed cognitive deficits in aging. Yet, the neuron number is mainly preserved within the hippocampus and is not the cause of learning impairments related to aging in rats [38].

Apart from neurons, both synaptic and structural plasticity are influenced by aging. A diminished number of synapses accompany various morphological changes. For example, in aged rats, the return mechanism of microtubule-associated protein 1B(MAP1B) is not effective as in the younger rats [39]. Long-term potentiation (LTP) and long-term depression(LTD) are two main mechanisms of synaptic plasticity for learning and memory and LTP is significantly diminished in aged rats [40] which has consequences for cognitive impairments, especially on hippocampal-related tasks. Morphological changes can be encountered in the presynaptic and postsynaptic terminals, the number of synaptic boutons is subject to change on the terminals.

In aged rodents and monkeys, a reduced number of postsynaptic spines on the cortex and hippocampus are detected [36].

The accumulation of neurofibrillary tangles which are mainly composed of phospho-tau generally in the amygdala and hippocampus as well as amyloid-β deposits which are one of the hallmarks of AD are among the protein accumulation examples [41]. They can be detected in both normal and diseased brains in the course of aging.

Glial cells are the other type of cells within the brain, they are divided into three oligodendrocytes, microglia, and astrocytes. The effects of aging can be observed in these cells too. Both the number and size of the microglia and astrocytes are increased, especially the number of activated astrocytes and microglia is boosted. This can lead to negative consequences for example the increased production of pro-inflammatory cytokines which advances the inflammatory response. However, the increased number of glial cells can contribute to protective responses for instance advanced production of anti-inflammatory cytokines [37]. Additionally, the expression profile of autophagy, ROS, and many other related inflammatory markers change depending on the alterations within the non-neuronal cells of the brain. All of these alterations eventually form the neuroinflammatory response profile of the central nervous system(CNS).

1.4 Neuroinflammation

Neuroinflammation can be defined as the multi-factorial inflammatory response within the brain and spinal cord [42]. The activation of the non-neuronal cells such as microglia and astrocytes lay the foundation of neuroinflammation, generally. Neuroinflammation is a common mechanism behind many neurodegenerative disorders including AD, PD, multiple

sclerosis (MS), and dementia, although the progress patterns differ within these disorders [43]. It can be said that systemic/chronic inflammation takes place in the case of neurodegenerative disorders, the activation and the downstream effects of glial cells and macrophages are increased and sustained for longer durations. In this case, the damage is accumulated in time and may exert its effects later [44].

Since systemic/chronic inflammation takes a long time to investigate the neuroinflammatory profile within the brain, acute inflammation is also possible and may lead to a similar neuroinflammatory profile. In the case of acute inflammation, the inflammatory responses can be initiated by various environmental toxins which act as inflammatory agents such as lipopolysaccharide (LPS) and copper sulfate ($CuSO_4$), spinal cord, and/or brain injury. Once the inflammatory response is needed to be initiated T cells, astrocytes, and microglia work as a team to start this response and exert neuroprotective effects later [43]. Now it has been generally accepted that neuroinflammation is a process that has both beneficial and harmful effects on the cells within the CNS. On the one hand, through the secretion of pro-inflammatory cytokines and ROS elements and the toxic nature of microglia, neuroinflammation would be harmful. On the other hand, the activation of microglia, astrocytes, and oligodendrocytes would stimulate cellular repair and the clearance of aggregated proteins [45]. The duration, dosage of the inflammatory stimuli, and the existence of other protective factors within the CNS would determine the outcome of the neuroinflammatory process.

1.4.1 Microglia

Microglia are among the macrophages of the CNS but they are different from other glial cells such as astrocytes and oligodendrocytes by their gene expression patterns and origins [46]. Microglia become activated as a response to an inflammatory stimulus. There are two main

types of phenotypes that microglia display, M1 state, and M2 state. M1 state can be defined as the pro-inflammatory response state of the microglia, many pro-inflammatory cytokines such as TNF-α, IL-1β, various chemokines, ROS elements, and nitric oxide(NO) are secreted from the M1 state of microglia. M2 state works as an immunosuppressor mechanism, neuronal survival, clearance of toxic aggregate proteins, and the secretion of neurotrophic factors for example IL-8 is seen in this state [45]. For some pathological conditions such as obesity and type 2 diabetes, the transition from the M2 state to the M1 state is detected. This transition is a risk factor for the progression of the pathological condition by the accelerated production of pro-inflammatory cytokines [46].

Apart from M1 and M2 microglial states, microglial activation is also separated into 3 phases: classical phase, alternative phase, and acquired deactivation phase depending on the factors that stimulate them [47]. The classical phase is defined through the activation of the M1 microglial state, T cell responses are initiated through the upstream activation of pro-inflammatory cytokines in this state [48]. In alternative activation and acquired deactivation phases, the M2 microglial state is dominant, and chemokines such as interleukin-13 (IL-13) and interleukin-4 (IL-4) are secreted. This mechanism is more focused on the "anti-inflammatory" process of the inflammatory response, also with the production of interleukin-10(IL-10) and transforming growth factor-β (TGF-β) [49].

1.4.2 Astrocytes

Astrocytes are among the non-neuronal cells together with microglia and oligodendrocytes. They take important roles in regulating inflammatory responses in the course of acute and/or chronic inflammation and they are mainly subject to moderation by microglia [50]. Astrocytes are generally involved in CNS damage and to do this they exhibit functional heterogeneity.

Reactive astrocytes are responsible for the feedback replies towards neuroinflammation, and they are considered to be divided into 2 groups as in the case of microglia, A1 astrocytes, and A2 astrocytes. A1 astrocytes are in charge of neurotoxic activity whereas neuroprotective effects are provided by A2 astrocytes [51]. For almost all CNS diseases and acute and/or chronic inflammation cases, astrocytes display binary responses. On the one hand, they take part in repairing CNS damage, and the healing process. On the other hand, they initiate and maintain inflammation within the CNS, release cytokines and pro-inflammatory chemokines, and accelerate the neuroinflammatory process [52]. More research is needed to decipher tissue, inflammation type, duration, and species-specific effects of astrocytes in the CNS. Astrocytes are also involved in the regulation of many signaling pathways such as the NF-κB, the mitogen-activated protein kinase (MAPK), and the calcineurin (CN) pathways [52].

1.4.3 M1 Microglial State Markers

M1 microglial state is associated with an increased inflammatory response immediately after the inflammation, especially in acute cases. Many pro-inflammatory cytokines, various chemokines, NO, and ROS elements are synthesized from the microglia at the M1 state. Microglia particularly respond to pathogen-associated molecular patterns (PAMPs) and damage-associated molecular patterns (DAMPs) at this stage for the further recruitment of T cells and leukocytes [48], [49].

1.4.3.1 Cyclooxygenase-2 (COX-2)

Cyclooxygenase (COX) enzymes belong to the prostaglandin-endoperoxide synthase (PTGS) enzyme family which work as reaction catalyzers. There are 2 isoforms of the COX enzyme: COX-1 and COX-2. Both isoforms have roles in inflammation regulation. COX-2 is generally

localized around neurons under normal conditions. However, astrocytes and microglia express COX-2 after inflammatory stimuli in both *in vivo* and *in vitro* experiments [53]. The expression of COX-2 is thought to be a moderating factor for the expression of other pro-inflammatory cytokines which take part in the NF-κB signaling pathway. However, in one study, the expression of COX-2 has been detected to be independent of the expression profile of IL-1β and TNF-α in human monocytes [54]. These differences may come from the type of inflammatory agents, the duration of the inflammation, and the experimental conditions [53].

COX-2 has many effects on the CNS, some of them are related to inflammatory responses but some of them are not. COX-2 facilitates neuronal plasticity within CNS under normal conditions. There is compelling evidence that states that COX-2 expression is enhanced during the process of LTP and LTD which are fundamental mechanisms of memory formation and consolidation [55]. On the other hand, cognitive dysfunctions are increased in aging rats via overexpression of COX-2 neurons, and the inhibition of COX-2 expression ameliorated these dysfunctions [56]. This shows that COX-2 expression at normal levels might be necessary for cognitive mechanisms and this relation may be moderated via the inflammatory pattern of the CNS.

Disruptions of glutamatergic transmission within the brain lead to excitotoxic cell death of neurons which is known as excitotoxicity. Excitotoxicity, oxidative stress, ROS secretion, and COX-2 expression are interconnected with each other [57]. The inhibition of COX-2 expression compensates for the injury which is caused by the excitotoxic cell death *in vivo* models [58] and induced ROS activity by cadmium can increase cellular COX-2 expression [59]. As stated previously, COX-2 activity is upregulated in the cases of both chronic and acute inflammation. Therefore, increased COX-2 expression is also detected in chronic

neurodegenerative disorders such as in hippocampal neurons of AD patients [60], and dopaminergic neurons of substantia nigra pars compacta in PD patients [61], and post-mortem spinal cord tissue from amyotrophic lateral sclerosis (ALS) patients [62].

1.4.3.2 Nuclear factor kappa-light-chain-enhancer of activated B cells (NF-κB)

NF-κB signaling pathway has been proposed as one of the main intermediary pathways of aging and neuroinflammation. This pathway involves many cellular processes such as cell survival, cellular stress and senescence, inflammation, expression of cytokines and chemokines, oxidative responses, and apoptosis [63]. Many other signaling pathways which are associated with aging and cellular senescence such as IGF-1, mTOR, sirtuin (SIRT), and FOXO are related to NF-κB signaling. Many pathogens, viruses, and related inflammation-stimulating agents for example LPS are known to activate this pathway [64]. Additionally, TNF and interleukin-1 (IL-1) are both catalysts and downstream transcriptional targets of NF-κB signaling [63].

NF-κB signaling is divided into 2 pathways mainly based on their functions: canonical and non-canonical. Canonical pathway is known as NF-κB essential modulator (NEMO) dependent IκB kinase (IKK) and is stimulated by pro-inflammatory signals. Therefore, the canonical pathway is more important for aging-associated pathologies and inflammation. On the other hand, the non-canonical pathway is required for the cellular development particularly B cells and T cells development throughout p52/RelB heterodimer complex [65]. Both of these pathways are interconnected and induce the transcription of many cytokines such as IL-1α/β, IL-2, 3, 6, 12, TNF-α in the cases of inflammation [63].

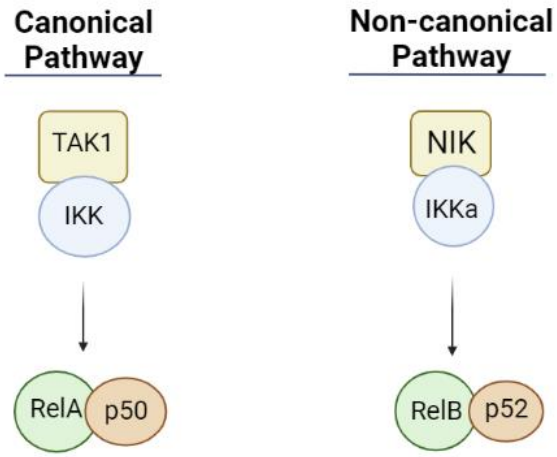

Figure 1.1 Schematic representation of canonical and non-canonical pathways in which NF-κB signaling function. The illustration is adapted from Cong Sun (2011) [155] and the figure is created with BioRender.

NF-κB signaling is also crucial for the functionalities of glial and neuronal cells. NF-κB works as a modulator for the expression of pro-inflammatory cytokines such as IL-6, IL-1, TNF, neuropeptides, and COX-2. This modulation is conducted through the proteasome IκB kinase pathway as a response to various factors such as oxidative stress, nerve growth factors, and glutamate toxicity [66]. In the cases of traumatic brain injury and viral infection, the expression levels of IL-1 and TNF are known to be upregulated via NF-κB signaling in glial cells [67]. Moreover, NF-κB takes a role in regulating synaptic plasticity together with COX-2. As stated before, COX-2 enzymatic activity is required for neuronal and synaptic plasticity under normal conditions. Elementary COX-2 expression for synaptic plasticity has been observed to be co-localized with increased NF-κB expression in neurons of the hippocampus in the rat brain [68]. This may indicate a necessary association between NF-κB and COX-2 signaling under baseline conditions within the brain. Also, the expression of NF-κB signaling and COX-2 enzymatic activity is anticipated to be increased in the cases of inflammation.

1.4.3.3 Interleukin-8 (CXCL8) (IL-8)

IL-8 is a cytokine that belongs to the CXC chemokine family and works in pathological inflammation [69]. IL-8 is generally secreted by macrophages, epithelial cells, astrocytes, and neurons in response to an inflammatory agent such as the entrance of bacteria, viruses, or another chemical and/or toxic molecule [70], [71], [72], [73]. One of the key factors of IL-8 expression is that its also a neutrophil chemokine, depending on the type and/or duration of the infection IL-8 can immigrate to the infection site [72]. The NF-κB signaling pathway is quite important for IL-8 gene expression. After the inflammatory response is initiated by a related inflammatory agent, NF-κB transcriptional activity is required through the IKK pathway [74]. IKK pathway is related to the canonical pathway of NF-κB signaling which is activated after the pro-inflammatory signal. Therefore, IL-8 can be regarded as a crucial cytokine, being an important indication of the inflammatory response. In one study, methamphetamine (METH) induced cells triggered the expression of IL-8 through the involvement of astrocytes, also neuronal apoptosis is increased again *in vitro* [72]. IL-8 expression is enhanced not only in acute inflammation but also in neurodegenerative disorders. Microglia cultured cells obtained from post-mortem AD patients reveal higher IL-8 expression compared to controls. Similarly, increased IL-8 expression is detected in the brains of Huntington's disease (HD) patients and within the cerebrospinal fluid (CSF) of ALS patients [75]. Therefore, IL-8 plays a crucial role in both acute and chronic inflammation through the NF-κB pathway.

1.4.3.4 Interleukin-1β (IL-1β)

Acute and/or chronic inflammation that takes place in the CNS initiates the activation of microglia and astrocytes by increasing their reactivity. As a result, the levels of pro-

inflammatory cytokines are boosted as mentioned previously. IL-1β is one of these pro-inflammatory cytokines. This cytokine belongs to the IL-1 family, it is one of two different proteins together with interleukin-1α (IL-1α) [76]. The elevated mRNA and protein levels of IL-1β after an inflammatory stimulus is detected on many occasions. In one study, adolescent rats are voluntarily administered alcohol and increased mRNA levels of IL-1β are identified in the medial prefrontal cortex (mPFC) by activating microglia [77]. IL-1β is associated with acute inflammation and is regarded as one of the important mediators of further pro-inflammatory responses. After inflammation initiation, both neuronal and non-neuronal cells undergo cellular hypertrophy by the elevated expression of cell-surface immune proteins. The direct injection of IL-1β induces the expression of other pro-inflammatory cytokines and cyclooxygenase enzymes [76]. These further effects are also capable of influencing the synaptic formation and integrity mechanisms. In one study, lipopolysaccharides (LPS) are injected into the hippocampal slice cultures from mice, and then IL-1β mRNA levels are elevated. Additionally, IL-1β direct injection causes the decline of synaptophysin protein levels in the culture [78]. IL-1β can be also related to chronic inflammatory states which are observed in neurodegenerative disorders. The expression of this cytokine is increased in post-mortem tissues of AD and vascular dementia (VD) patients [79].

1.4.3.5 Tumor necrosis factor-alpha (TNF-α)

TNF-α is one of the pro-inflammatory cytokines which is mainly secreted from microglia. Although astrocytes and neurons can produce this cytokine up to some extent, the main source is microglial cells. TNF-α has an important role in regulating neuroinflammatory responses via carrying both neuroprotective and neurotoxic effects. Apart from being a prominent indicator of microglial activation in both acute and chronic inflammation also in

neurodegeneration, it is known to modulate glutamate-regulated cytotoxicity [80]. TNF-α affects the expression levels of many other pro-inflammatory cytokines such as IL-1β and IL-6. In one study, TNF-α direct injection into the mice increases serum and brain levels of IL-6 together with robust sickness response [81]. Furthermore, in another research, TNF-α synthesis suppressor 3,6'-dithiothalidomide decreases TNF-α levels by rescuing LPS-mediated neuroinflammation. In the same study, decreased TNF-α levels also mitigate aberrant hippocampal plasticity which is caused by LPS neurotoxicity [82]. TNF-α is believed to modulate these synaptic plasticity changes as well as LTP and LTD mechanisms together with IL-1β expression through the findings from the research about neurodegenerative disorders [83]. Finally, TNF-α is a mediator in AD pathophysiology, LPS injection to AD animal models elevates the detrimental effects of AD in terms of amyloid precursor protein (APP) and amyloid beta-peptide (Aβ) plaques through increased levels of TNF-α [84].

1.4.4 M2 Microglial State Markers

Inflammation within the CNS can have many detrimental consequences. Astrocytes and microglia are specialized non-neuronal cells for the recognition and the construction of essential responses within the CNS in the case of an inflammatory challenge, especially after acute inflammation. PAMPs and DAMPs are among the response targets of these cells. These responses are associated with the M1 microglial state and are quite important for the recruitment of leukocytes, T cells and helper cells, the release of pro-inflammatory cytokines is in this response group. However, neuroprotective responses are needed to be initiated to ameliorate the long-term detrimental effects of inflammation. Therefore, immunosuppressive/anti-inflammatory cytokines are secreted. This process also indicates the transition from the M1 microglial state to the M2 microglial state [85].

1.4.4.1 Interleukin-10 (IL-10)

IL-10 is one of the crucial anti-inflammatory cytokines. Macrophages, dendritic cells, and microglia can secrete IL-10 which exerts neuroprotective and immunosuppressive effects in both acute and chronic inflammation [86]. In one study, LPS stimulated inflammatory challenge to the primary neuronal cell culture is rescued by IL-10 receptor (IL-10R) and JAK-STAT3 pathway activation [87]. This rescue mechanism is considered to be exerted by the downregulation of pro-inflammatory cytokines. For instance, LPS-induced inflammation of the primary ventral mesencephalic (VM) cultures causes neuronal destruction and neuronal loss as well as increased expression of pro-inflammatory cytokines such as IL-1β, TNF-α, and COX-2. In this case, IL-10 can reduce neuronal deficiency and the elevation of pro-inflammatory cytokines [88]. Another evidence of IL-10 neuroprotective effects comes from ischemic stroke and traumatic brain injury(TBI) studies [89]. In one study, after cortical stroke, IL-10 is injected into the mice. This administration decreases the elevation of pro-inflammatory cytokines and genes which are related to inflammation as shown by quantitative polymerase chain reaction (qPCR) in the acute phase of the brain injury [90]. Therefore, IL-10 is among the important modulators of anti-inflammatory responses.

1.4.4.2 Transforming Growth Factor-Beta (TGF-β)

TGF-β is one of the well-known anti-inflammatory cytokines with robust neuroprotective effects after inflammation. Reactive astrocytes play an important role in TGF-β expression and this role has supported the correlation between the expression levels of glial fibrillary acidic protein(GFAP) and TGF-β signaling. However, T cells and B cells are also known to produce this cytokine even at low levels [91]. TGF-β is known to diminish neuronal deficiency through the downregulation of immune cell infiltration. In one study, the expression of astrocytic TGF-

β is suppressed through a genetically engineered mouse model of $GFAP^+$ astrocytes *in vivo*. The upregulation of immune cell infiltration and deficiency in motor behaviors are detected [92]. TGF-β signaling is also important for the progression of neurodegenerative disorders as seen in AD. Research with post-mortem tissues has revealed that TGF-β expression is increased in CSF and plasma in the brains of AD patients [93]. This may be related to the increased need for neuroprotective effects in the course of AD development. Therefore, TGF-β signaling and its associated downstream targets should be evaluated for therapeutic objectives for both acute and chronic neuroinflammation cases.

1.5 Neuroinflammation and Synaptic Integrity

In 1949, Donal Hebb has made an important statement that constitutes the basis of brain plasticity: "Cells that fire together, wire together" [94]. A lot has changed since then, today it is acknowledged that brain plasticity has also many biological routes and subdomains within the CNS. Neuronal differentiation and migration, neurogenesis, axonal growth, and dendritic branching are among the cellular basis of brain plasticity. Synaptic plasticity is also one of these subdomains and is considered to be the cellular base of learning and memory through LTP and LTD mechanisms. The neuroinflammatory status of the brain inevitably affects synaptic plasticity, there is a mutual relation between neuroinflammation and synaptic plasticity. Non-neuronal cells, for example, glial cells, affect many cellular mechanisms that control pre- and post-synaptic formation/integrity in the course of neuroinflammation and neurodegeneration [95].

Neuroinflammation is revealed to be correlated with the reduction of synaptic integrity and formation, also the increment of synaptic deficiency [96]. This mechanism is thought to be modulated by neuronal excitotoxicity. Microglial activation, in the course of

neuroinflammation, causes NO release. NO prevents glutamate reuptake at pre-synaptic sites which induce N-methyl-$_D$-aspartic acid (NMDA) receptors overactivation. This overactivation leads to the release of pro-inflammatory cytokines through arachidonic acid (AA) activation.

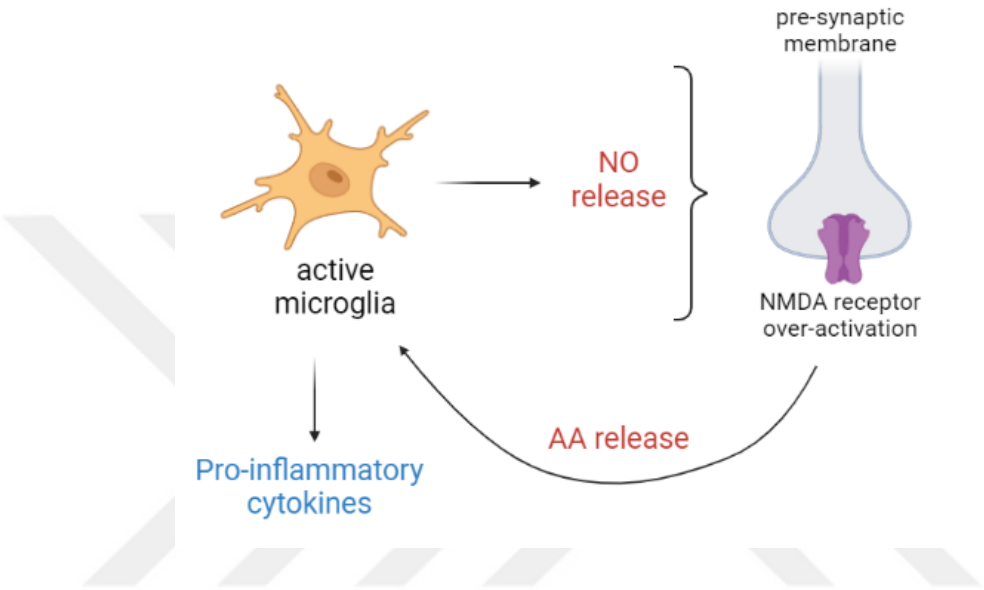

Figure 1.2 Schematic representation of NO and AA release during the secretion of pro-inflammatory cytokines. The figure is created with BioRender.

Under these conditions, pre-synaptic markers synaptophysin (SYN) and drebrin are also decreased [97]. SYN is a vesicle membrane pre-synaptic marker and drebrin is localized in dendrites and dendritic spines as a neuron-specific marker. Drebrin is found to decrease in the case of chronic inflammation in the neurodegenerative disease models [98], and LPS exposure to organotypic hippocampal slice cultures (OHSC) has caused a decrease in SYN protein levels [99].

Chronic neuroinflammation which is often seen in neurodegenerative disorders also causes synaptic plasticity dysregulations. This mechanism is one of the reasons for deficiency in

neuroprotective processes during disorders as well as a crucial mediator of cognitive disruptions observed during the disease progression [95].

1.5.1 Post Synaptic Density-95 (PSD-95)

PSD-95 is one of the scaffold proteins which is crucial for the NMDA receptors (NMDAR), dendritic spines, and excitatory signaling. NMDARs are important for LTP and LTD mechanisms which are the cellular bases of learning and memory within the brain. PSD-95 binds to the NMDARs so contributes to the excitatory activity between neurons [100]. Moreover, PSD-95 involves in the construction process of new dendritic spines again as a scaffold protein [96]. It can be claimed that this protein is one of the fundamental aspects of synaptic plasticity. However, the relation between neuroinflammation and the expression of PSD-95 is not simple. In one study, Freund's adjuvant (CFA) which is an antigen solution that stimulates inflammation is injected into mice brains and causes a decrease in PSD-95 protein levels in the cortex but not in the hippocampus. This may indicate a region-specific modulation of PSD-95 levels, which may also be dependent on the inflammatory agent and the duration [101]. In another study, resveratrol administration ameliorates morphine tolerance and suppresses neuroinflammation by modulating NMDARs expression through the loss of PSD-95 protein. This study shows the importance of PSD-95 for the NMDARs and the ameliorating effect of resveratrol may present itself by decreasing NMDAR levels in the course of inflammation [102]. Finally, another study has found that LPS administration to mice hippocampus induces elevated PSD-95 levels. This could work as a compensatory mechanism, LPS may increase the need for the birth of new neurons so NMDARs and excitatory activity could be upregulated especially in the early phases of synaptogenesis [103]. Therefore, it can be said that PSD-95 expression depends on many factors in the course of neuroinflammation

such as the inflammatory agent, the duration of the exposure, and the developmental stage of the neurogenesis and/or synaptogenesis. More research is needed to decipher this relation in a detailed manner.

1.5.2 Synaptophysin (SYN)

SYN is another crucial synaptic integrity protein that accumulates on presynaptic vesicle membranes [96]. SYN has important regulatory roles in learning and memory. Since the neuroinflammatory condition is known to damage these abilities, SYN is expected to be downregulated in the presence of neuroinflammation. In one study, glutaminase C overexpressing transgenic mice models have developed neuroinflammation as well as learning and memory deficits, also decreased SYN levels showing through Western blot [104]. Apart from overexpressing brain enzymes, external factors such as aging and brain trauma may downregulate SYN levels, throughout intensifying neuroinflammatory effects due to aging in the presence of surgical brain trauma [105]. Finally, in the course of neurodegeneration, the expression of SYN may also be at low levels. Aβ treated astrocytes are co-cultured with CD4+ T cells and again SYN levels are decreased [106]. These findings might partly explain the debilitating cognitive outcomes seen in the chronic neuroinflammation cases, for example in neurodegenerative disorders.

1.5.3 Gephyrin (GEP)

Gephyrin is a scaffolding protein like PSD-95, but it is mainly found in inhibitory synapses – GABAergic synapses. Therefore, it plays a major role in inhibitory signaling and the excitatory/inhibitory (E/I) balance of the CNS [107]. Gephyrin is inevitably affected by the neuroinflammatory status of the brain. Although increased inhibitory synaptic activity is

related to various neurodegenerative disorders [108], gephyrin modulation may be depended on the type of neuroinflammation. In one study, a group of mice is exposed to social isolation for 4 weeks. This isolation leads to anxiety-like behaviors and the following neuroinflammation by reducing gephyrin protein levels in the hippocampi, measured by the Western blot method [109]. On the other hand, in another study, mice hippocampal neurons that are exposed to Human Immunodeficiency Virus (HIV)-induced neuroinflammation in culture, show increased inhibitory synaptic activity and gephyrin levels by confocal imaging [110]. The pathways of socially-induced neuroinflammation and HIV-induced neuroinflammation are not the same so this could cause different gephyrin outcomes. GABAergic synapses are crucial for the progression of anxiety disorders so this could be a more direct mechanism. The source of the inflammation, signaling pathways, the nature of the studies(*in vitro* vs *in vivo*), measurement methods, and maybe the duration of the inflammatory signaling might significantly affect the gephyrin levels in the brain [110].

1.6 Neuronal & Glial Cell Markers

1.6.1 HuC

Drosophila ELAV protein has been recognized as a crucial neuronal marker since its being expressed in all neurons, identifying as a pan-neuronal marker [111]. Similarly, HuC protein belongs to the Hu/*elav* RNA binding protein family together with HuD and these proteins are believed to be the earliest neuronal markers in zebrafish. Both HuC and HuD are expressed in the central and peripheral nervous systems. The temporal and spatial expression patterns of HuC and HuD are different from each other, with HuC more effective in the neural determination while HuD being more effective in neural differentiation [112]. HuC is competent as a neuronal precursor in the course of early development. In one study, neurogenin

which supports neuronal specialization is administered to zebrafish embryos and this leads to HuC expression in the forebrain, hindbrain, and midbrain at 11 hours post-fertilization (hpf) [113]. HuC is also important for the neuronal precursor and therefore also for neurogenesis which is the creation of new neurons.

1.6.2 Glial Fibrillary Acidic Protein (GFAP)

Although GFAP is often known as a prominent marker of glial cells, GFAP can affect the fate of neurons in the CNS in the course of development. In one study GFAP+ progenitor cells have upregulated oligodendrocytes and neurons in mice [114]. Moreover, GFAP expressing cells are among the important regulators of adult neurogenesis in the mouse forebrain [115]. The upregulated GFAP expression particularly by astrocytes is among the indicators of neuroinflammation and even aging. In one study, GFAP expression is significantly increased in CSF of MS patients' brains. This can be interpreted as a sign of astrogliosis which is the upregulated astrocyte levels within the CNS possibly due to inflammation [116]. Similarly, GFAP levels are measured from grey matters of schizophrenic patients through the real-time polymerase chain reaction (RT-PCR) method, and upregulated GFAP expression is found only in patients with altered astrocyte morphology and astrogliosis [117]. *In vitro* studies via the usage of inflammation-stimulating agent for example LPS has proven increased GFAP expression as well as the upregulation of COX-2. Since GFAP is among the symbols of reactive glial cells, it is expected be interacting with pro-inflammatory cytokines, too [118]. GFAP upregulation is encountered not only in acute inflammation but also in low-level chronic inflammation for example in the course of neurodegenerative disorders. In one study, post-mortem hippocampal tissues of AD patients express GFAP by neurons. This also proves the

extent of GFAP, it is not only seen in glial cells but takes a role both in the production and progression of the neuronal cells [119].

1.7 Mammalian Target of Rapamycin Signalling Pathway (mTOR)

mTOR is a serine-threonine kinase from the PI3K family and has crucial roles in anabolic processes associated with cell growth, survival, and cellular proliferation, it is also evolutionarily conserved in zebrafish (*Danio rerio*). mTOR signaling pathway is related to deregulated nutrient sensing which is one of the hallmarks of aging. In the course of aging, the balance of nutrient signaling for cells has been dysregulated via the negative contributions of the hormonal ISS pathway, FOXO transcription, and mTOR signaling. These pathways are also associated with longevity and aging-related disorders. mTOR pathway has implications on the downregulation of autophagy-related gene expressions, and even tumor formation, especially at an advanced age. Apart from mTOR and the phospho-mTOR (p-mTOR) proteins, ribosomal protein S6 (S6), phospho-ribosomal protein S6 (p-S6), eukaryotic translation initiation factor 4E-binding protein 1 (4E-BP1) and phospho-4E-BP1 (p-4E-BP1) are among the downstream targets of mTOR pathway and indicate the activity of mTOR signaling [25], [26].

Rapamycin is known as an immunosuppressing chemical, it is also a proven mTOR pathway inhibitor [24]. Rapamycin has been approved to be used in humans by the United States Food and Drug Administration (FDA) [120] and it has been experimented with for a long time for the usage of pharmacological intervention. Apart from suppressing mTOR signaling, it can prevent LPS-induced acute neuroinflammation so would be classified as a potential therapeutic target for neuroinflammation-related diseases. In the course of inflammation, levels of hypoxia-inducible factor 1α (HIF1α) which is the main transcriptional factor that arranges

adequate responses to several pathologies are upregulated together with mTOR protein levels. Rapamycin exposure inhibits this upregulation by ensuring neuroprotective signals [121]. However, the exact mechanism is not clear, it may be depended on the mTOR pathway or rapamycin might act as an immunosuppressor independent of the mTOR pathway. Therefore, the exact implications, usage conditions, dose, and duration protocols are not clear, yet. In one research, age-dependent effects of rapamycin are observed on zebrafish [26], but its suppressing effects in the presence of inflammation are worth investigating.

1.8 Tuberous Sclerosis Complex (TSC)

Tuberous sclerosis complex (TSC) is an autosomal dominant disorder characterized by the formation of multiple tumors. This disorder is caused by the mutations in TSC1 and/or TSC2 genes. These genes do not only cause TSC disorder, they are also crucial for various cellular signals such as sensing environmental cues to create effective responses in terms of cellular growth, proliferation, and stress signals. TSC1 protein which is also known as hamartin and TSC2 protein which is also known as tuberin constitute the TSC1-TSC2 protein complex together and work as a negative regulator of the mTOR pathway, especially for the mTORC1 signaling by undertaking the aforementioned tasks. Therefore, when these genes are not available, overactivation of the mTOR pathway is possible [122]. A TSC2 mutant model would be useful to investigate the mTOR pathway over-activation and its relation to neuroinflammation in the framework of age and pharmacological intervention interactions.

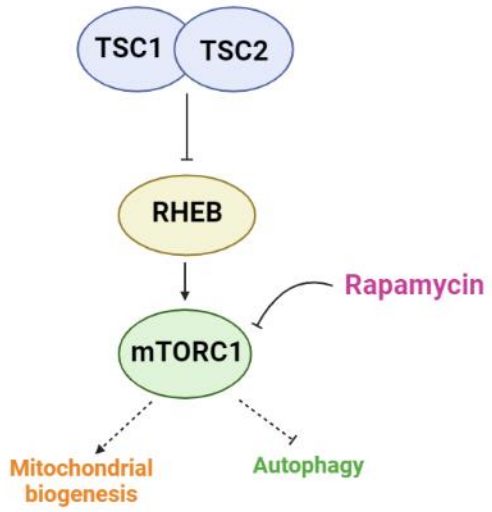

Figure 1.3 Schematic representation of TSC1-TSC2 complex and its relation to mTOR signaling. The figure is created with BioRender.

1.9 Copper Sulfate ($CuSO_4$) As an Inflammatory Agent

LPS is a widely used chemical to stimulate inflammation within the brain in both *in vivo* and *in vitro* models [78], [84], [88], [121]. Although it is useful, other chemicals are also worth investigating in terms of their inflammatory potential. Copper sulfate ($CuSO_4$) is a widespread chemical that can be one of the main sources of environmental toxicity. Copper is important for nutrition, various enzymatic reactions, and cellular events at trace amounts but its levels are arranged carefully within the organism. Higher amounts of copper might cause cellular toxicity and induce inflammation [123]. Ceruloplasmin and transcuprein are major copper-binding proteins, ceruloplasmin is also responsible for copper entry into the brain. Copper toxicity can cause neuroinflammatory events and the upregulation of ROS levels within the brain [124].

Copper induces ROS generation through the Fenton reaction. Since copper is a cation with +2 charges, it can decompose with hydrogen peroxide (H_2O_2) to generate free oxidizing agents. These oxidizing agents damage macromolecules and cause inflammatory events [123].

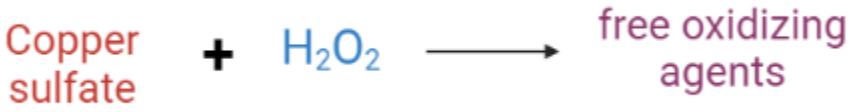

Moreover, copper has a role in the accumulation of Aβ protein. Long-term exposure to copper causes Aβ aggregation followed by oxidative damage and microglial activation. In AD animal models, this pattern is detected as well as increased pro-inflammatory cytokines such as TNF-α and IL-1β [125]. These findings show that copper would be an effective inflammatory agent to be used in various model organisms.

1.10 Zebrafish As A Model Organism

There is an emerging interest in zebrafish as a model organism, especially in translational and biomedical research. Zebrafish are cost-efficient model organisms, that can produce hundreds of offspring in one breeding [126]. Zebrafish embryos are transparent so they are quite suitable for early genetic interventions, drug screening, and chemical toxicity experiments [127]. They have a fully sequenced genome, their brain organizations are similar to mammals and they have a 69% similar genetic profile to humans which makes them quite appropriate model organisms to study complex brain diseases such as neuropsychiatric and neurodevelopmental disorders. [128], [129]. Zebrafish telencephalon is considered to be homologous to mammalian amygdala and hippocampus so neurobiological changes related to learning-memory deficits as well as social behavior can be investigated [130]. Moreover, zebrafish telencephalon expresses

adult neurogenesis [131] and high regenerative capacity in CNS [132]. All these features make zebrafish a useful model organism for neurobiological research at both embryo and adult levels.

1.11 Aims of This Thesis

As mentioned previously, primary, antagonistic and integrative hallmarks of aging constitute the aging profile of the organism. The free radical/oxidative stress theory of aging comprehensively summarizes this profile. According to this theory, the upregulated inflammatory status leads to enhanced ROS production together with less efficient anti-inflammatory cytokine expression mechanisms. This process is followed by the increased production of M1 microglial state markers such as pro-inflammatory cytokines and astrocyte reactivity [20]. In the course of this process, the mTOR signaling may become over-active together with deregulated nutrient sensing and dysfunctional autophagy [26]. NLRP3/NALP3 inflammasome activation, upregulation of NF-κB signaling pathway, and its downstream targets lead to increased cytokine levels. This neuroinflammatory status of the brain induces dysregulated synaptic integrity and impaired neurogenesis. Finally, cognitive/behavioral consequences are applied in addition to neurodegenerative disorders. This whole mechanism is also known as “oxy-inflammaging” which was pointed out by De La Fuente in 2008 [133].

In the light of this information, there were several objectives of this thesis. The first objective was to develop copper sulfate as an inducer of neuroinflammation in both zebrafish embryos and adults. Copper sulfate is an efficient inflammatory reagent due to its contribution to ROS production and Aβ accumulation [123], [124], [125]. Therefore, it would give expected outcomes for the development of neuroinflammation. The second objective was to assess the effect of the acute inflammatory response on mTOR signaling, synaptic integrity responses

and the inhibitory capacity of rapamycin in the course of neuroinflammation in very old (38 months) adult male and female zebrafish. Increased mTOR signaling and its downstream targets are detected in the hippocampus of AD patients via post-mortem studies [134]. Additionally, the suppression of mTOR signaling leads to a decreased neuroinflammatory response in the cerebral palsy mouse model [135]. Rapamycin can also downregulate neuroinflammation in both *in vitro* and *in vivo* models, apart from being a proven inhibitor for the mTOR pathway [121], so interactions between rapamycin, mTOR signaling, and neuroinflammation are worth investigating in aged organisms. The third objective was to characterize $tsc2^{+/-}$ mutants genotypically. Previously, $tsc2^{-/-}$ zebrafish embryos show higher inflammatory responses through over-active mTOR signaling [136], so the inflammatory status of the very old $tsc2^{+/-}$ adults would provide valuable insights for neuroinflammation. The final objective of this thesis was to decipher the effect of rapamycin treatment on an over-active mTOR pathway that is seen in very old (33 months) $tsc2^{+/-}$ animals. Also the impact of $CuSO_4$ treatment on very old (43 months) $ztor^{+/-}$ animals was aimed to be examined on a less-active mTOR pathway. In other words, we investigated the scope of chemical interventions in the inflammatory responses.

CHAPTER 2

Methods

The first objective of this thesis was to develop $CuSO_4$ as an inflammatory-stimulating agent in zebrafish embryos. To do this aim, zebrafish embryos at 3 days post fertilization (dpf) were exposed to 2 different types of $CuSO_4$ exposure in 24 well plates in E3 medium: long-term treatment and short-term treatment. The long-term treatment took 4 days with methylene blue and the short-term treatment took 4 hours or 24 with or without methylene blue. The objective of the long-term copper treatment was to mimic chronic inflammation whereas the aim of the short-term treatment was to mimic the acute inflammation. Since methylene blue was found to be therapeutic in oxidative-stress related degeneration [137], the effect of this substance to the inflammatory condition should have been taken into consideration. The overall objective of the embryo study was to determine the effective dosage of $CuSO_4$ as an inflammatory reagent in terms of its effectiveness on mRNA levels of various pro- and anti-inflammatory cytokines.

2.1 Gene Expression Experiments with Embryos

2.1.1 Subjects

ZebTech Housing System (Tecniplast, Italy) takes place in Bilkent University Zebrafish Facility and is used for the maintanence of the fish. The temperature and pH level of the circulating water were controlled regulary with carbon and mechanical filters. The temperature of the system was 28^0C and pH levels were kept in between 7.0-7.5. All of the fishes were fed with dry flakes twice a day and artemia once a day. They were kept in either 3.5 liter or 8 liter of tanks with a 14 hours of light and 10 hours of dark cycle. A total of 300 3 dpf offsprings of wild type fish were used for

both long-term and short-term $CuSO_4$ exposure study. The protocol for animal experiments in this study was approved by Bilkent University Animal Experiments Local Ethics Committee (BILHADYEK) with the decision number 2019/14.

2.1.2 Experimental Procedure

In order to obtain embryos, one adult female and one adult male wild type fish were placed in breeding tanks with a seperator, for at least 15 hours.

After seperators were opened in the following day, emrbyos were collected and placed into the E3 medium with methylene blue in petri dish. Emrbyos were fed with dry flakes (Sera, Germany) and kept in 30.5^0C incubator for 3 days. The collection time of the embryos were noted and they were taken into the experiments exactly after 72 hours.

Table 2.1 E3 Medium (60X)

Substance	**Amount**
NaCI (Sigma Aldrich, 13423)	17.2 g
KCI (Sigma Aldrich, 12636)	0.76 g
$CaCI_2$. $2H_2O$ (Carlo Erba, 327 607)	2.9 g
$MgSO_4$. $7H_2O$ (Sigma, M2773-1)	4.9 g
ddH_2O	Up to 1 L

2.1.3 Long-term Treatment Condition

The $CuSO_4$ concentrations in this condition were as the following: 0 uM (control), 2.5 uM, 5 uM, and 7.5 uM. In the beginning of the experiment, $CuSO_4.5H_2O$ (Sigma-Aldrich; Catalog #: 209198)

was dissolved in E3 medium with methylene blue to obtain 100 uM concentrated stock solution. Later, copper solutions at different concentrations were obtained through serial dilution. At 3 dpf, embryos were taken into the 24 well plates. In each well, there were 5 embryos and 2 ml dissolved $CuSO_4$ in E3 medium with methylene blue at different concentrations. There were at least 3 control wells(15 embryos) in each 24-well plate. These well plates were again kept in 30.5^0C incubator until the experiment was ended. At every 24 hours, the E3 medium was changed. Also, checkpoints were arranged and at every checkpoint dead embryos were removed. Checkpoints were decided as the following:

Table 2.2 Checkpoint chart for long-term treated embryos

Checkpoint – 1	3 hours later
Checkpoint – 2	6 hours later
Checkpoint – 3	12 hours later
Checkpoint – 4	18 hours later
Checkpoint – 5	24 hours later – Medium change
Checkpoint – 6	48 hours later – Medium change
Checkpoint – 7	72 hours later – Medium change
Checkpoint – 8	96 hours later – Medium change

In total, 5 technical replicas were conducted for this study. After treatment, embryos were collected in 1.5 ml eppendorf tubes as being 10 emrbyos in each tube. The collected embryos were immediately snap-frozen in liquid nitrogen and stored into the -80^{0}C.

2.1.4 Short-term Treatment Condition

Long-term treatment was conducted to mimic chronic inflammation in order to investigate the inflammatory response at mRNA level. However, the mortality rate of animals was quite high in the end of this treatment. This could be due to the duration, 4 days of $CuSO_4$ exposure could be too long. In addition, methylene blue which was a common chemical reagent used in embryo mediums has anti-inflammatory feature [137]. For these reasons, short-term $CuSO_4$ treatment was conducted as a follow-up study with shorter $CuSO_4$ exposure duration and the usage of E3 medium in both with and without methylene blue options.

Again at 3 dpf, embryos were taken into the 24 well plates. In each well, there were 5 embryos in 2 ml E3 medium which contained 10 uM dissolved $CuSO_4$ with or without methylene blue. There were at least 3 control wells(15 embryos) in each 24-well plate. These well plates were again kept in 30.5^{0}C incubator until the experiment was ended. Initial mortality rate was not high so checkpoints were not applied. At least 30-40 embryos were collected after 4 hours and the same number were collected after 24 hours with corresponding controls for each duration. In total, 3 technical replicas were conducted for this study. Again, every 1.5 ml eppendorf tube contains 10 emrbyos. The collected embryos were immediately snap-frozen in liquid nitrogen and stored into the -80^{0}C.

The summary of long-term and short-term treatment conditions are as follows:

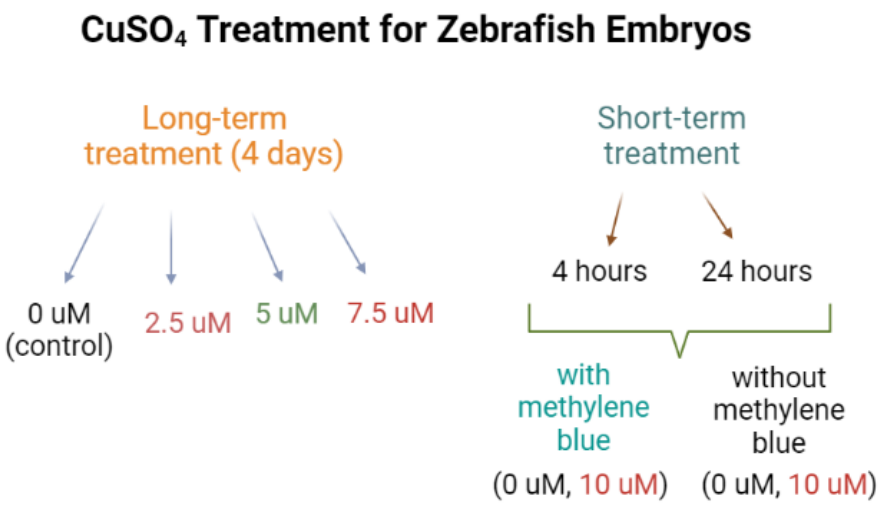

Figure 2.1 CuSO4 treatment for 3 dpf zebrafish embryos. The figure is created with BioRender.

2.1.5 RNA Isolation from Zebrafish Embryos

For RNA isolation, 10 embryos were pooled and at least 10 embryos were used from each technical replica for each concentration and time point. Each pooled embryo set was homogenized with 250 µl Trizol (Trizol ® Reagent, Ambion, 19367501) by using a syringe. Then, samples were centrifuged at 12.000 x g for 5 minutes at +4^{0}C. Embryos were sinked at the bottom of the tube and the clear supernatant was transferred into the another tube. 5 minutes incubation was applied at room temperature to allow the complete dissociation of nucleoproteins. Then, 50 µl Chloroform (Chloroform, Merck, 1.02245.2500) was added into each tube, Trizol and Chloroform was allowed to mix by gentle spin-down movements. After 3 minutes of incubation at room temperature, samples were centrifuged at 12.000 x g for 15 minutes at +4^{0}C. After centrifuge, samples were dissociated into 3 phases: bottom Trizol layer, middle organic layer and top aqeous phase which contains RNA. The top layer was transferred to another tube and 125 µl isopropanol was added to tubes to precipitate the RNA. Again 10 minutes incubation at room temperature was performed and samples were centrifuged at 12.000 x g for 10 minutes at +4^{0}C. The total RNA precipitated as

a white-gel at the bottom of the tube. The supernatant was decanted and the precipitation was washed with 250 µl 75% ethanol. After a brief vortex, samples were centrifuged at 12.000 x g for 5 minutes at $+4^0$C. The ethanol was removed by pipetting gently, and the samples were left within the bench for 5 minutes for air-dry. Then, RNA pellets were dissolved with 10 µl nuclease-free water (Thermo Fisher Scientific, USA, AM9937) and placed into the 55^0C heat block for 10 minutes to ensure complex dissolution. Final RNA concentrations were determined on NanoDrop™ 2000 and samples are removed to -80^0C fridge to be used later.

2.1.6 DNase Treatment and Complementary DNA (cDNA) Synthesis

TURBO DNA-free™ Kit (AM1907, Ambion, USA) was used for DNase treatment to eliminate the DNA residues within the RNA. After quick spin of RNA samples, 7 µl nuclease-free water (Thermo Fisher Scientific, USA, AM9937), 2 µl 10X buffer and 1 µl DNase enzyme were added for each sample. Then, samples were incubated at 37^0C for 30 minutes. After incubation, 2 µl DNase inactivation buffer was added to stop the reaction. Samples were incubated at room temperature for 5 minutes and they were centrifuged for 2 minutes at 11.000 x g. The inactivation buffer precipitated at the bottom of the tube, the supernatant which contained the DNase-free RNA was taken into the new tube. The RNA concentration was again measured on NanoDrop™ 2000.

DNase treatment was followed by cDNA synthesis. cDNA synthesis kit (iScript cDNA Synthesis Kit, 100 reactions, BioRad, USA, 1708891) was used to synthesize 500 ng cDNA. The final RNA concentrations were used to calculate the required RNA amount. In order to obtain 20 µl cDNA, samples were diluted with 15 µl nuclease-free water then 4 µl 5X buffer and 1 µl reverse-transcriptase enzyme within the kit were added. Samples were centrifuged for a few seconds and incubated at 25^0C for 5 minutes, at 46^0C for 20 minutes finally at 95^0C for 1 minute at the thermal

cycler (Thermal Cycler C1000, BioRad) machine. Samples were kept at -80^{0}C for long-term experiments.

2.1.7 Quantitative Polymerase Chain Reaction (qPCR)

2.1.7.1 Primers Used in The Study

Gene expression and mRNA levels were measured through qPCR. Some of the primers used in the study such as COX-2, NF-κB and IL-8 were taken from the literature [69]. Other primers such as IL-1β, TNF-α, IL-10, TGF-β, lc3-b and atg-5 were validated by our group. As the housekeeping gene, ribosomal protein L13a (rpl13-a) was used [138], [139]. The relative gene expression levels of each gene were specified based on the rpl13-a gene. The annealing temperature, the melting temperature, the length, and the length of the products could not be specified in the reference source. Therefore, the National Center for Biotechnology Information (NCBI) Primer Blast program was used to analyze the obtained primers. The detailed information about the used primers can be found in Table 2.3.

Table 2.3 Forward and reverse sequences and the final concentrations of primers

Gene	Forward primer (5'-3')	Reverse primer (5'-3')	Concentration in reaction
cox-2	ACAGATGCGCTACCAGTCTT	CCCATGAGGCCTTTGAGAGA	1 µM
nf-κB	GGTCGGACAGAGATCACGGATT	TGCTGTTCTTCACGTCCTCT	0.5 µM
IL-8	GTGCGCCAATGAGGGTGAA	ACCCACGTCTCGGTAGGATT	1 µM
IL-1β	GATCCGCTTGCAATGAGCTAC	TCAGGGCGATGATGACGTTC	1 µM

TNF-α	AGGAACAAGTGCTTATGAGCCATGC	AAATGGAAGGCAGCGCCGAG	1 µM
IL-10	TCACGTCATGAACGAGATCC	CCTCTTGCATTTCACCATATCC	0.5 µM
TGF-β	TGTACCCGCAATCCTTGACC	CCGACTGAGAAATCGAGCCA	1 µM
lc3-b	CCTCCAACTCAACTCCAACC	GCCGTCTTCGTCTCTTTCC	1 µM
atg-5	CAACTGTGGATGGGTCTG	GAGCGTCTGGATGAATGG	1 µM
rpl13-a	TCTGGAGGACTGTAAGAGGTATGC	AGACGCACAATCTTGAGAGCAG	1 µM

2.1.7.2 Dilutions of Primers and Samples

After new primers arrived, they were dissolved in nuclease-free water (Thermo Fisher Scientific, USA, AM9937) as specified on their product sheet to achieve 500 µM of final primer concentration. Then, these primers were optimized by using trial cDNA which was obtained from non-treated and $CuSO_4$ treated embryos. For each primer pair, undiluted, 1:2, 1:4 and 1:8 diluted versions of cDNA samples were used. After this optimization, primers were decided used as follows:

Table 2.4 Product lengths and sample dilutions of primers

Gene	Product Length	Sample Dilution
cox-2	240	1:8
nf-κB	210	1:8
IL-8	195	undiluted
IL-1β	109	1:2
TNF-α	157	1:2
IL-10	151	1:2

TGF-β	169	1:4
Lc3b	112	undiluted
rpl13-a	148	1:8

2.1.7.3 Quantitative Polymerase Chain Reaction (qPCR) Protocol

For both optimization and actual experiments, the protocol was the same. The total reaction volume for each sample was 20 µl which included 10 µl LightCycler® 480 SYBR Green 1 Master (Roche, Switzerland, 04707516001), 6 µl nuclease-free water, 2 µl diluted primers and 2 µl cDNA. First, SYBR Green 1 Master and nuclease-free water were mixed (MasterMix). Then, primer dilutions were prepared, for 1:20 dilution 2.5 µl forward, 2.5 µl reverse primer were mixed with 95 µl nuclease-free water. For 1:10 dilution 5 µl forward, 5 µl reverse primer were mixed with 90 µl nuclease-free water. Then MasterMix was mixed with a diluted version of each primer(premix). Each well of Roche 96 well plate (Roche, Switzerland, 04707516001) was filled with 18 µl of this premix. Finally, cDNA was added to each well according to the agreed sample dilutions. The plate was sealed and centrifuged at 1500 rpm for 2 minutes. After centrifugation, the plate was placed into the LightCycler® 480 Instrument (Roche) and the reaction was initiated. The reaction conditions are stated in Table 2.5.

Table 2.5 Reaction Conditions for Quantitative Polymerase Chain Reaction

Preincubation	95^0C for 10 seconds		
Amplification – 45 cycles	95^0C	10 seconds	4.4 ramp rate
	60^0C	15 seconds	2.2 ramp rate
	72^0C	15 seconds	4.4 ramp rate

Melting Curve	95^0C	5 seconds	4.4 ramp rate
	55^0C	30 seconds	2.2 ramp rate
	72^0C	continuous	0.29 ramp rate
Cooling	40^0C for 10 seconds		

Two technical replicas were conducted for each sample. The gene expression levels were calculated based on the $2^{-\Delta\Delta CT}$ method by the normalization for rpl13-a housekeeping gene. First, rpl13-a Ct values were subtracted from the Ct values of the gene of interest, so delta Ct values were obtained. Then, 0 µM copper sulfate treated samples (control samples) were determined as the control samples and their average values were subtracted from the delta Ct values. These final values were delta delta Ct values (ΔΔCT) and fold change gene expression levels were obtained through $2^{-\Delta\Delta CT}$ method. For some experimental cohorts, fold change values were transformed to the log2 values to normalize the data and to apply the homogeneity of variances assumptions.

2.2 Protein Expression Experiments

Section titles indicated with one asterisk (*) states that those prodecures were performed by Dr. Ergül Dilan Çelebi Birand.

The second aim of this thesis was to assess the effect of the mTOR signaling on an acute inflammatory response, synaptic integrity responses and the inhibitory capacity of rapamycin in the course of neuroinflammation in very old (38 months) adult male and female zebrafish.

2.2.1 Subjects

All of the animal subjects were taken from the Bilkent University Zebrafish Facility whose conditions were mentioned previously. There are 16 adult (7 females, 9 males) 38 months old

zebrafish were used in this experiment. Before the experiment, all fish were fed twice a day with standard fish flakes (Sera, Germany), and once a day with artemia (Sera, Germany) in the tank system. The protocol for very old wild-type adults, genotyping of $tsc2^{+/-}$ adults and the gene expression experiments of $tsc2^{+/-}$ and $ztor^{+/-}$ adults was approved by Bilkent University Animal Experiments Local Ethics Committee (BILHADYEK) with the decision number 2019/14.

2.2.2 *Experimental Procedure

There were 4 groups in this experiment: dimethyl sulfoxide (DMSO) treatment group, $CuSO_4$ treatment group, rapamycin (RAPA) treatment group and $CuSO_4$ and then rapamycin treatment ($CuSO_4$ + RAPA) treated group. There were 4 animals assigned in each treatment group.

Table 2.6 Distribution of animals across experimental groups. DMSO: DMSO treated control group, $CuSO_4$: Copper sulfate treatment group, RAPA: rapamycin treatment group, $CuSO_4$ + RAPA: Copper sulfate and then rapamycin treated group.

Group Name	**Treatment**	**Male number**	**Female number**
DMSO	1 hour of DMSO treatment	2	2
$CuSO_4$	1 hour of copper treatment	2	2
RAPA	1 hour of DMSO + 3 hours of rapamycin treatment	3	1
$CuSO_4$ + RAPA	1 hour of copper + 3 hours of rapamycin treatment	2	2

All treatments were conducted in separate 4 L of tanks on the indicated durations in the table. The standard temperature and lighting conditions were maintained for the fish during the treatment. Both rapamycin and $CuSO_4$ were dissolved in DMSO. Basically, 25 mM $CuSO_4$ was obtained in 1 ml DMSO (Applichem, Germany, A3672) and this working solution was added to the 4 L of tank water. Therefore, the final $CuSO_4$ concentration was 25 µM. Similarly, 96 µl RAPA (Sigma, USA, R0395) was dissolved in 904 µl DMSO. And this amount was added to the 4 L tank water so the final RAPA concentration was 24 µM. After drug treatments were conducted as on the indicated durations in Table 2.6, all of the animals were euthanized on the ice and fish are decapitated using a sterile surgical blade. Trunks were visualized on the light microscopy to confirm genders. Gills, eyes and brains of the animals were dissected separately and collected in different eppendorf tubes. After collection, tissues were snap-frozen immediately with liquid nitrogen and stored at -80^0C .

2.2.3 *Protein Isolation from Brain Tissues

Each of the brain tissues was homogenized in freshly prepared RIPA buffer with a 25-gauge 2 ml syringe (Beybi, Turkey). The recipe for the 1 ml RIPA buffer can be found in Table 2.7.

Table 2.7 The recipe for the 1 ml RIPA buffer

Reagent Name	**Amount**
2 M NaCI (Sigma-Aldrich, Germany, 7647145)	75 µl
1 M Tris-HCI (pH=8) (Sigma Aldrich, Germany, 1185531)	50 µl
1 % NP-40 (NP40S)	10 µl
Sodium dodecyl sulfate (SDS, 10%) (Sigma, T9281)	10 µl

ddH_2O	355 µl
2X Protease Inhibitor (Sigma, 05892970001)	500 µl

60 µl RIPA buffer was used for each 1 mg of tissue. After complete homogenization, homogenates were left in ice for 30 minutes for the lysis. Then, samples were centrifuged at 13.000 rpm for 20 minutes at $+4^0$C. Supernatants were removed gently with the micropipette, they were aliquoted and stored at -80^0C.

2.2.4 *Bradford Assay

Bradford assay was used to measure the protein concentrations which were isolated from brains. In this measurement, 1 mg/ml bovine serum albumin (BSA) protein was the standard control protein. In 96-well plates, BSA (Sigma, USA, A2153) standards were prepared with ddH_2O as stated on the Table 2.8.

Table 2.8 BSA Standars (µl) for Bradford Assay

	1	**2**	**3**	**4**	**5**	**6**	**7**
BSA	0	0.5	1	2	3	4	5
ddH_2O	5	4.5	4	3	2	1	0

All protein samples were prepared as 0.5 µl protein and 4.5 µl ddH_2O. Then, 250 µl of Bradford reagent (Sigma, USA, B6916) was added to each well. Standards and protein samples were prepared as duplicates. The plate was shaken briefly and incubated for 10 minutes. On the Microplate Reader (SpectraMax M5, Molecular Devices, Sunnyvale, CA, USA), absorbance

values at 595 nm were read. After reading, a standard curve was obtained based on the BSA values and the concentration of proteins was calculated.

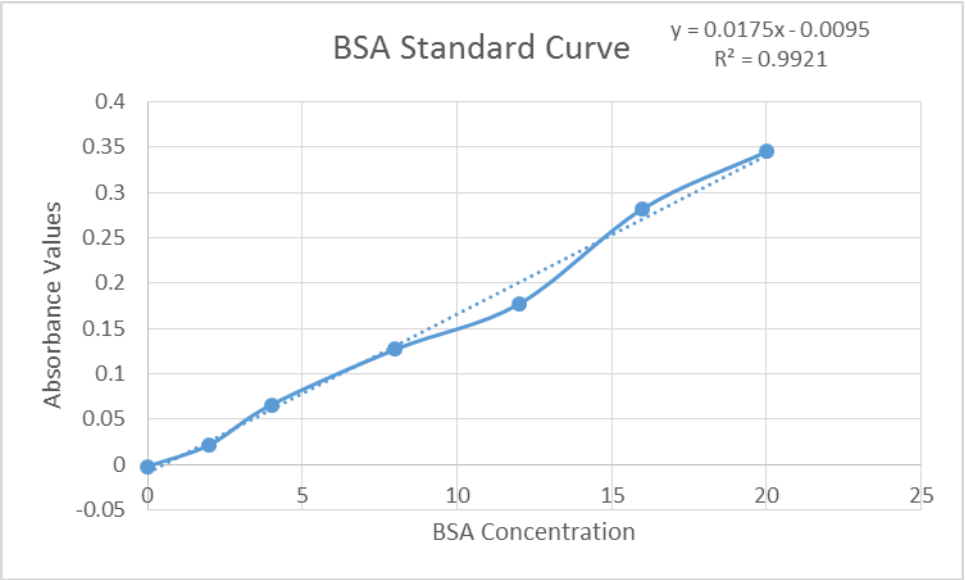

Figure 2.2 BSA Standard Curve results for the calculation of protein concentrations from the brains.

2.2.5 Western Blot Procedure

2.2.5.1 Sample Preperation for Western Blot

To avoid the saturation of proteins, all of them were loaded into the gel as a total of 40 µg. This amount was decided previously in Adams Lab by optimization experiments. The housekeeping protein tubulin also gave unsaturated results with 40 µg loading. Protein samples were mixed with ddH_2O and 2X loading dye according to their obtained concentrations. The total volume for each sample was set as 40 µl. Before adding 2X loading dye, 10% dithiothreitol (DTT) was added freshly to the 2X loading dye mixture.

Table 2.9 2X Loading Dye

Reagent Name	Amount
10% SDS	4 ml
Glycerol	2 ml
Bromophenol blue	100 µl
0.125 M Tris-HCI (pH=6.8)	2.5 ml

After samples were prepared, they were boiled at 95^0C for 10 minutes. Then they were ready to be loaded into the SDS-PAGE gel.

2.2.5.2 SDS-PAGE Gel Preperation

For Western Blot experiments, two types of gels were prepared: 10% resolving and 5% stacking gels. Stacking gels were required for the generation of wells and protein loading whereas resolving gels were for the running of the proteins. The concentration of the gels depended on the protein of interest, smaller proteins run better at concentrated gels. At each experiment, 2 gels were loaded with proteins.

Table 2.10 10% Resolving Gel (for 2 gels)

Reagent Name (for 2 gels)	Amount
ddH_2O	9.3 ml
1.5 M Tris (pH=8.8)	5 ml
10% SDS	200 µl
30% Acrylamide/bis-acrylamide mix (Sigma, A6050)	5.3 ml

10% Ammonium persulfate (APS)	200 µl
N,N,N'N'-tetramethylethane-1,2-diamine (TEMED) (Sigma, T9281)	30 µl

Table 2.11 5% Stacking Gel (for 2 gels)

Reagent Name (for 2 gels)	**Amount**
ddH_2O	4.76 ml
0.5 M Tris (pH=6.8)	2 ml
10% SDS	80 µl
30% Acrylamide/bis-acrylamide mix (Sigma, A6050)	1060 µl
10% Ammonium persulfate (APS)	80 µl
N,N,N'N'-tetramethylethane-1,2-diamine (TEMED) (Sigma, T9281)	8 µl

2.2.5.3 Sample Loading and Gel Electrophoresis

1.5 mm glass plates were aligned with the shorter one facing inward. The potential leakage was checked with ddH_2O. Then, 10% resolving gel was poured slowly with a pipette. Isopropanol was added to the gel immediately to prevent any bubble generation. After the resolving gel was polymerized completely, the isopropanol was discarded and its residues were cleaned with ddH_2O. Then, 5% stacking gel was poured on top of the resolving gel again with a pipette. Bubbles were

removed with 10 µl pipette tips and a 10-wells gel comb was placed slowly to produce wells. The gel took 15 minutes to polymerize completely.

Gels within the glass plates were removed from the gel cassettes and placed into the electrode assembly (Mini-PROTEAN Tetra Cell Electrophoresis System, BioRad, USA). The tank was filled with 1X running buffer (Table 2.12). 10-well combs were removed slowly not to damage protein wells. Protein samples were loaded slowly into the wells to prevent any formation of bubbles. PageRuler Prestained Protein Ladder (Thermo Fisher Scientific, USA, 26616) and PageRuler Prestained Protein Ladder (Thermo Fisher Scientific, USA, 26619) were used as protein markers and loaded as 1.5 µl into the first well and last two wells in each gel. All wells were loaded with protein samples and/or 2X loading dye. After loading was completed, the 1X running buffer was poured until the 4-gels line and samples were run at 90 V for 30 minutes to align all samples. During this duration samples were expected to leave stacking gel. Then, the voltage was increased to 120 V, and samples were run in the gel for 120 minutes at this voltage. Each sample was run at least two times per protein of interest.

Table 2.12 10X Running Buffer (pH=8.3, 1 L)

Reagent Name	**Amount**
250 mM Tris	30.285 g
1.9 M Glycine	144.134 g
10% SDS	100 ml
ddH_2O	Up to 1 L

2.2.5.4 Transfer of Proteins

The required equipment for the transfer system was prepared before the gel running ends. Gel holder cassettes, 4 Whatman papers per gel holder cassette and foam pads were soaked into the 1X Transfer buffer (Table 2.13). In the meantime, Polyvinylidene difluoride (PDVF) membranes were also soaked into the 100% methanol for 1 minute in order to activate them. Then, membranes were also taken into the 1X Transfer buffer after activation. Also, the sandwich system for the gel transfer was prepared (Figure 2.3). The running time for electrophoresis was checked, and protein markers should have been opened. The running was stopped and cassette sandwiches were opened with gel releasers. The stacking gel was discarded and the resolving gel was carefully placed within the gel holder cassette on top of the Whatman paper. Then, the PDVF membrane was placed, and two Whatman papers and a sponge were followed. Then, gel holder cassettes were closed, placed into the Mini Trans-Blot Cell Module (BioRad, CA, USA). The cooling unit was placed into the tank, and the transfer process was conducted at +40C. It took 90 minutes at 100 V.

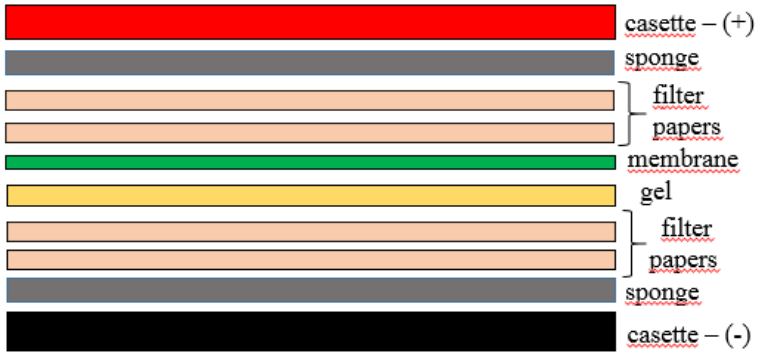

Figure 2.3 The sandwich blot system for the transfer of proteins.

Table 2.13 1X Transfer Buffer (2 L)

Reagent Name	Amount
25 mM Tris base	6 g

195 mM Glycine	28 g
Methanol	400 ml
ddH_2O	Up to 1.6 L

2.2.5.5 Blocking & Primary and Secondary Antibody Incubation

In the process of transfer, blocking buffers were prepared with either 5% non-fat dry milk or 5% bovine serum albumin (BSA) in 1X-TBS-T (Tris Buffered Saline – 3% Tween-20) (Table 2.14) in 50 ml falcons. After the transfer was ended, membranes were removed from the Trans-Blot Cell Module system and cut into pieces according to the size of the protein of interest based on the protein ladders. Then, they were placed into either milk or BSA solutions and left for incubation on the shaker for 1 hour at room temperature. This blocking step was required for the elimination of the undesired proteins from the membrane. In the meantime, primary antibodies were prepared in 5% milk or BSA in 1X-TBS-T solutions at previously optimized concentrations. After blocking, membranes were left for incubation with primary antibodies at $+4^0$C overnight.

Table 2.14 10X Tris Buffered Saline (TBS) (pH=7.6, 1 L)

Reagent Name	**Amount**
Tris base	12 g
NaCI	80 g
ddH_2O	Up to 1 L

In order to obtain TBS-T, this solution was diluted to 1X and 3 ml Tween-20 (Sigma, 8221841000) was added to 1 L of 1X TBS.

After overnight incubation with primary antibodies, membranes were washed with 1X TBS-T several times as indicated durations in Table 2.17. Membranes were subjected to secondary antibody incubation at room temperature for 1 hour. Then, they were again washed with 1X TBS-T under the same conditions in Table 2.17. Therefore, membranes were ready for chemiluminescent detection.

Table 2.15 Primary Antibodies Used in the Western Blot Experiments

Primary Antibody	**Company**	**Catalog Number**	**Dilution Ratio**	**Dilution Buffer**
α-Gephyrin	Santa Cruz Biotechnology, USA	sc-6411	1:1000	5% BSA in TBS-T
α-GFAP	Abcam, UK	ab53554	1:1000	5% BSA in TBS-T
α-PSD-95	Abcam, UK	ab18258	1:5000	5% milk in TBS-T
α-Synaptophysin	Abcam, UK	ab32594	1:10.000	5% milk in TBS-T
α-HuC	Abcam, UK	ab184267	1:1000	5% milk in TBS-T
α-mTOR	Cell Signaling Technology, USA	2983S	1:5000	5% milk in TBS-T
α-p-mTOR	Cell Signaling Technology, USA	2974	1:2000	5% BSA in TBS-T
α- TNF-α	Z-Fish®	AS-55383s	1:4000	5% milk in TBS-T

α-p-S6	Cell Signaling Technology, USA	4858	1:1000	5% BSA in TBS-T
α-β-Tubulin	Cell Signaling Technology, USA	2146	1:5000	5% milk in TBS-T

Table 2.16 Secondary Antibodies Used in Western Blot Experiments

Secondary Antibody	**Company**	**Catalog Number**	**Dilution Ratio**	**Dilution Buffer**
α-goat	Abcam, UK	ab97100	1:5000	5% BSA in TBS-T
α-rabbit	Cell Signaling Technology, USA	7074	1:5000	5% milk in TBS-T

Table 2.17 Membrane Washing Conditions for Western Blot Experiments

Duration	5 minutes	5 minutes	10 minutes	5 minutes	5 minutes

2.2.5.6 Chemiluminescent Detection

Supersignal West Femto Maximum Sensitivity Substrate (Thermo Fisher Scientific, Rockford, USA, 34095) was used for the band detection. Peroxide and enhancer detection solutions were used in a 1:1 ratio for imaging. Later, this mixture was used to cover membranes and they were left for

incubation for 5 minutes in the dark. Membranes were visualized on the BioRad ChemiDocTM XRS+ Imaging System (BioRad, CA, USA) on both signal accumulation and automatic exposure modes because the exposure depended on the protein of interest.

2.2.6 Image Quantification

The quantification of images was conducted by Narin Ilgım Ardıç Avcı who was blind to experimental conditions and the order of protein samples. The obtained band intensities were double-normalized. First, within-gel normalization was conducted by dividing the band intensity of the protein of interest by the average band intensity of that within the same gel. Within-gel normalization aimed to eliminate differences between technical replicas. Then, tubulin normalization was calculated by dividing the within-gel normalized value of the protein of interest by the within-gel normalized value of the tubulin.

Within-gel normalization: (band intensity of the protein) / (average band intensity of that protein)

Tubulin normalization: (within-gel normalized value of the protein) / (within-gel normalized value of the tubulin)

2.3 Genotyping Experiments for $tsc2^{+/-}$ Animals & Gene Expression Experiments for TSC2 and mTOR Mutants

The third objective was to optimize the genotyping protocol for $tsc2^{+/-}$ mutants and to investigate the outcomes of the genetic susceptibility for an over-active mTOR signaling.

2.3.1 Genotyping Experiments for $tsc2^{+/-}$ Animals

2.3.1.1 Tissue Collection for Deoxyribonucleic Acid (DNA) Extraction

Gills from individual adult fishes were used for DNA extraction. Tissues were collected in separate tubes during the dissection and snap-frozen immediately by using liquid nitrogen. Then, samples were placed into the -80^{0}C fridge. One piece of gill and/or half of the tail was enough for DNA extraction.

2.3.1.2 DNA Extraction

This process took 2 consecutive days. On the first day, tissues were placed into the separate tubes which were filled with 300 µl lysis buffer beforehand.

Table 2.18 DNA Extraction (Lysis) Buffer – 30 ml

Substance	**Amount**
100 mM EDTA	3 ml
1 M Tris-HCI (pH = 8.23)	3 ml
2 M NaCI	3 ml
10% SDS	1.5 ml
ddH_2O	19.5 ml

Then, 3 µl proteinase k (20 mg/ml) was added to each tube, and samples were left at 55^{0}C incubation overnight. On the second day, samples were heated at 95^{0}C in a heat bath for 20 minutes for the inactivation of Proteinase K. Then, samples were centrifuged at 13.000 rpm for 20 minutes, at +4^{0}C. After this centrifuge, DNA remained in the supernatant so it was slowly removed into another tube. 275 µl isopropanol was added to each sample, and another centrifuge was conducted again at 13.000 rpm for 20 minutes, at +4^{0}C. After this centrifuge, DNA precipitated as a white-gel pellet at the bottom of the tube. The isopropanol supernatant part was removed slowly and DNA

samples were washed with 500 µl, 70% ethanol. Again the centrifugation was conducted under the same conditions and the ethanol supernatant was finally removed. The eppendorf tubes were placed horizontally within the petri dishes for air drying, it took approximately 7-8 minutes. DNA pellets were dissolved in 10 µl nuclease-free water by pipetting up and down on the eppendorf walls. Finally, DNA concentrations were measured at NanoDrop^{TM} 2000, and samples were removed to a -20^{0}C fridge to be used later. Some of the obtained DNA concentrations from adult fishes for the genotyping experiments are as follows:

Table 2.19 Some of the DNA Concentrations from Adult Zebrafish Tissues for Genotyping

Sample Name	DNA Concentration	260/280 Value	260/230 Value
Sample-1	115.4	1.71	1.16
Sample-2	1329.6	1.71	1.26
Sample-3	1064.1	1.83	1.58
Sample-4	280.3	1.77	1.58
Sample-5	756.6	1.76	1.66

2.3.1.3 Primers for Tuberous Sclerosis Complex 2 (TSC2) Mutant Characterization

Primers were taken from Kim et al. (2011) article, the research group that developed tsc2$^{+/-}$ zebrafish animals [140].

Table 2.20 Primers Used for TSC2 Genotyping

Primer Name	Product Length	Final Concentration	Sequence (5'-3')

TSC2 – forward	151 bp	1 µM	CCAGCACCACCTGCAGTCTGG
TSC2 - reverse	151 bp	1 µM	CTCTTGGGCAGAGCAGAGAAGTTGG

Before usage primers were diluted as 1/10 ratio and final concentration in the reaction was finalized as 1 µM.

2.3.1.4 Polymerase Chain Reaction (PCR)

For each sample, 25 µl PCR was prepared in 200 µl eppendorf tubes. The reagents in the reaction included nuclease-free water, DMSO (NEB, M0536l), the mixture of forward and reverse primers(premix), Phusion® Hot Start Flex 2X Master Mix (NEB, M0536L), and individual DNA for each sample.

Table 2.21 The reagents of 25 µl PCR

Reagent Name	Amount for 25 µl reaction
Nuclease-free water	8.25 µl
DMSO	0.75 µl
Premix	2.5 µl
Hot Start Flex 2X Master Mix	12.5 µl
DNA	1 µl

At the beginning of each experiment, Master Mix which contained all reagents except DNA was prepared. Then, 24 µl was put from Master Mix to each sample and finally, DNA was added. The samples were placed into the thermal cycle (TC-512, Techne) under the following cycling conditions. Annealing took 30 cycles.

Table 2.22 Thermal Cycyling Conditions for PCR

Initial Denaturation	980C – 30 seconds
Annealing	980C – 10 seconds

	700C – 30 seconds
	720C – 30 seconds
Final Extension	720C – 10 minutes

After PCR experiment, samples were kept in -20^{0}C until restriction enzyme(RE) reaction.

2.3.1.5 Restriction Enzyme (RE) Reaction

HpyCH4IV(NEB, R0619L) restriction-digestion enzyme was used for this step. 30.5 µl reaction was prepared for each sample.

Table 2.23 The reagents of 30.5 µl restriction enzyme reaction

Reagent Name	Amount for 30.5 µl Reaction
Nuclease-free water	23 µl
PCR product(individual)	4 µl
CutSmart 10X Buffer (NEB)	3 µl
HpyCH4IV Enzyme (NEB)	0.5 µl

Then samples were taken into the thermal cycle (2720 Thermal Cycler, Applied Biosystems) for the following conditions: 37^{0}C for 40 minutes + 80^{0}C for 15 minutes. After restriction enzyme experiment, samples were kept in -20^{0}C until they were loaded into the agarose gel.

2.3.1.6 Sample Preparation & Sample Loading

Both PCR and RE samples were loaded into the agarose gel. 8 µl PCR sample was mixed with 2 µl 5X DNA Loading Dye (5X DNA Loading Buffer Blue, 5400200-1000) and a 28 µl RE sample was mixed with 7 µl dye. Afterward, samples were loaded into the agarose gel electrophoresis together with a 1.5 µl DNA ladder (GeneRuler 100bp, Thermo Scientific, SMO243). After loading, they were left to run for 40 minutes at 100 V by using a 1X TAE buffer. BioRad ChemiDocTM XRS+ Imaging System (BioRad, CA, USA) was used for gel imaging.

Table 2.24 50X TAE Buffer – 1 L

Substance	Amount
Trisma Base (Sigma Aldrich, 77861)	242 g
Glacial Acetic Acid (Sigma Aldrich, 64197)	57.1 ml
EDTA	18.6 g
ddH_2O	Up to 1 L

Table 2.25 2.5% Agarose Gel with EtBr

Substance	Amount
Agarose (BioReagent, low EEO, 9012366)	2.5 g
1X TAE Buffer	100 ml
EtBr	2 µl

2.3.2 Gene Expression Experiments for $tsc2^{+/-}$ & $ztor^{+/-}$ Animals and Wild Type Siblings

Gene expression experiments for $tsc2^{+/-}$ and $ztor^{+/-}$ animals together with their wild-type siblings were conducted with very old zebrafish adults (33 months and 43 months) on qPCR. The genotyping experiments of $ztor^{+/-}$ animals were conducted by Serena Sevdiye Aktürk. On $tsc2^{+/-}$ animals the tuberin protein was not able to encode due to the non-sense mutation in the gene of interest and this led to the over-active TOR signaling. On $ztor^{+/-}$ animals, TOR signaling was suppressed due to TOR haploinsufficiency [141]. Therefore, $tsc2^{+/-}$ animals could be defined as the accelerated aging model whereas $ztor^{+/-}$ animals could be defined as the deaccelerated aging model. In this experiments, 24 µM rapamycin treatment was applied to the TSC2 animals for 3 hours, and

25 µM $CuSO_4$ treatment was applied to the ztor animals for 1 hour together with their wild-type siblings on the previously described conditions (Section 2.2.2). After tissues were collected, brains were split into two as the left and right hemispheres, and snap-frozen immediately. Then RNA isolation, DNase treatment, and cDNA synthesis experiments were conducted as described previously. Gene expression experiments were conducted on qPCR for various pro- and anti-inflammatory markers and some autophagy markers.

2.4 Statistical Analysis

All statistical tests and data visualizations were conducted in R(4.2.0) programming language. For gene expression experiments, diagnostic tests were applied to both fold change and log2 expression values before the statistical analyses. Shapiro Wilk and Levene's Tests were used to check the normality and homogeneity of variances assumption, respectively. The majority of the genes accorded normality and homogeneity of variances assumptions. For the long-term $CuSO_4$ exposure experiments, one-way ANOVA was applied if these assumptions were met. If not, the Kruskal-Wallis test was conducted. For the short-term $CuSO_4$ exposure experiments, three-way ANOVA was applied for 3 independent variables: $CuSO_4$ dosage, the medium, and the duration of exposure. If one of these variables was not significant, then this variable was dropped from the analysis and two-way ANOVA was applied to investigate factors together and/or individually.

For protein expression experiments, again diagnostic tests were applied to check normality and homogeneity of variances assumption. If these assumptions were met, one-way ANOVA was applied for only one independent variable which was the exposed substance to animals. If these assumptions were not met, the non-parametric alternative of one-way ANOVA which was the Kruskal-Wallis Test was applied. The significance levels were set at $p \leq 0.05$ in all experiments.

CHAPTER 3

Results

3.1 Gene Expression Experiments with Embryos

3.1.1 Long-Term $CuSO_4$ Exposed Embryos

The main objective of this study was to asses the capability of $CuSO_4$ to induce inflamatory response in zebrafish. Therefore, we checked the gene expression levels of two pro-inflammatory cytokines, COX-2 and IL-8, also one anti-inflammatory cytokine IL-10 in the long-term $CuSO_4$ exposed embryos. There was no significant effect of $CuSO_4$ dosage ($F(3,20) = 0.258$, $p = 0.855$) on the log2 fold change values of COX-2 (Figure 3.1.1 (a)). Also, there was no significant effect of $CuSO_4$ treatment ($F(3,20) = 1.463$, $p = 0.255$) on log2 fold change values of IL-8 (Figure 3.1.1 (b)).

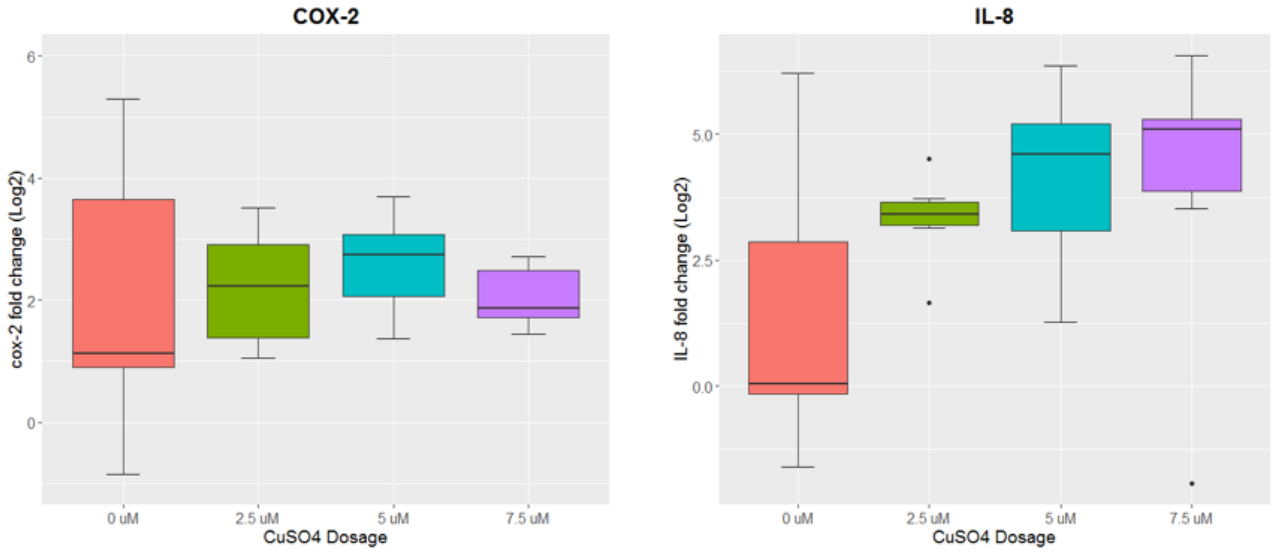

(a) (b)

Figure 3.1.1: Log2 fold change values in the expression levels of two pro-inflammatory cytokines, COX-2 and IL-8. There were no significant effects of $CuSO_4$ dose on COX-2 (a) and IL-8 (b). Error bars represent the 95% confidence interval. The top and the bottom of the box represent the 25th and 75th percentiles. The line inside the box is the 50th percentile. Outliers are represented by closed circles. (***: $p \leq 0.001$, **: $p \leq 0.01$, *: $p \leq 0.05$, #: $p \leq 0.1$, ns: $p > 0.1$)

In terms of the gene expression levels of the anti-inflammatory cytokine IL-10, there was a marginally significant effect of $CuSO_4$ dosage ($F(3,14) = 3.221$, $p = 0.05$) on the log2 fold change values of IL-10 (Figure 3.1.2 (a)). The difference between IL-10 log2 fold change values at 0 µM copper treated condition (control group) and 7.5 µM treated condition was significant ($p = 0.04$, 95% C.I. = [0.095], [4.451]) (Figure 3.1.2 (b)).

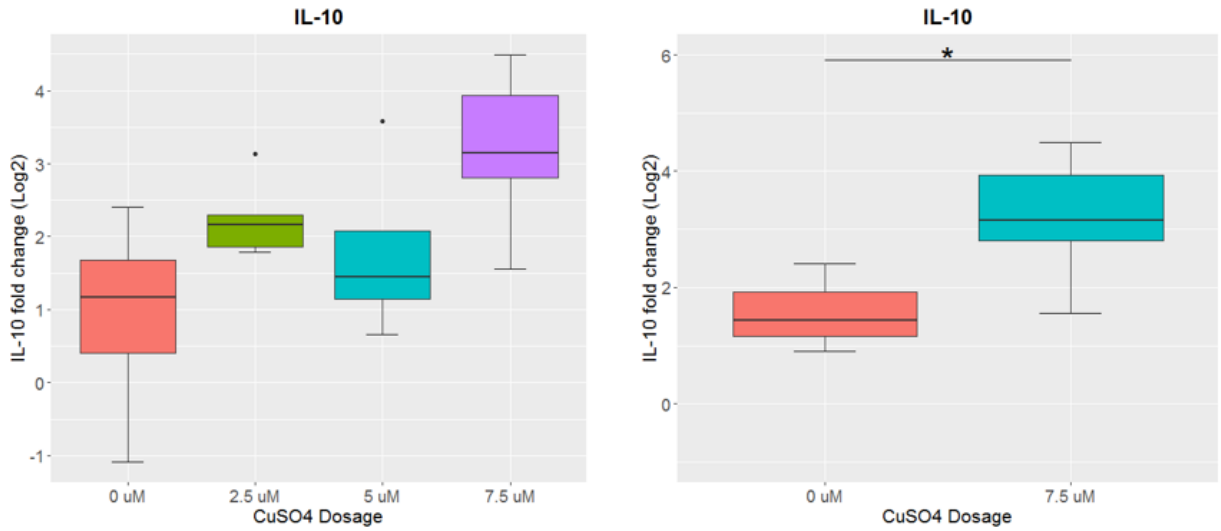

(a) (b)

Figure 3.1.2: Log2 fold change values in the expression levels of the anti-inflammatory cytokine, IL-10 (a). There was a marginally significant effect of $CuSO_4$ dose on log2 fold change values of IL-10. Error bars represent the 95% confidence interval. The top and the bottom of the

box represent 25th and 75th percentiles. The line inside the box is the 50th percentile. Outliers are represented by closed circles. (***: p≤ 0.001, **: p≤ 0.01, *: p≤ 0.05, #: p≤ 0.1, ns: p> 0.1)

3.1.2 Short-term $CuSO_4$ Exposed Embryos

The long-term $CuSO_4$ treatment was not very effective for embryos. There was higher mortality rate and embryos were quite lethargic during the experiment. Also, methylene blue has immuno-suppressive effects and it could prevent the generation of inflammatory response. However, adult fishes do not need methylene blue in tank water. Therefore, an additional short-term $CuSO_4$ exposure study has been conducted to test the effect of methylene blue and $CuSO_4$ exposure duration on 3 dpf zebrafish embryos. In this study, we checked the gene expression levels of pro-inflammatory cytokines COX-2, NF-κB, IL-8, IL-1β, TNF-α and anti-inflammatory cytokines IL-10 and TGF-β.

There was a significant effect of only $CuSO_4$ dosage ($F(1,20) = 5.079$, $p = 0.035$) on the log2 fold change values of COX-2 (Figure 3.1.3 (a)). There was not an interaction effect between dose and duration and dose and medium. Also, there was a significant effect of only $CuSO_4$ treatment ($F(1,16) = 4.649$, $p = 0.046$) on log2 fold change values of NF-κB (Figure 3.1.3 (b)). Again, there was not an interaction effect between dose and duration and dose and medium.

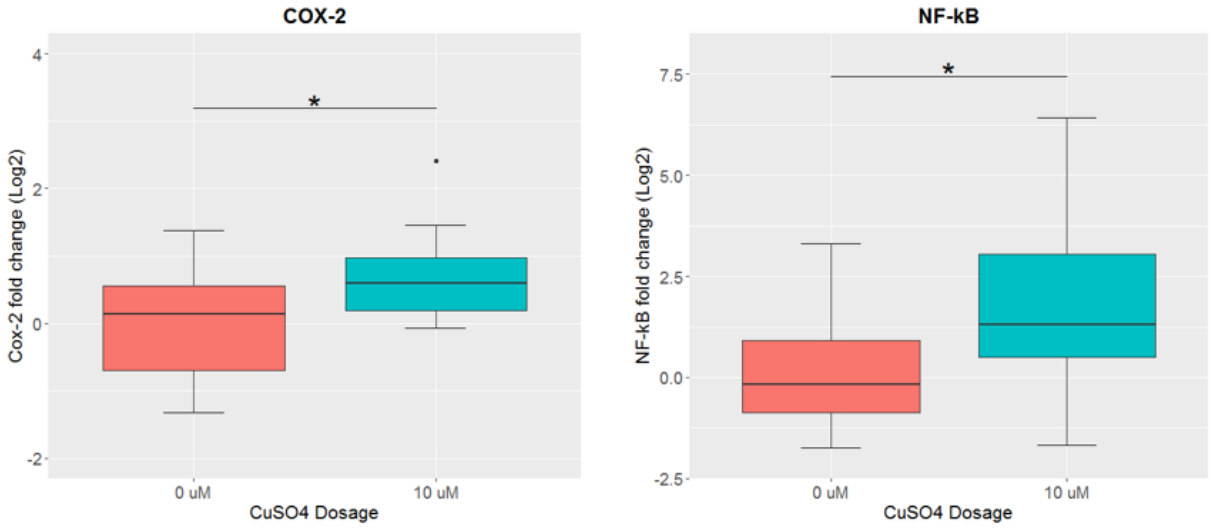

(a) (b)

Figure 3.1.3: Log2 fold change values in the expression levels of the pro-inflammatory cytokines, COX-2 (a) and NF-κB (b). There was a significant effect of $CuSO_4$ dose on log2 fold change values of COX-2 and NF-κB. Error bars represent the 95% confidence interval. The top and the bottom of the box represent the 25th and 75th percentiles. The line inside the box is the 50th percentile. Outliers are represented by closed circles. (***: $p \leq 0.001$, **: $p \leq 0.01$, *: $p \leq 0.05$, #: $p \leq 0.1$, ns: $p > 0.1$)

For another pro-inflammatory cytokine IL-8, there was a statistically significant interaction between $CuSO_4$ dosage and duration ($F(1,20) = 6.344$, $p = 0.02$). Therefore, simple main effect analysis showed that 10 µM CuSO4 treatment had a significant effect on IL-8 fold change log2 values on 4 hours treated condition ($F(1,10) = 51.7$, $p < 0.001$) (Figure 3.1.4 (a)). Also, 10 µM CuSO4 treatment had a significant effect on IL-8 fold change log2 values on 24 hours treated condition ($F(1,10) = 6.124$, $p = 0.03$) (Figure 3.1.4 (b) & Figure 3.1.5).

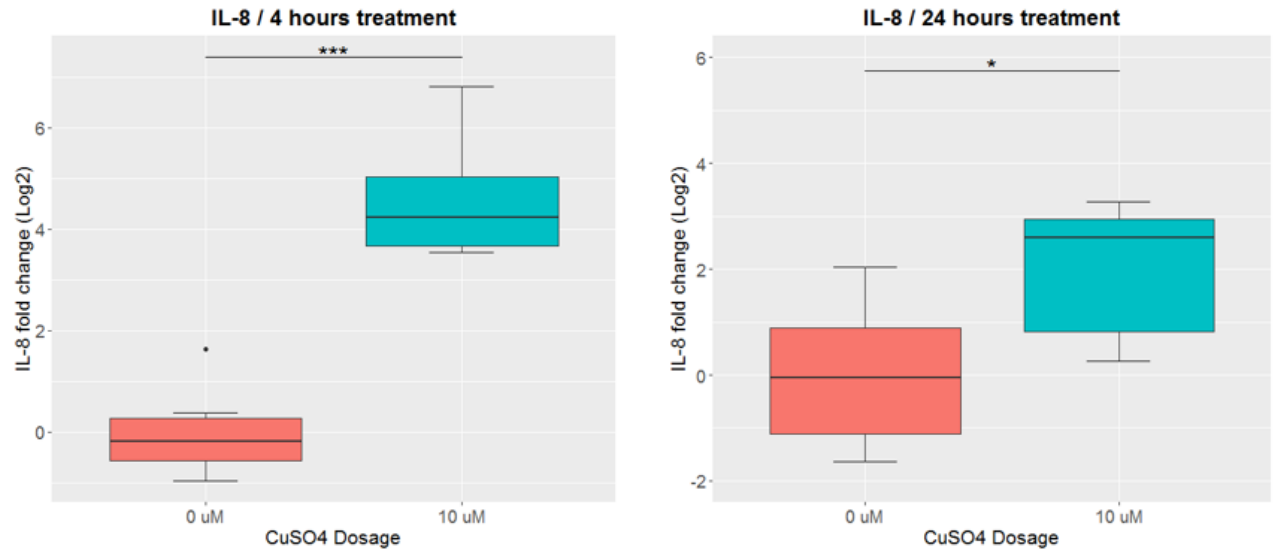

(a) (b)

Figure 3.1.4: Log2 fold change values in the expression levels of the pro-inflammatory cytokine IL-8 on 4 hours treated condition (a) and 24 hours treated condition (b). There was a significant effect of $CuSO_4$ dose on log2 fold change values of IL-8 in both conditions. Error bars represent the 95% confidence interval. The top and the bottom of the box represent the 25th and 75th percentiles. The line inside the box is the 50th percentile. Outliers are represented by closed circles. (***: $p \leq 0.001$, **: $p \leq 0.01$, *: $p \leq 0.05$, #: $p \leq 0.1$, ns: $p > 0.1$)

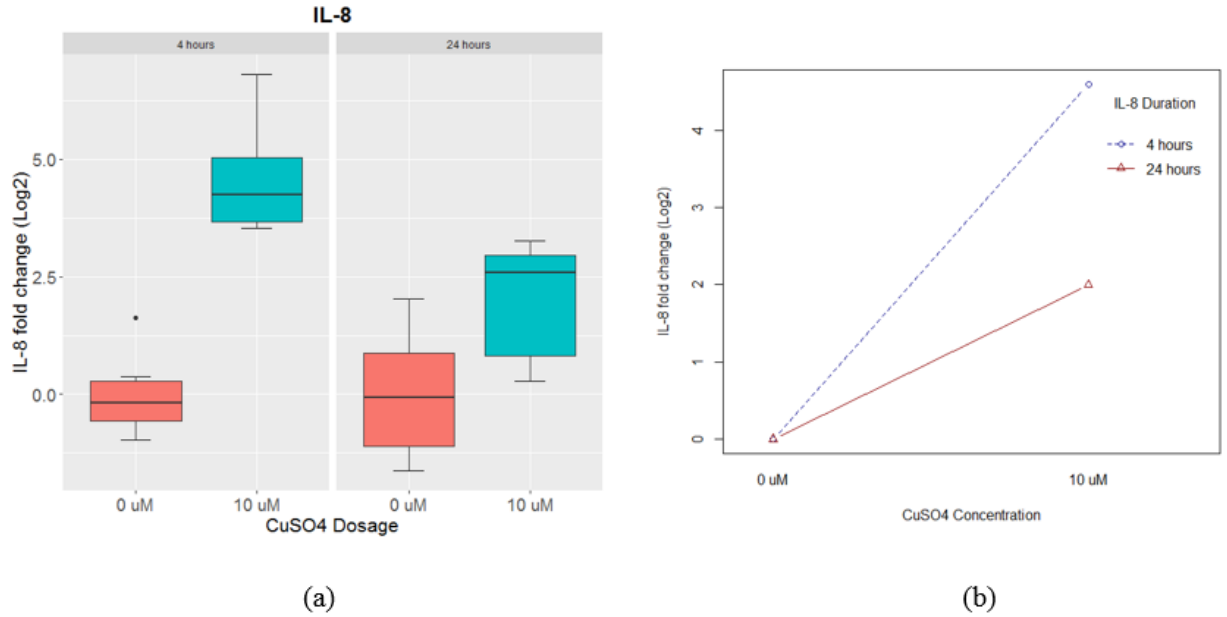

Figure 3.1.5: Log2 fold change values in the expression levels of the pro-inflammatory cytokine IL-8 (a). IL-8 log2 fold change levels increase earlier upon the exposure of $CuSO_4$ (b). There was a significant effect of $CuSO_4$ dose on log2 fold change values of IL-8 in both conditions. Error bars represent the 95% confidence interval. The top and the bottom of the box represent the 25th and 75th percentiles. The line inside the box is the 50th percentile. Outliers are represented by closed circles. (***: $p \leq 0.001$, **: $p \leq 0.01$, *: $p \leq 0.05$, #: $p \leq 0.1$, ns: $p > 0.1$)

For another pro-inflammatory cytokine IL-1β, there was a statistically significant interaction between $CuSO_4$ dosage and medium (with or without methylene blue) ($F(1,20) = 5.944$, $p = 0.024$). Therefore, simple main effect analysis showed that 10 µM $CuSO_4$ treatment had a significant effect on IL-1β fold change log2 values on without methylene blue treated condition ($F(1,10) = 16.29$, $p < 0.01$) (Figure 3.1.6 (a)). On the other hand, 10 µM $CuSO_4$ treatment did not have a significant effect on IL-1β fold change log2 values on with methylene blue treated condition ($F(1,10) = 0.112$, $p = 0.745$) (Figure 3.1.6 (b)).

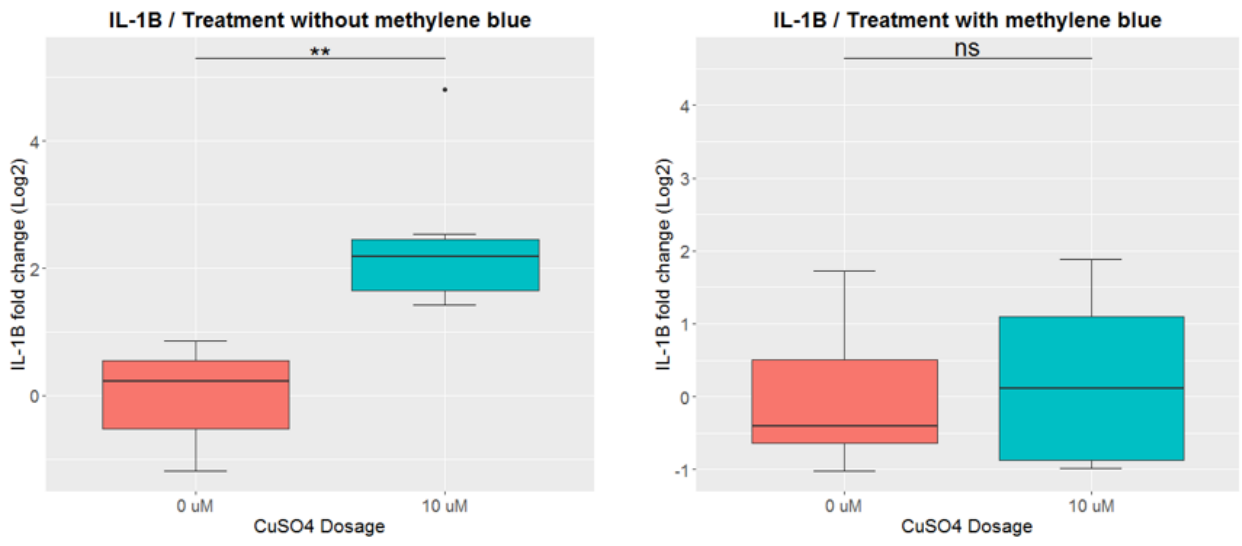

(a) (b)

Figure 3.1.6: Log2 fold change values in the expression levels of the pro-inflammatory cytokine IL-1β on treatment without methylene blue condition (a) and on treatment with methylene blue condition (b). There was a significant effect of $CuSO_4$ dose on log2 fold change values of IL-1β on treatment without methylene blue condition. Error bars represent the 95% confidence interval. The top and the bottom of the box represent the 25th and 75th percentiles. The line inside the box is the 50th percentile. Outliers are represented by closed circles. (***: $p \leq 0.001$, **: $p \leq 0.01$, *: $p \leq 0.05$, #: $p \leq 0.1$, ns: $p > 0.1$)

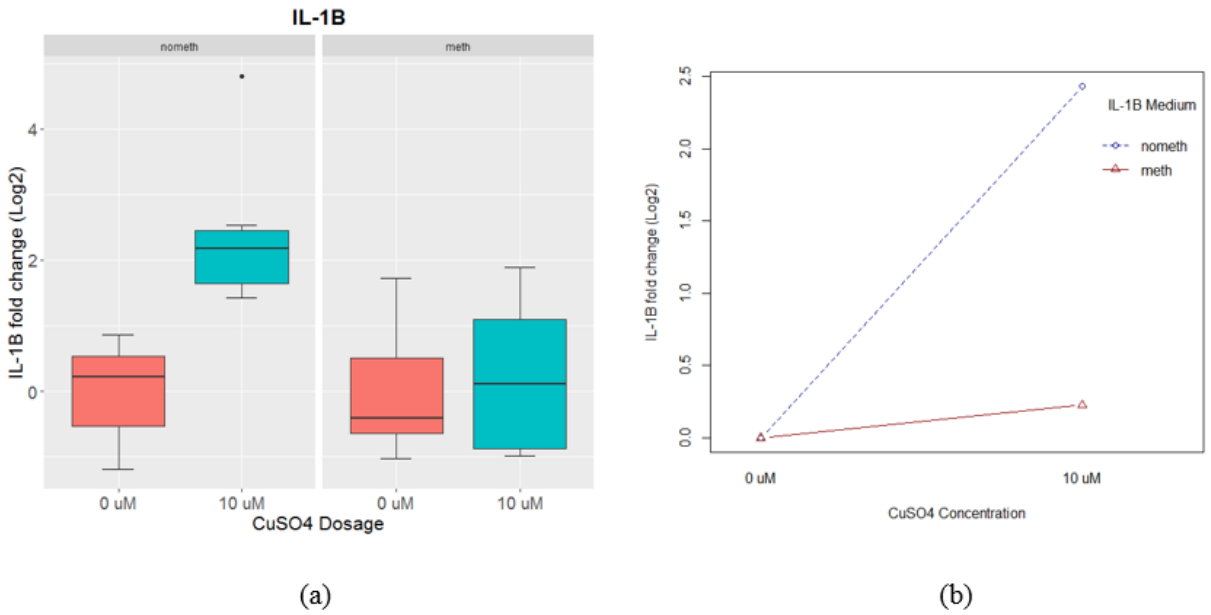

(a) (b)

Figure 3.1.7: Log2 fold change values in the expression levels of the pro-inflammatory cytokine IL-1β (a). IL-1β log2 fold change levels increase significantly only on the without methylene blue treatment condition upon the exposure of $CuSO_4$ (b). Error bars represent the 95% confidence interval. The top and the bottom of the box represent the 25th and 75th percentiles. The line inside the box is the 50th percentile. Outliers are represented by closed circles. Nometh: without methylene blue, meth: with methylene blue. (***: $p \leq 0.001$, **: $p \leq 0.01$, *: $p \leq 0.05$, #: $p \leq 0.1$, ns: $p > 0.1$)

For pro-inflammatory cytokine TNF-α there was not a significant effect of $CuSO_4$ dosage ($F(1,17) = 1.624$, $p = 0.219$), duration of the treatment ($F(1,17) = 1.117$, $p = 0.305$) and the medium condition ($F(1,17) = 0.767$, $p = 0.393$) on the log2 fold change values of TNF-α (Figure 3.1.8). There was not an interaction effect between dose and duration and dose and medium.

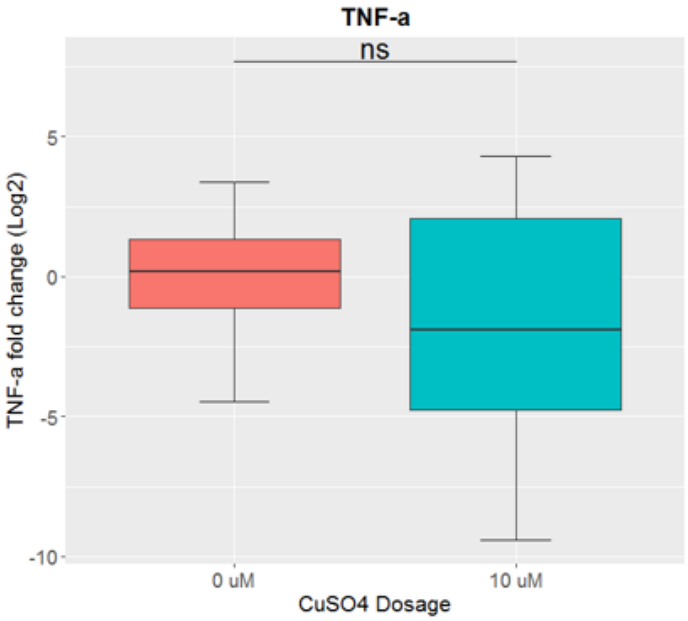

Figure 3.1.8: Log2 fold change values in the expression levels of the pro-inflammatory cytokine, TNF-α. There was not a significant effect of $CuSO_4$ dose on log2 fold change values of TNF-α. Error bars represent the 95% confidence interval. The top and the bottom of the box represent the 25th and 75th percentiles. The line inside the box is the 50th percentile. Outliers are represented by closed circles. (***: $p \leq 0.001$, **: $p \leq 0.01$, *: $p \leq 0.05$, #: $p \leq 0.1$, ns: $p > 0.1$)

In terms of anti-inflammatory cytokine IL-10, there was a statistically significant interaction between $CuSO_4$ dosage and treatment duration ($F(1,17) = 9.329$, $p = 0.007$). Therefore, simple main effect analysis showed that 10 µM 4 hours $CuSO_4$ treatment did not have a significant effect on IL-10 fold change log2 values ($F(1,9) = 0.306$, $p = 0.594$) (Figure 3.1.9 (a)). On the other hand, 10 µM 24 hours $CuSO_4$ treatment had a significant effect on IL-10 fold change log2 values ($F(1,8) = 31.48$, $p < 0.001$) (Figure 3.1.9 (b)).

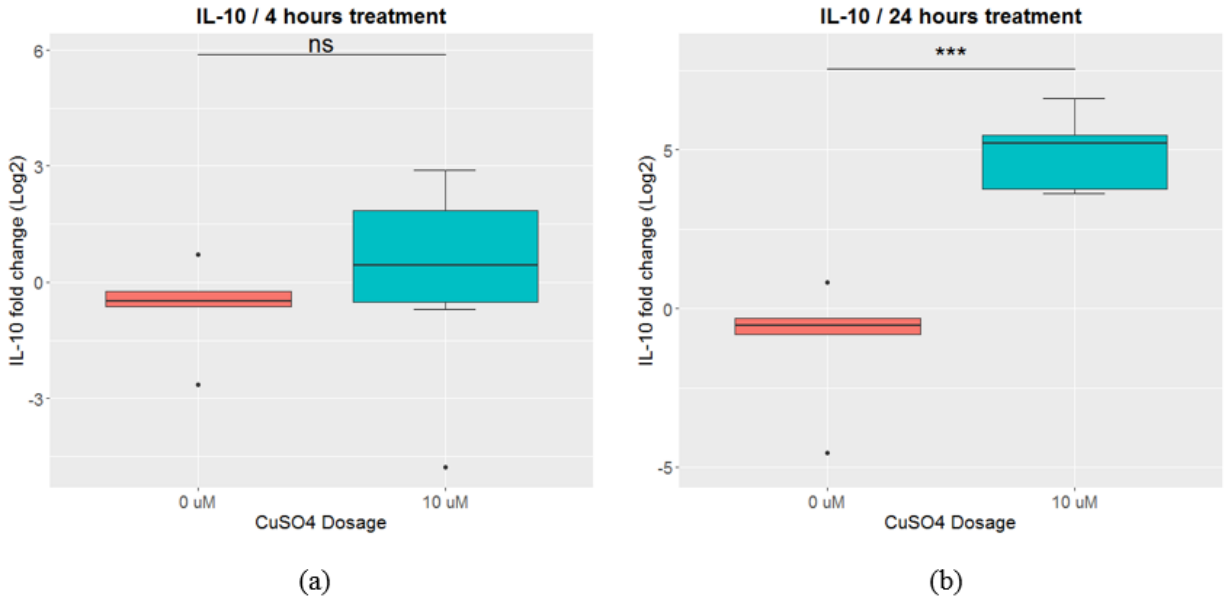

Figure 3.1.9: Log2 fold change values in the expression levels of the anti-inflammatory cytokine IL-10 on CuSO4 treatment for 4 hours (a) and 24 hours (b). There was a significant effect of $CuSO_4$ dose on log2 fold change values of IL-10 only on 24 hours treatment condition. Error bars represent the 95% confidence interval. The top and the bottom of the box represent the 25th and 75th percentiles. The line inside the box is the 50th percentile. Outliers are represented by closed circles. (***: $p \leq 0.001$, **: $p \leq 0.01$, *: $p \leq 0.05$, #: $p \leq 0.1$, ns: $p > 0.1$)

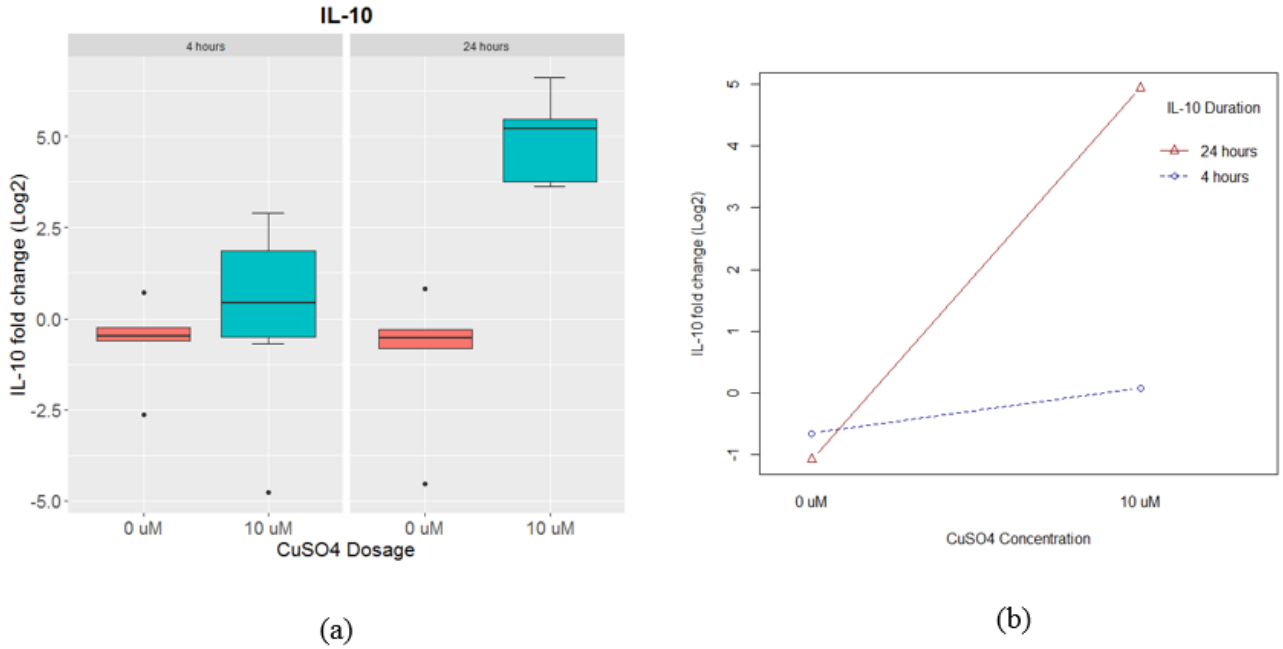

Figure 3.1.10: Log2 fold change values in the expression levels of the anti-inflammatory cytokine IL-10 (a). IL-10 log2 fold change levels increase significantly only on the 24 hours treated condition upon the exposure of $CuSO_4$ (b). Error bars represent the 95% confidence interval. The top and the bottom of the box represent the 25th and 75th percentiles. The line inside the box is the 50th percentile. Outliers are represented by closed circles. (***: $p \leq 0.001$, **: $p \leq 0.01$, *: $p \leq 0.05$, #: $p \leq 0.1$, ns: $p > 0.1$)

Another anti-inflammatory cytokine TGF-β, there was not a significant effect of $CuSO_4$ dosage ($F(1,17) = 0.00$, $p = 0.998$), duration of the treatment ($F(1,17) = 0.858$, $p = 0.367$) and the medium condition ($F(1,17) = 2.104$, $p = 0.165$) on the log2 fold change values of TGF-β (Figure 3.1.11). There was not an interaction effect between dose and duration and dose and medium.

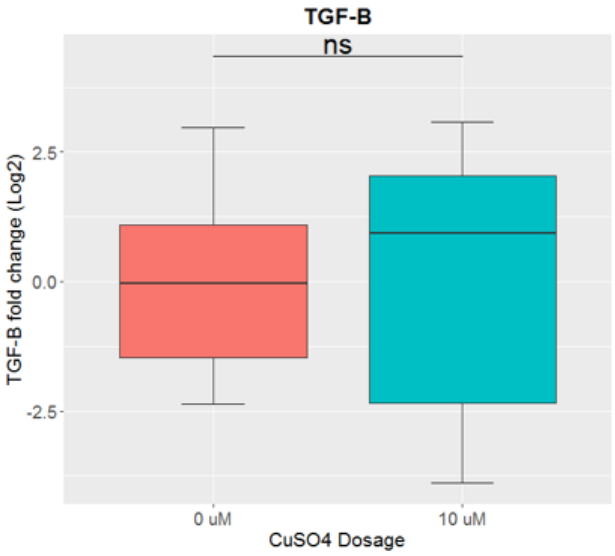

Figure 3.1.11: Log2 fold change values in the expression levels of the anti-inflammatory cytokine, TGF-β. There was not a significant effect of $CuSO_4$ dose on log2 fold change values of TGF-β. Error bars represent the 95% confidence interval. The top and the bottom of the box represent the 25th and 75th percentiles. The line inside the box is the 50th percentile. Outliers are represented by closed circles. (***: p≤ 0.001, **: p≤ 0.01, *: p≤ 0.05, #: p≤ 0.1, ns: p> 0.1)

3.2 Protein Expression Experiments with Very Old (38 months) Adult Zebrafish

The second aim of this thesis is to assess the effect of the acute inflammatory response which was caused by copper on mTOR signaling and the synaptic integrity response in the course of neuroinflammation in very old (38 months) adult male and female zebrafish. Also, the inhibitory capacity of rapamycin in terms of mTOR signaling and neuroinflammation has been investigated.

3.2.1 Changes in mTOR Pathway Markers (*)

Our results showed that there was not a statistically significant difference between mTOR protein expression ($F(3,12) = 0.563$, $p = 0.65$) (Figure 3.2.1(a)), p-mTOR protein expression ($F(3,12) =$

0.02, p = 0.996) (Figure 3.2.1(b)) upon $CuSO_4$ and RAPA treatment. Similarly, the ratio of p-mTOR to mTOR was not significant (F(3,12) = 0.182, p = 0.907) (Figure 3.2.1(c)). However, there was a significant difference between protein expression level of p-S6, specifically rapamycin treatment after CuSO4 exposure significantly down-regulated p-S6 levels (F(3,12) = 7.274, p = 0.004) (Figure 3.2.1(d)).

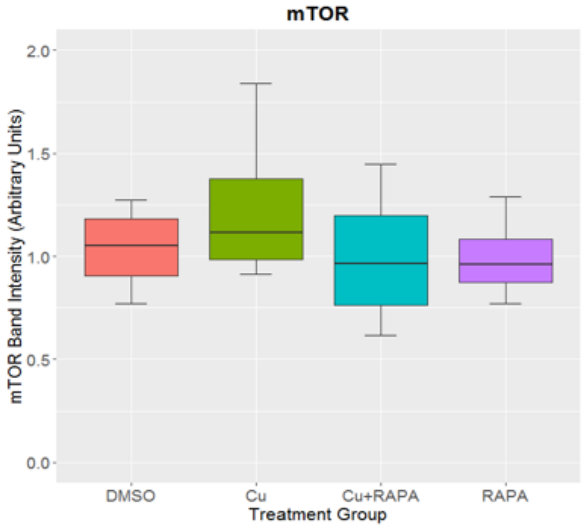

(a)

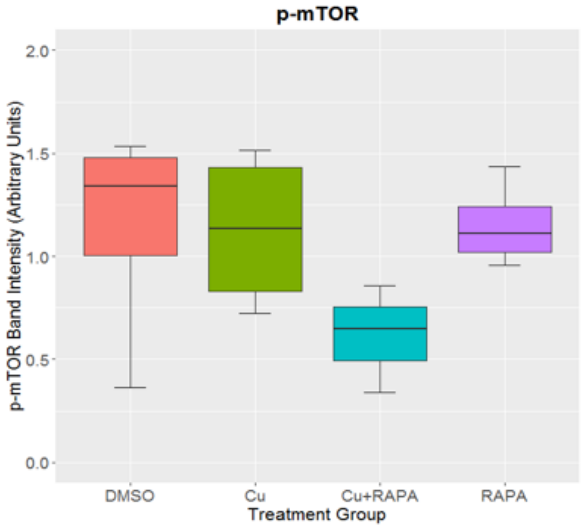

(b)

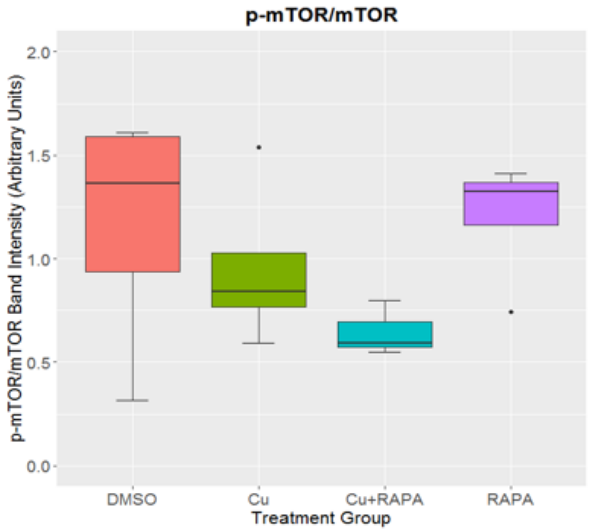

(c)

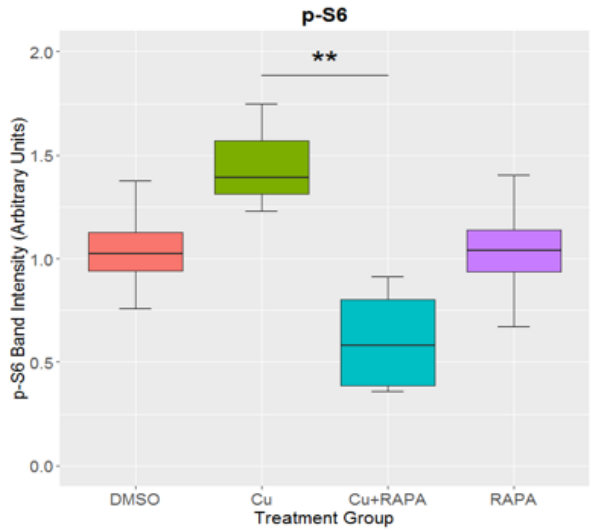

(d)

Figure 3.2.1 Changes in the expression levels of mTOR, p-mTOR, p-mTOR/mTOR and p-S6 proteins in response to $CuSO_4$ and RAPA treatment in very old (38 months old) animals. mTOR, p-mTOR and p-mTOR / mTOR levels (a), (b), (c) are stable among the treatment groups whereas RAPA treatment after $CuSO_4$ exposure significantly down-regulates p-S6 levels (d). The double-normalized mean band intensity values are given in arbitrary units. Error bars represent the 95% confidence interval. The top and the bottom of the box represent the 25th and 75th percentiles. The line inside the box is the 50th percentile. Outliers are represented by closed circles. DMSO: DMSO treated control group, Cu: $CuSO_4$ treated group, Cu+RAPA: $CuSO_4$ and rapamycin treated group, RAPA: rapamycin treated group. (***: $p \leq 0.001$, **: $p \leq 0.01$, *: $p \leq 0.05$)

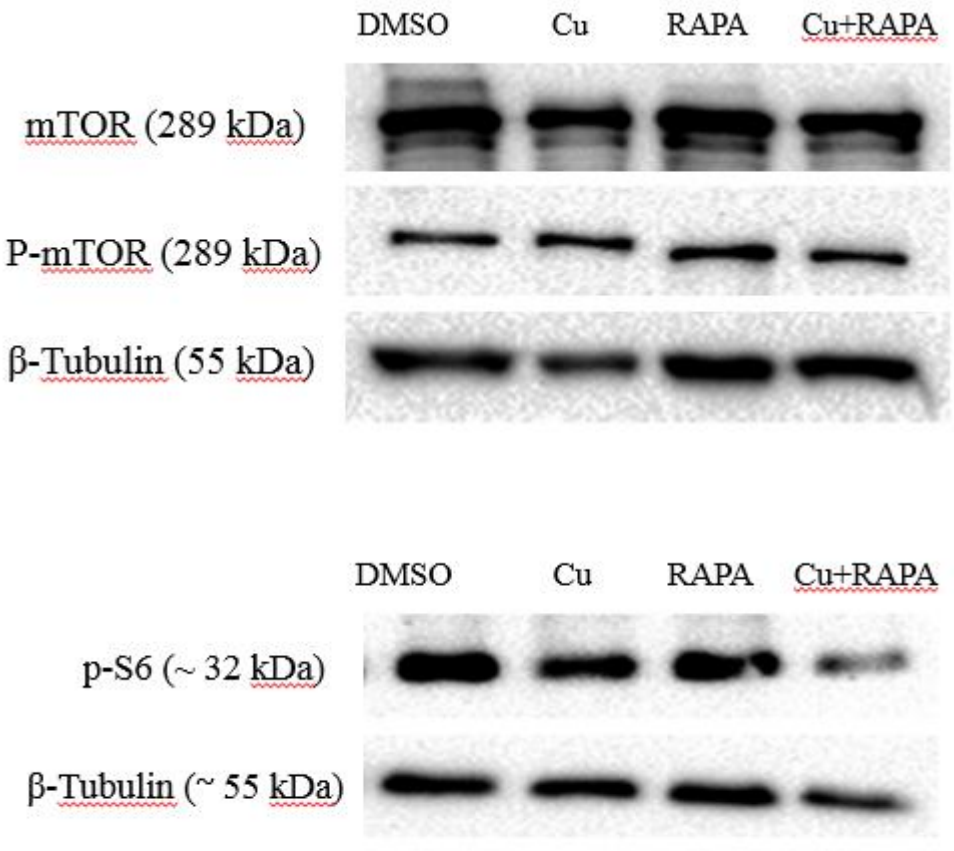

Figure 3.2.2 Representative western blots for mTOR, p-mTOR, p-S6 and β-tubulin. The bands at approximately 289 kDa correspond to mTOR and its phosphorylated version. The bands at 55 kDa correspond to β-tubulin. DMSO: DMSO treated control group, Cu: $CuSO_4$ treated group, Cu+RAPA: $CuSO_4$ and rapamycin treated group, RAPA: rapamycin treated group

3.2.2 Changes in Synaptic Integrity / Neuronal Markers

Our results showed that there was not a statistically significant difference between gephyrin protein expression ($F(3,10) = 0.793$, $p = 0.525$) (Figure 3.2.3(a)), PSD-95 protein expression ($F(3,11) = 1.095$, $p = 0.392$) (Figure 3.2.3(b)) and the ratio of PSD-95 to gephyrin was not significant ($F(3,11) = 0.207$, $p = 0.889$) (Figure 3.2.3(c)).

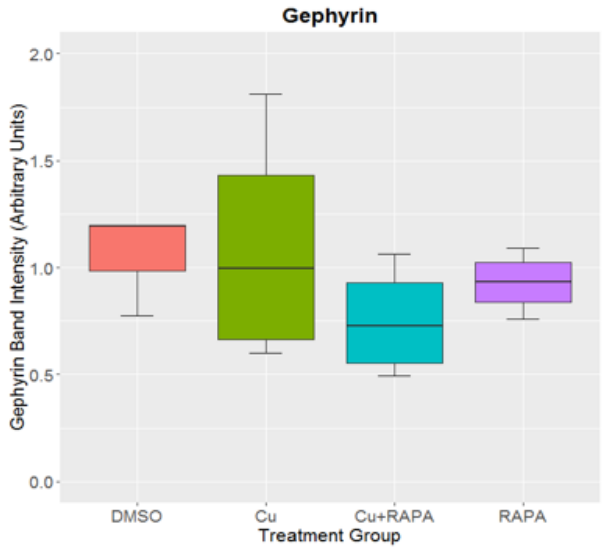

(a)

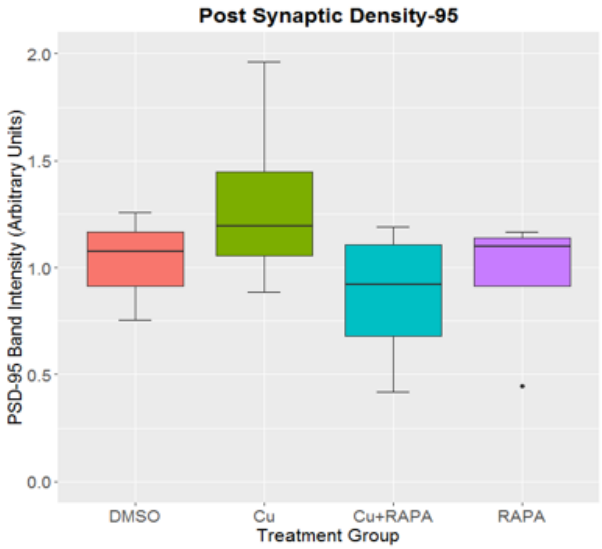

(b)

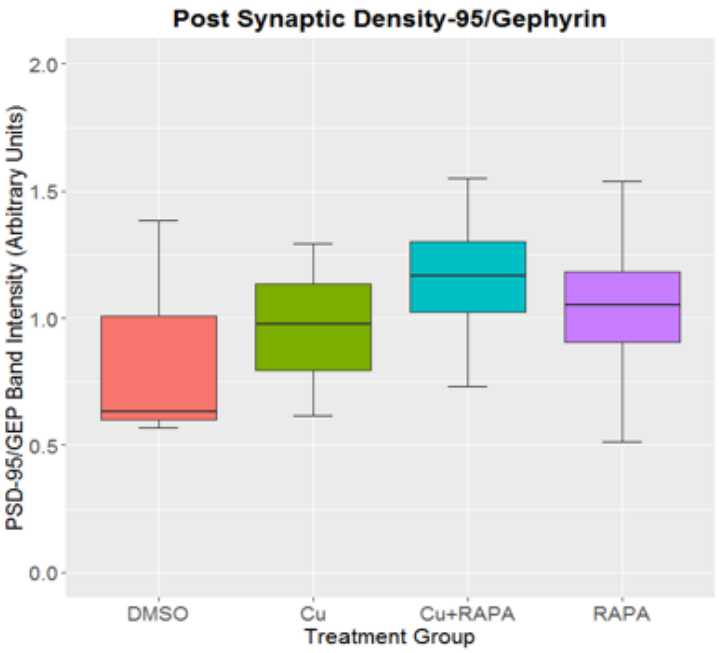

(c)

Figure 3.2.3 Changes in the expression levels of gephyrin, PSD-95 and PSD-95/gephyrin proteins in response to $CuSO_4$ and RAPA treatment in very old (38 months old) animals. PSD-95, gephyrin and PSD-95 / gephyrin levels (a), (b), (c) are stable among the treatment groups. The double-normalized mean band intensity values are given in arbitrary units. Error bars represent the 95% confidence interval. The top and the bottom of the box represent the 25th and 75th percentiles. The line inside the box is the 50th percentile. Outliers are represented by closed circles. DMSO: DMSO treated control group, Cu: $CuSO_4$ treated group, Cu+RAPA: $CuSO_4$ and rapamycin treated group, RAPA: rapamycin treated group. (***: $p \leq 0.001$, **: $p \leq 0.01$, *: $p \leq 0.05$)

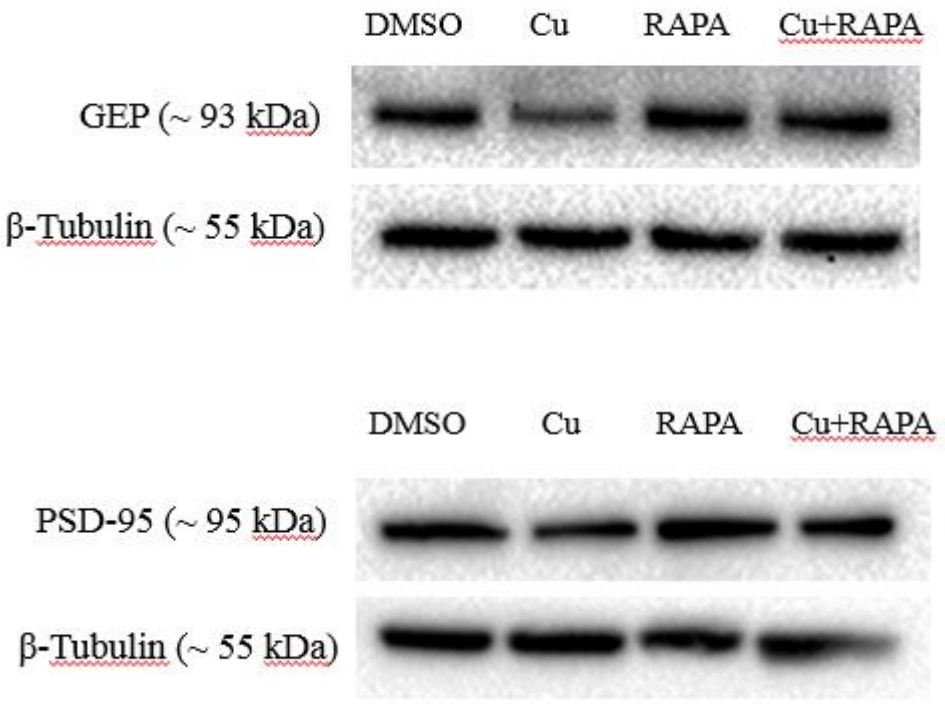

Figure 3.2.4 Representative western blots for gephyrin, PSD-95, and β-tubulin. The bands at approximately 93 kDa correspond to gephyrin. The bands at 95 kDa correspond to PSD-95. The bands at 55 kDa correspond to β-tubulin. DMSO: DMSO treated control group, Cu: $CuSO_4$ treated group, Cu+RAPA: $CuSO_4$ and rapamycin treated group, RAPA: rapamycin treated group

Also, SYN ($F(3,12) = 1.128$, $p = 0.377$) (Figure 3.2.5(a)), HuC ($F(3,11) = 0.401$, $p = 0.755$) (Figure 3.2.5(b)) and GFAP ($F(3,10) = 2.813$, $p = 0.094$) (Figure 3.2.5(c)) levels are mostly stable upon $CuSO_4$ and RAPA treatment.

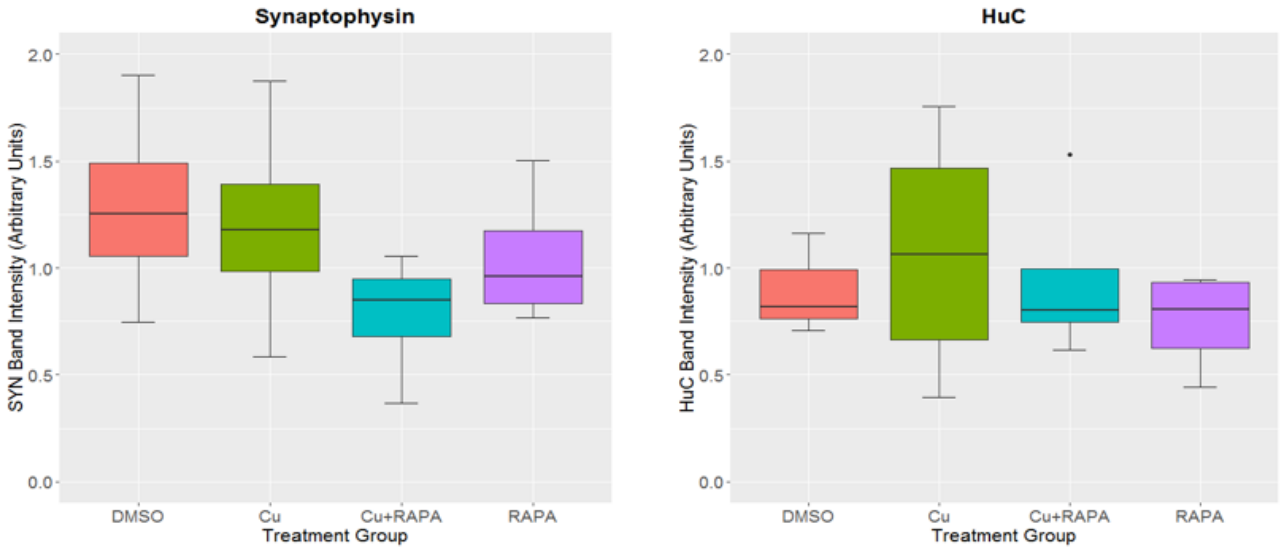

(a)

(b)

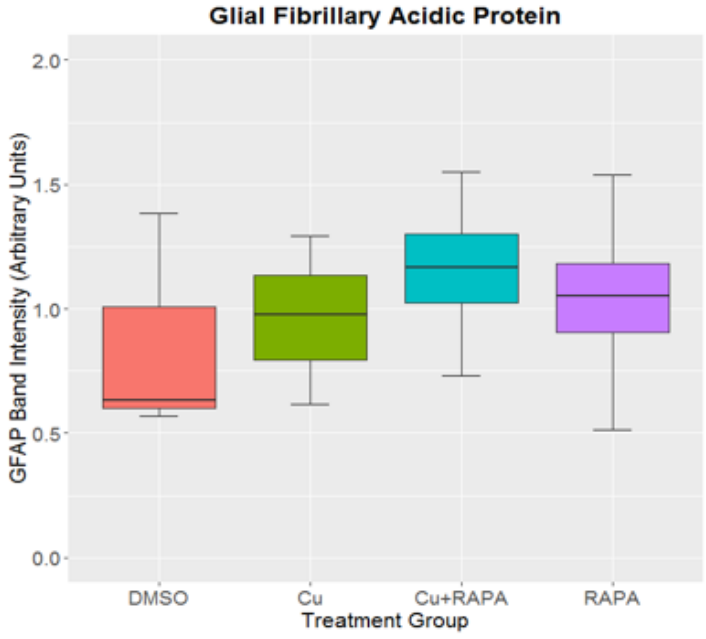

(c)

Figure 3.2.5 Changes in the expression levels of SYN, HuC and GFAP proteins in response to $CuSO_4$ and RAPA treatment in very old (38 months old) animals. SYN, HuC and GFAP

levels (a), (b), (c) are stable among the treatment groups. The double-normalized mean band intensity values are given in arbitrary units. Error bars represent the 95% confidence interval. The top and the bottom of the box represent the 25th and 75th percentiles. The line inside the box is the 50th percentile. Outliers are represented by closed circles. DMSO: DMSO treated control group, Cu: $CuSO_4$ treated group, Cu+RAPA: $CuSO_4$ and rapamycin treated group, RAPA: rapamycin treated group. (***: $p \leq 0.001$, **: $p \leq 0.01$, *: $p \leq 0.05$)

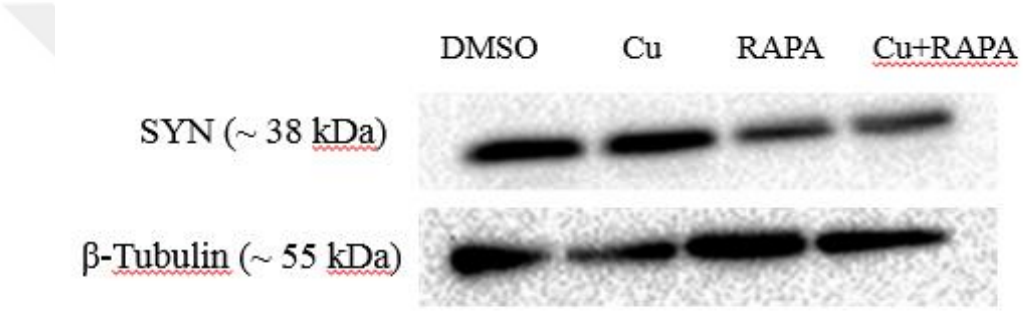

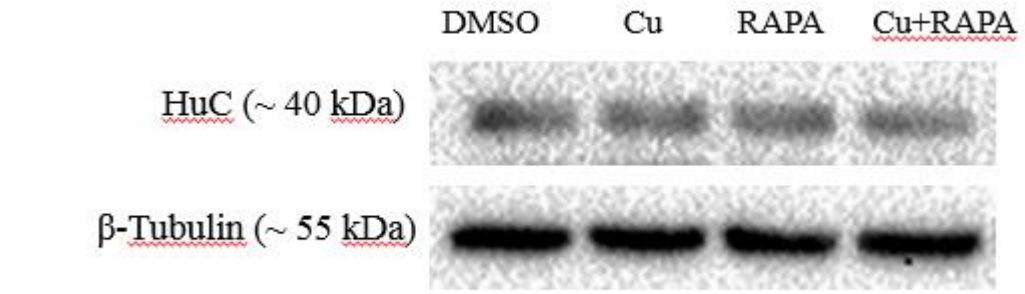

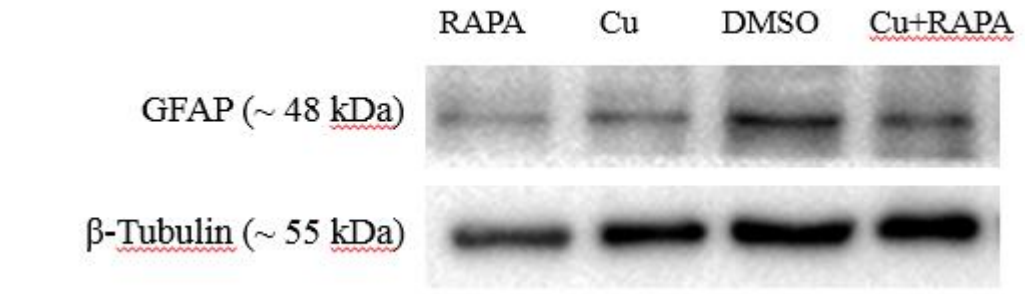

Figure 3.2.6 Representative western blots for SYN, HuC, GFAP and β-tubulin. The bands at approximately 38 kDa correspond to SYN, 40 kDa correspond to HuC and 48 kDa correspond to GFAP. The bands at 55 kDa correspond to β-tubulin. DMSO: DMSO treated control group, Cu: $CuSO_4$ treated group, Cu+RAPA: $CuSO_4$ and rapamycin treated group, RAPA: rapamycin treated group

3.2.3 Changes in Inflammatory Markers (*)

Our results showed that there was not a significant difference upon $CuSO_4$ and rapapmycin treatment for IL-6 protein expression ($H(3) = 2.404$, $p = 0.492$) (Figure 3.2.7(a)) and TNF-α protein expression ($F(3,11) = 2.027$, $p = 0.168$) (Figure 3.2.7(b)).

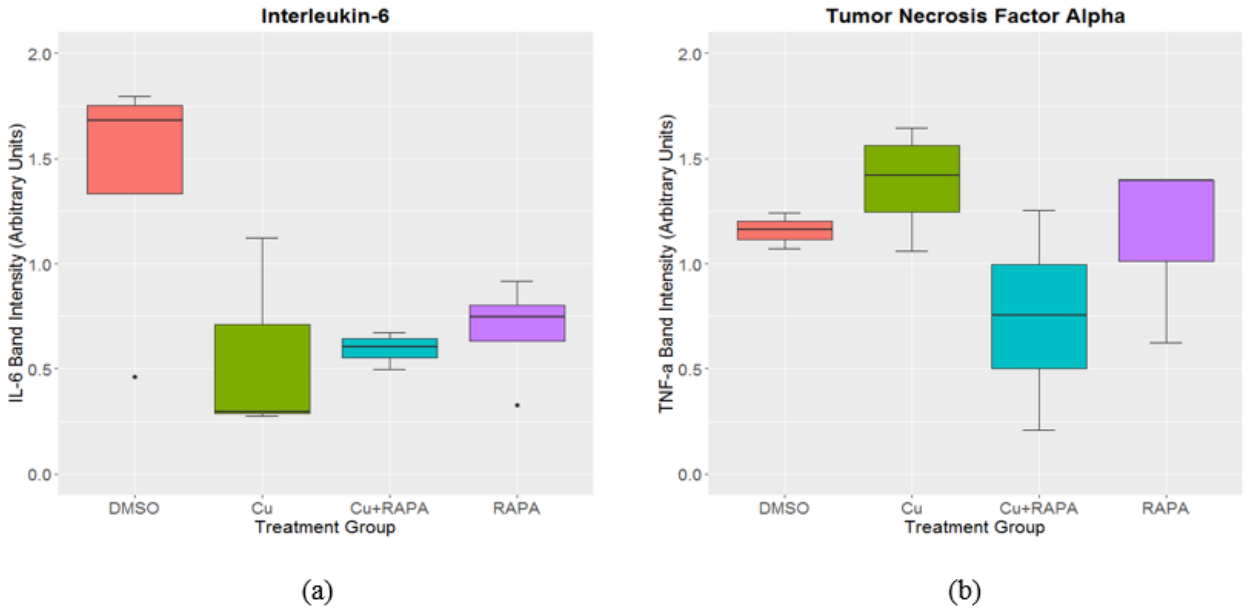

Figure 3.2.7 Changes in the expression levels of IL-6 and TNF-α in response to $CuSO_4$ and RAPA treatment in very old (38 months old) animals. SYN, HuC and GFAP levels (a), (b) are stable among the treatment groups. The double-normalized mean band intensity values are given in arbitrary units. Error bars represent the 95% confidence interval. The top and the bottom of the

box represent the 25th and 75th percentiles. The line inside the box is the 50th percentile. Outliers are represented by closed circles. DMSO: DMSO treated control group, Cu: $CuSO_4$ treated group, Cu+RAPA: $CuSO_4$ and rapamycin treated group, RAPA: rapamycin treated group. (***: $p \leq 0.001$, **: $p \leq 0.01$, *: $p \leq 0.05$)

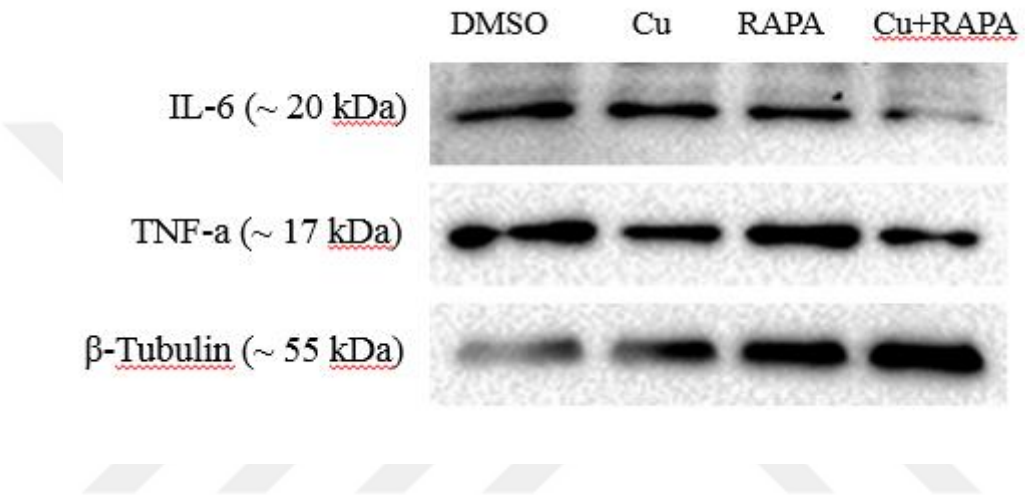

Figure 3.2.8 Representative western blots for IL-6, TNF-α and β-tubulin. The bands at approximately 20 kDa correspond to IL-6, 17 kDa correspond to TNF-α. The bands at 55 kDa correspond to β-tubulin. DMSO: DMSO treated control group, Cu: $CuSO_4$ treated group, Cu+RAPA: $CuSO_4$ and rapamycin treated group, RAPA: rapamycin treated group

3.3 Genotyping Experiments with Tuberous Sclerosis Complex 2 ($tsc2^{+/-}$) Adult Zebrafish

In order to understand wild-type (WT) and heterozygote adult fishes, both PCR and restriction enzyme digested (RE) products are loaded into the agarose gel in each experiment. PCR products are expected to give bands at 151 base pair (bp). The HpyCH4IV (NEB) restriction enzyme recognizes the DNA sequence for the WT allele so it provides efficient cut for WT animals. Since heterozygote animals have two alleles, one of them is WT allele and the other one is the mutant allele, heterozygote animals can not produce efficient cuts upon RE treatment. Therefore, wild-

type restriction enzyme (WT-RE) products give cut results at 120 bp and 30 bp while heterozygote animals give inefficient cut results at 151 bp, 120 bp and 30 bp.

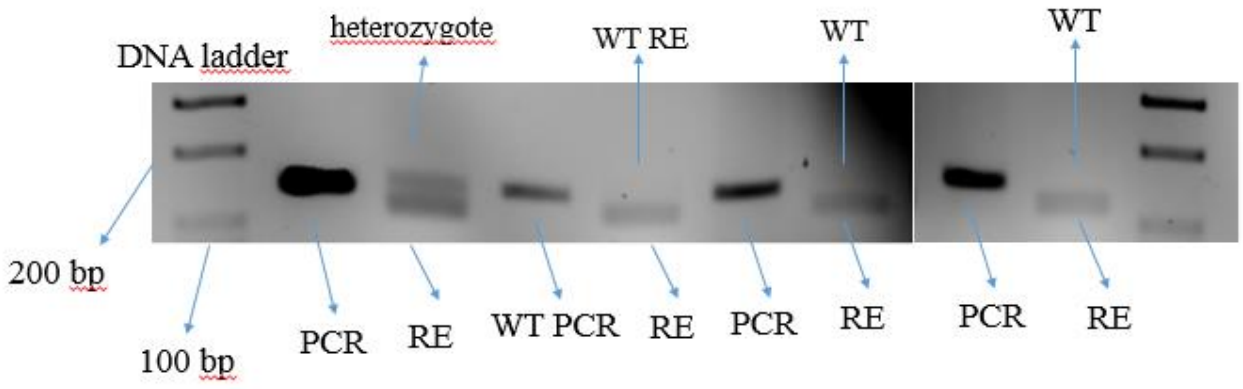

Figure 3.3.1 The representative agarose gel image of tsc2$^{+/-}$ adult zebrafish genotyping. All PCR products give bands at 151 bp. WT-RE products give efficient cut results at 120 bp and heterozygote-RE products give cut results at 151 bp and 120 bp.

3.4 Gene Expression Experiments with tsc2$^{+/-}$ Old Adults and Their WT Siblings with Rapamycin Treatment

Old tsc2$^{+/-}$ adults are treated with rapamycin for 3 hours together with their wild type siblings. Our results demonstrated that there was not a significant difference between rapamycin treated mutant (heterozygote) and wild-type old adult fishes on fold change values of two pro-inflammatory cytokines, COX-2 ($t(4) = 0.157$, $p = 0.882$) (Figure 3.4.1(a)) and TNF-α ($t(4) = -0.44$, $p = 0.682$) (Figure 3.4.1(b)).

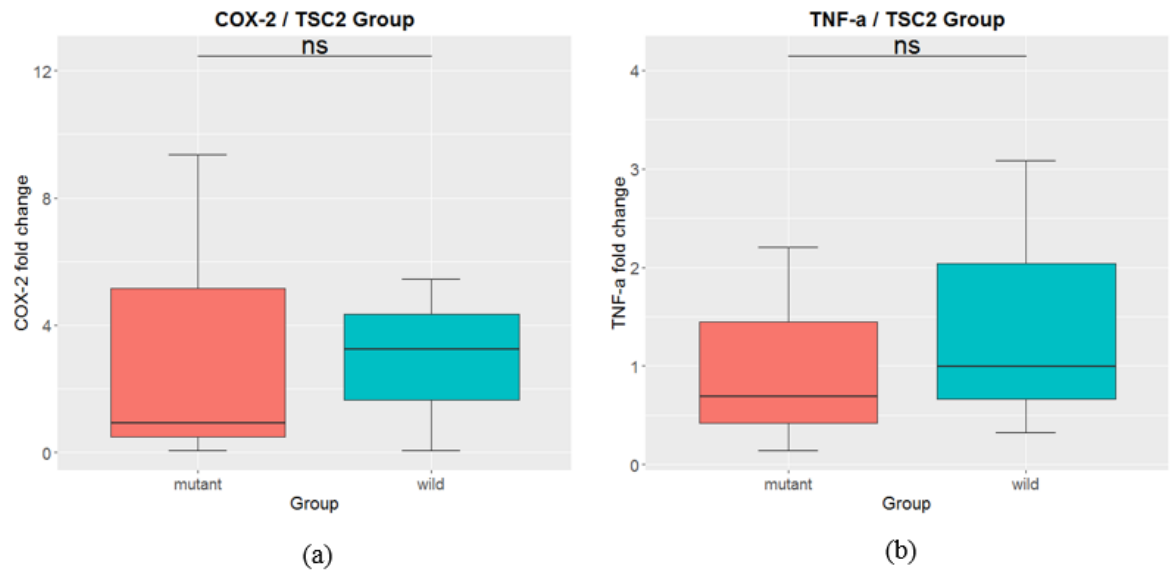

Figure 3.4.1: Log2 fold change values in the expression levels of the two pro-inflammatory cytokines, COX-2 and TNF-α. There was not a significant effect of animal type on fold change values. Error bars represent the 95% confidence interval. The top and the bottom of the box represent the 25th and 75th percentiles. The line inside the box is the 50th percentile. Outliers are represented by closed circles. (***: $p \leq 0.001$, **: $p \leq 0.01$, *: $p \leq 0.05$, #: $p \leq 0.1$, ns: $p > 0.1$)

Also, there was not a significant difference between rapamycin treated mutant (heterozygote) and wild-type old adult fishes on fold change values of autophagic marker lc3b ($t(4) = 0.425$, $p = 0.693$) (Figure 3.4.2).

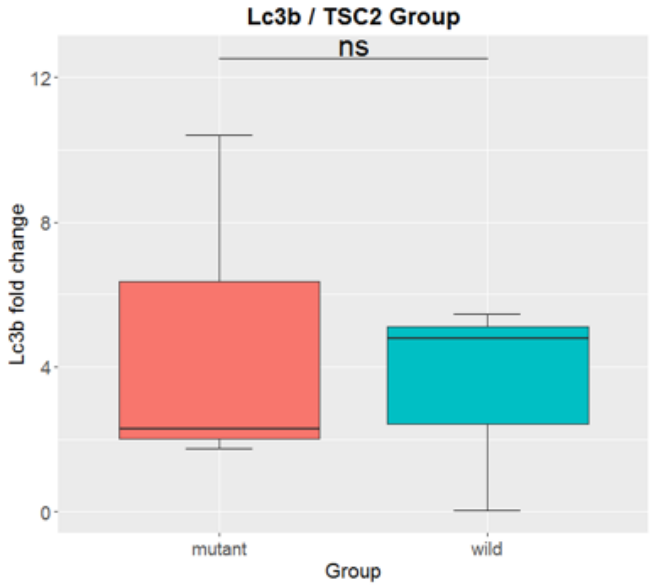

Figure 3.4.2: Fold change values in the expression levels of the lc3b. There was not a significant effect of animal type on fold change values. Error bars represent the 95% confidence interval. The top and the bottom of the box represent the 25th and 75th percentiles. The line inside the box is the 50th percentile. Outliers are represented by closed circles. (***: $p \leq 0.001$, **: $p \leq 0.01$, *: $p \leq 0.05$, #: $p \leq 0.1$, ns: $p > 0.1$)

3.5 Gene Expression Experiments with ztor$^{+/-}$ Old Adults and Their WT Siblings with $CuSO_4$ Treatment

Old ztor$^{+/-}$ adults are treated with $CuSO_4$ for 1 hour together with their wild type siblings. The results showed that there was not a significant difference between $CuSO_4$ treated mutant (heterozygote) and wild-type old adult fishes on fold change values of two pro-inflammatory cytokines, COX-2 ($t(4) = -1.27$, $p = 0.273$) (Figure 3.5.1(a)) and TNF-α ($t(4) = -0.974$, $p = 0.385$) (Figure 3.5.1(b)).

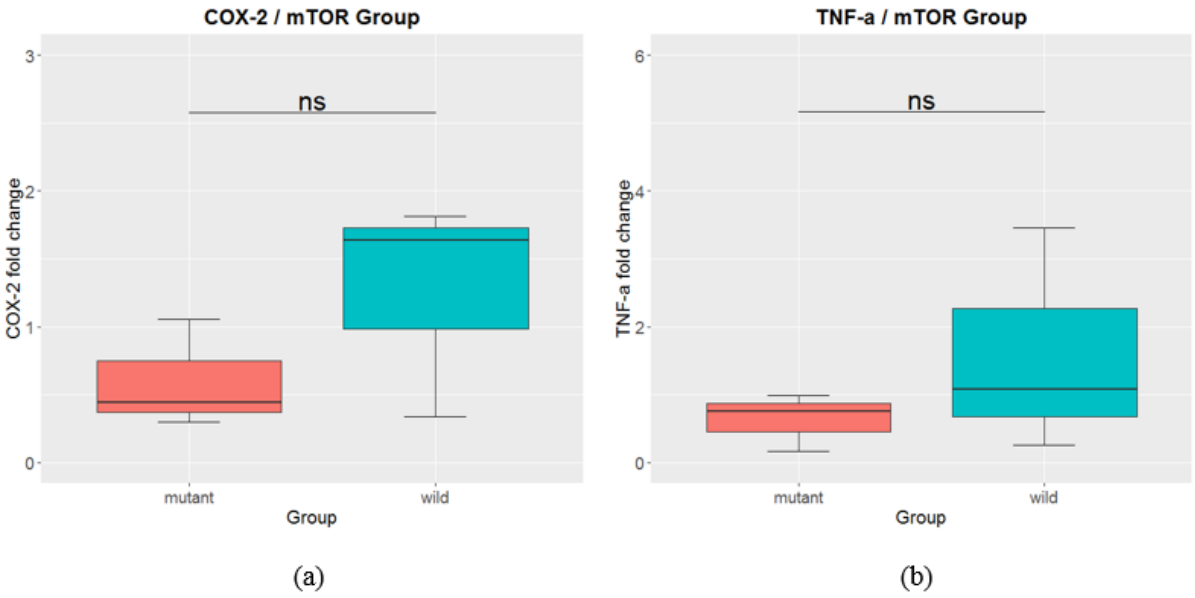

Figure 3.5.1: Fold change values in the expression levels of the two pro-inflammatory cytokines, COX-2 and TNF-α. There was not a significant effect of animal type on fold change values. Error bars represent the 95% confidence interval. The top and the bottom of the box represent the 25th and 75th percentiles. The line inside the box is the 50th percentile. Outliers are represented by closed circles. (***: $p \leq 0.001$, **: $p \leq 0.01$, *: $p \leq 0.05$, #: $p \leq 0.1$, ns: $p > 0.1$)

There was a significant difference between $CuSO_4$ treated mutant (heterozygote) ztor and wild-type old adult fishes on fold change values of autophagic marker lc3b ($t(4) = -3.141$, $p = 0.03$) (Figure 3.5.2).

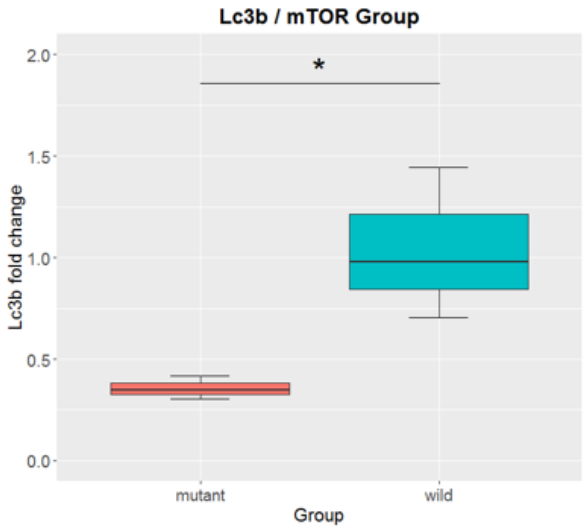

Figure 3.5.2: Fold change values in the expression levels of the lc3b. There was a significant effect of animal type on fold change values. Wild type animals have higher lc3b gene expression level than mTOR heterozygote animals. Error bars represent the 95% confidence interval. The top and the bottom of the box represent the 25th and 75th percentiles. The line inside the box is the 50th percentile. Outliers are represented by closed circles. (***: $p \leq 0.001$, **: $p \leq 0.01$, *: $p \leq 0.05$, #: $p \leq 0.1$, ns: $p > 0.1$)

CHAPTER 4

Discussion

The free radical/oxidative stress theory of aging indicates mechanisms of aging throughout the regular aging process. Increased mTOR signaling activation, dysfunctional autophagy, upregulated NLRP3/NALP3 inflammasome and elevated NF-κB pathway function constitute the "oxy-inflammaging" status of the organism. This study investigated some aspects of the "oxy-inflammaging" process on neuroinflammatory and mTOR pathway response levels on both wild-type and mutant zebrafish by utilizing $CuSO_4$ as an inflammation-stimulating agent.

4.1 The Response of Embryos to Inflammation

The embryo part of the research was conducted to investigate the inflammatory capacity of $CuSO_4$ in zebrafish. $CuSO_4$ has strong implications in terms of ROS production within the organism due to the Fenton reaction [124]. The first part of the embryo study involves long-term (4 days) CuSO4 treatment with 3 dpf embryos with different concentrations. Two pro-inflammatory cytokines COX-2 and IL-8 gene expression levels did not increase whereas the anti-inflammatory cytokine IL-10 level upregulated in response to $CuSO_4$. In short-term (4 hours and 24 hours) $CuSO_4$ treatment, COX-2 and, NF-κB gene expression levels also increased together with upregulating IL-10 level only during the 24 hours treated condition. This shows that the anti-inflammatory response may have started later than the pro-inflammatory response and late increased levels of IL-10 may act as a suppressor for pro-inflammatory cytokines in the long-term treated condition.

Another pro-inflammatory cytokine IL-8 gene expression level increased earlier. The gene expression levels of IL-8 were higher in the 4 hours treated condition compared to the 24 hours

treated condition. This would be due to the relation between IL-8 and the recruitment of neutrophils. Neutrophils are one of the hallmarks of acute inflammation, they initiate early immune responses in the case of inflammation. IL-8 cytokine is responsible for the recruitment and the activation of neutrophils [142]. Therefore, IL-8 may act as an activator for neutrophils through early increasing levels.

Another pro-inflammatory cytokine IL-1β level upregulated only in the without methylene blue condition for embryos. This would explain the anti-inflammatory feature of methylene blue [137]. Interestingly, IL-1β involves in the activation of many cytokines such as IL-6 and TNF-α through various intracellular signaling events; mitogen-activated protein kinases (MAPKs) / activator protein -1 (AP-1) and IKK / IKβ / NF-κB [143]. Also, in one study, reversine which has antitumor effects has suppressed IL-1β and caused JNK / AP-1 activation and ROS production [144]. IL-1β can act as a master regulator for the initiation of inflammatory responses through various signaling pathways. More research is needed to understand the relation between IL-1β and these inflammatory kinases.

Another pro-inflammatory cytokine, TNF-α levels were stable in response to short-term CuSO4 treatment. TNF-α expression may be dependent on the activation of other cytokines especially anti-inflammatory cytokines for example IL-10. In one study, IL-10 suppressed TNF-α and IL-1β cytokines at the protein level on the activated microglial cells with amyloid-beta plaques [145]. The presence of astrocytes can also affect the expression of related cytokines and so TNF-α levels [146].

4.2 The Response of Very Old Adults to Inflammation

The adult study aimed to investigate the effect of the acute inflammatory response caused by copper on mTOR signaling, the modulation of synaptic integrity, and the inhibitory capacity of rapamycin in the course of neuroinflammation in very old adult male and female zebrafish. In the results, the p-S6 protein level was significantly downregulated on rapamycin exposure after CuSO4 treatment. mTOR signaling pathway has many downstream targets and p-S6 is one of those. Therefore, rapamycin can be regarded as an effective substance to partially inhibit mTOR activity. The direct suppression of mTOR activity can be detected through the suppression of mTOR autophosphorylation which is the decrease of p-mTOR protein expression. However, p-mTOR levels are generally stable across the treatment groups. In another study, the age-dependent effects of rapamycin treatment were observed as well, mTOR activity inhibition was only seen in young adult zebrafish in response to the rapamycin treatment [26]. mTOR has two complexes: mTORC1 and mTORC2, although rapamycin is more effective in mTORCI, it also downregulates mTORC2 activity [147]. On the other hand, mTORC2 activity increases robustly in the course of aging, so in our study mTORC2 levels may be upregulated further to compensate rapamycin-induced mTORCI inhibition in very old animals [148]. Therefore, the inhibitory effect of rapamycin may not be present in these animals.

In terms of synaptic integrity and other neuronal markers, there was not a statistically significant difference across treatment groups. PSD-95 and GEP are important post-synaptic scaffolding proteins for the maintenance of the excitatory/inhibitory balance of the brain. At an advanced age, this balance may be disrupted toward a more inhibitory state. Therefore, the brain may try to increase PSD-95 protein levels to reach a more excitable state in to compensate for this imbalance. However, $CuSO_4$ and rapamycin treatment in old age may damage this compensatory mechanism through more stable scaffolding protein levels.

Although GFAP is mostly known to be a marker of reactive astrocytes, it is also important for neural stem cells and progenitor cells [149]. Although not significant, GFAP levels were downregulated after $CuSO_4$ exposure. Neurogenesis is known to be heavily dysregulated in the advanced age [150] and the neuroinflammatory status of the brain contributes to this through increased chemokine and cytokine production [151]. Exposure to the inflammatory stimulating agent at an advanced age may damage the neurogenesis potential of the brain and short-term rapamycin treatment is not effective to rescue this damage. Similarly, HuC is an indicator of immature neurons and has implications for neural determination. In the developmental trajectory of the brain, GFAP is expressed earlier than the HuC since the former regulates neuronal precursor cells whereas the latter regulates immature neurons. Our results indicated that HuC levels were also mostly stable. Longer $CuSO_4$ and/or rapamycin treatments may slightly change HuC levels as well.

In terms of inflammatory markers, we did not observe any significant difference across treatment groups for both IL-6 and TNF-α. This could be explained by the ceiling effect in very old animals. These adult zebrafish which are used in the experiments are 38 months old, $CuSO_4$ treatment may not change their inflammatory status because they could have already reached an inflammatory status. Although not significant, rapamycin treatment after $CuSO_4$ treatment slightly rescues TNF-α inflammatory response. This may indicate that rapamycin may act more effectively when there is a robust inflammation within the brain.

Also, the effectiveness of $CuSO_4$ within the tank water would be an issue. These animals were treated with 25 µM $CuSO_4$ in tank water for 1 hour. At the beginning of the treatment, they were not lethargic and maintained usual swimming patterns. However, they started to swim at the bottom of the tank and their movements were slower towards the end of the treatment. Therefore, the

duration and dosage of the copper could be regarded as efficient but direct cerebral ventricular injection (CVMI) to the zebrafish brain would be another option.

4.3 The Response of Very Old $tsc2^{+/-}$ & $ztor^{+/-}$ Adults to Inflammation

The third objective of this thesis was to characterize TSC2 heterozygote mutants ($tsc2^{+/-}$) genotypically. TSC2 animals were imported from abroad and they have been bred both incross and outcross methods in the Bilkent University Zebrafish Facility. During breedings, homozygote embryos died at 11 dpf at most due to lack of swim bladders. Since we are mainly interested in outcomes related to the mTOR signaling in the course of aging, it was important for us to optimize the characterization protocol for $tsc2^{+/-}$ adults.

TSC2 mutants ($tsc2^{+/-}$) were originally developed by Kim et al. (2011) through the Targeting Induced Local Lesions in Genomes (TILLING) technique [140]. This technique is quite beneficial to induce point mutations by using denaturing and reannealing pre-amplified PCR products [152]. This non-sense point mutation induces a C3087 to A transversion within the genome and causes the loss of function on the gene of interest which encodes the tuberin protein. Also, this mutation eradicates the cutting site by the HpyCH4IV restriction enzyme which works effectively on the WT allele. Therefore, we could see efficient enzyme cuts for WT animals and non-efficient cuts for the mutant animals in the results.

TSC2 mutation induces a non-sense mutation which causes the loss of function for the TSC2 gene which encodes tuberin. This protein forms complexes with the hamartin protein which is encoded by the TSC1 gene and this complex suppresses the G protein Rheb. Rheb is known as an enhancer for the target of rapamycin (TOR) kinase. TOR kinase is evolutionarily conserved in humans, mice,

and Drosophila [140]. Therefore, the TSC1-TSC2 complex works as a negative regulator of the mTOR signaling.

As mentioned previously, the TOR pathway has important modulatory roles in cell growth, proliferation, and the development of some immune responses. This pathway involves two protein complexes TORC1 and mTORC2. The former one contains Raptor protein and rapamycin is an effective inhibitor for it. However, mTORC2 involves Rictor protein and rapamycin is not a useful suppressor [140]. In the light of this information, when the TSC1-TSC2 complex does not work adequately to suppress the mTOR pathway in a heterozygote mutant model, rapamycin would be useful to suppress mTORC1 signaling.

Additionally, ztor$^{+/-}$ animals have been developed by Ding et al. (2011) and their maintenance and breeding are being conducted at Bilkent University Zebrafish Facility. These animals were generated through an insertional mutagenesis screen to cause TOR haploinsufficiency. Therefore, TOR signaling is inhibited and an effective inflammatory stimulator for example $CuSO_4$ could be useful to activate mTORC1 signaling in these mutants in the course of aging [141].

The final objective of this thesis was to investigate whether rapamycin treatment would be effective in rescuing the over-active mTOR pathway in tsc2$^{+/-}$ animals and whether $CuSO_4$ treatment would be useful to reverse the less-active mTOR pathway in ztor$^{+/-}$ animals. In other words, we tried to investigate the possibility of chemical interventions to reverse inflammatory responses in animals that have a genetic susceptibility. On the results for tsc2$^{+/-}$ old animals, we did not see a statistically significant difference between WT and heterozygote animals that were treated with rapamycin on the gene expression levels of COX-2, TNF-α and Lc3b. For tsc2$^{+/-}$ old animals, rapamycin would suppress the over-active mTOR signaling as expected so both WT and heterozygote animals could show similar neuroinflammatory and autophagic responses. However, non-treated WT and tsc2$^{+/-}$

animals from the same cohort should be treated for a better comparison. On the results for ztor+/- old animals, again we did not see a significant difference between WT and heterozygote animals that were treated with $CuSO_4$ on the gene expression levels of COX-2 and TNF-α. On the other hand, the lc3b gene expression level was significantly higher in the copper-treated WT animals. Lc3b is among the prominent markers of autophagy and the suppression of the mTOR pathway leads to the increased autophagy and Lc3b expression [153], [154]. As a response to short-term copper treatment, WT animals could have needed more effective coping mechanisms for this robust inflammation so they could have increased the autophagy response. However, old $ztor^{+/-}$ animals could have already reached an autophagy potential due to less-active mTOR signaling so $CuSO_4$ treatment would not have been an effective autophagic signal for them. Aging could also be a modulatory factor in these responses. mTOR signaling has been suppressed efficiantly in young animals rather than the old animals in the previous research [26], so we should further check young and non-treated animals as well.

4.4 Changes in Cognitive Functioning In the Course of Aging

The importance of this study can also be evaluated in terms of the changes in cognitive functioning during aging. The neuroinflammatory status of the brain may lead to cognitive dysfunctionalities, especially at an advanced age. Many cognitive and executive functions including different types of learning, attention, memory comprehension, and higher-order executive tasks are appear to be affected by aging [31]. Memory is one of the cognitive functions that gain attention in aging-related cognitive functioning studies. Memory is a comprehensive construct and is generally divided into many subgroups such as short-term, long-term, episodic, and semantic memory. Different brain regions affect the execution of different memory procedures. Therefore, these cognitive functions may not react to aging in the same manner. In working memory, older adults generally exhibit a

lower performance compared to younger adults. Also, neuroimaging studies have shown that different regions in the prefrontal cortex(PFC) are recruited depending on age. However, the execution of working memory requires many components such as organization of the information, inhibition of the unrelated content, and control of the information flow. These factors also influence the working memory ability in aging[32].

In long-term memory, elderly people often believe that episodic memory which is related to the previously acquired memories in one's life is not affected by aging. This assumption can be partially true, especially for older memories. However, elderly people have difficulty in remembering the source of the memory compared to younger people [33] which again indicates an important distinction related to aging.

Memory, decision-making and other related executive control functions mainly rely on the PFC recruitment and neuroimaging studies have shown that there is a significant decline in the volume of PFC in older people[34]. PFC is the mainly responsible brain region behind these functions and can provide various outcomes depending on the age. These age-dependent alterations are not independent of each other, for both basic and higher-order cognitive functions. For example, in one study, aging-associated declines are observed in a motor learning task in mice and the confinement factor is related to explicit memory ability [35] which also decreases in the course of aging [32].

To understand the interaction between the neuroinflammation and cognitive functions in zebrafish, more research is needed by combining neuroimaging and behavioral studies. Conditioned place preference (CPP) and aversion paradigms would be useful behavior assessment tools and can provide important outcomes for the zebrafish brain.

CHAPTER 5

Conclusions and Future Prospects

In this study,we showed that copper sulfate is an efficient inflammatory reagent at both gene and protein expression levels. In embryos, the inflammatory status was quite straightforward with early increasing pro-inflammatory cytokines and later increasing anti-inflammatory cytokine. Also, the duration of the copper treatment affected the gene expression levels of cytokines. In adults, the age effect was robust in comparison to the embryos. Copper sulfate treatment did not cause a direct inflammatory response in very old animals possible due to the already elevated inflammatory status of the brain. Nevertheless, rapamycin treatment after copper exposure was successful in the suppression of p-S6 protein expression which is among the important downstream targets of mTOR signaling. This showed that copper can induce an over-active mTOR signaling pattern and rapamycin can reduce this response even in the elevated inflammation. In terms of synaptic integrity and other neuronal markers, we showed that copper sulfate also can inhibit neural progenitors and affect neurogenesis.

The genotypic characterization of $tsc2^{+/-}$ adults was achieved through the HpyCH4IV restriction enzyme for the adults. This mutant model would provide useful insights into the interaction between neuroinflammation and mTOR signaling through the over-active mTOR pathway. Similarly, $ztor^{+/-}$ adults would represent a deaccelerated aging model through less-active mTOR. We only observed significant result between WT and heterozygote animals on gene expression levels of Lc3b, and this would indicate that mTOR signaling has strong implications on autophagic response.

This study has some limitations and future research could eliminate them. First of all, the sample size for each treatment group in the adult study can be increased. There were some decreasing and increasing trends, especially in the protein expression levels of TNF-α and GFAP. These results could be significant by adding more animals. The usage of only very old animals is another limitation. The effect of rapamycin has been more evident in young rather than old animals. Also, the effectiveness of copper may not be enough to trigger an inflammatory response in very old animals since their brains may have already an inflammatory status. The inclusion of young and middle-aged animals would provide valuable insights in terms of neuroinflammatory progress. Although this study includes both male and female adult animals, sexually dimorphic responses have not been investigated. The development of neuroinflammation may occur differently between males and females so this kind of analysis should be conducted by adding more animals to the study. The inflammatory and autophagic responses could be detected within different brain regions through immunohistochemical methods such as the bromodeoxyuridine (BrdU) assay. The telencephalon region of the zebrafish brain is mainly responsible for the age-related neurobiological changes so this method would provide comprehensive outcomes. Also, changes in mRNA levels which are indicated by the gene expression do not always reflect the alterations within proteins. Post-translational modifications after mRNA synthesis change the levels of the protein expression. Therefore, qPCR results may not reflect the protein expression results. Related post-translational modifications and their effects onto the protein expression can be investigated as further study.

Consequently, this study showed that the modulation of neuroinflammatory responses occurs in an age-specific manner and genetic interventions via mutant models on the mTOR signaling pathway

would give comprehensive outcomes to understand the inflammatory profile of the brain in the course of aging.

Biblography

[1] C. López-Otín, M. A. Blasco, L. Partridge, M. Serrano, and G. Kroemer, "The hallmarks of aging," *Cell*, vol. 153, no. 6, pp. 1194–1217, Jun. 2013.

[2] "Ageing," World Health Organization. [Online]. Available: https://www.who.int/health-topics/ageing#tab=tab_1. [Accessed: 16-Jan-2022].

[3] "Maternal, Newborn, Child and Adolescent Health and Ageing," World Health Organization. [Online]. Available: https://platform.who.int/data/maternal-newborn-child-adolescent-ageing/indicator-explorer-new/mca/percentage-of-total-population-aged-60-years-or-over. [Accessed: 16-Jan-2022].

[4] G. Carbonaro, E. Leanza, P. McCann, and F. Medda, "Demographic decline, population aging, and modern financial approaches to Urban policy," *International Regional Science Review*, vol. 41, no. 2, pp. 210–232, 2016.

[5] H. Yotsuyanagi, M. Kurosaki, H. Yatsuhashi, I.-H. Lee, A. Ng, C. Brooks-Rooney, and M. H. Nguyen, "Characteristics and healthcare costs in the aging hepatitis B population of Japan: A nationwide real-world analysis," *Digestive Diseases*, vol. 40, no. 1, pp. 68–77, 2021.

[6] S. A. Youssef, M. T. Capucchio, J. E. Rofina, J. K. Chambers, K. Uchida, H. Nakayama, and E. Head, "Pathology of the aging brain in domestic and laboratory animals, and animal models of human neurodegenerative diseases," *Veterinary Pathology*, vol. 53, no. 2, pp. 327–348, 2016.

[7] W. Campos, A. Martinez, W. Sanchez, H. Estrada, N. A. Castro-Sánchez, and D. Mujica, "A systematic review of proposals for the social integration of elderly people using ambient intelligence and social networking sites," *Cognitive Computation*, vol. 8, no. 3, pp. 529–542, 2016.

[8] K. Zainabadi, “A brief history of modern aging research,” *Experimental Gerontology*, vol. 104, pp. 35–42, 2018.

[9] L. J. Niedernhofer, A. U. Gurkar, Y. Wang, J. Vijg, J. H. J. Hoeijmakers, and P. D. Robbins, “Nuclear genomic instability and aging,” *Annual Review of Biochemistry*, vol. 87, no. 1, pp. 295–322, 2018.

[10] J. Vijg and Y. Suh, “Genome instability and aging,” *Annual Review of Physiology*, vol. 75, no. 1, pp. 645–668, 2013.

[11] B. H. Howard, “Replicative senescence: Considerations relating to the stability of heterochromatin domains,” *Experimental Gerontology*, vol. 31, no. 1-2, pp. 281–293, 1996.

[12] M. A. Aon, S. Cortassa, M. Juhaszova, and S. J. Sollott, “Mitochondrial health, the epigenome and healthspan,” *Clinical Science*, vol. 130, no. 15, pp. 1285–1305, 2016.

[13] V. Bollati, J. Schwartz, R. Wright, A. Litonjua, L. Tarantini, H. Suh, D. Sparrow, P. Vokonas, and A. Baccarelli, “Decline in genomic DNA methylation through aging in a cohort of elderly subjects,” *Mechanisms of Ageing and Development*, vol. 130, no. 4, pp. 234–239, 2009.

[14] S. Maegawa, G. Hinkal, H. S. Kim, L. Shen, L. Zhang, J. Zhang, N. Zhang, S. Liang, L. A. Donehower, and J.-P. J. Issa, “Widespread and tissue specific age-related DNA methylation changes in mice,” *Genome Research*, vol. 20, no. 3, pp. 332–340, 2010.

[15] E. H. Blackburn, E. S. Epel, and J. Lin, “Human telomere biology: A contributory and interactive factor in aging, disease risks, and protection,” *Science*, vol. 350, no. 6265, pp. 1193–1198, 2015.

[16] K. Okuda, M. Y. Khan, J. Skurnick, M. Kimura, H. Aviv, and A. Aviv, "Telomere attrition of the human abdominal aorta: Relationships with age and atherosclerosis," *Atherosclerosis*, vol. 152, no. 2, pp. 391–398, 2000.

[17] M. A. Shammas, "Telomeres, lifestyle, cancer, and aging," *Current Opinion in Clinical Nutrition and Metabolic Care*, vol. 14, no. 1, pp. 28–34, 2011.

[18] J. Labbadia and R. I. Morimoto, "The biology of proteostasis in aging and disease," *Annual Review of Biochemistry*, vol. 84, no. 1, pp. 435–464, 2015.

[19] F. Demontis and N. Perrimon, "FOXO/4e-bp signaling in drosophila muscles regulates organism-wide proteostasis during aging," *Cell*, vol. 143, no. 5, pp. 813–825, 2010.

[20] F. Martinon, "Signaling by ROS drives inflammasome activation," *European Journal of Immunology*, vol. 40, no. 3, pp. 616–619, 2010.

[21] K. Wang and D. J. Klionsky, "Mitochondria removal by autophagy," *Autophagy*, vol. 7, no. 3, pp. 297–300, 2011.

[22] B. G. Childs, M. Durik, D. J. Baker, and J. M. van Deursen, "Cellular senescence in aging and age-related disease: From mechanisms to therapy," *Nature Medicine*, vol. 21, no. 12, pp. 1424–1435, 2015.

[23] D. E. Harrison, R. Strong, Z. D. Sharp, J. F. Nelson, C. M. Astle, K. Flurkey, N. L. Nadon, J. E. Wilkinson, K. Frenkel, C. S. Carter, M. Pahor, M. A. Javors, E. Fernandez, and R. A. Miller, "Rapamycin fed late in life extends lifespan in genetically heterogeneous mice," *Nature*, vol. 460, no. 7253, pp. 392–395, 2009.

[24] S.-B. Yang, A.-C. Tien, G. Boddupalli, A. W. Xu, Y. N. Jan, and L. Y. Jan, "Rapamycin ameliorates age-dependent obesity associated with increased mtor signaling in hypothalamic POMC neurons," *Neuron*, vol. 75, no. 3, pp. 425–436, 2012.

[25] E. Dazert and M. N. Hall, "mTOR signaling in disease," *Current Opinion in Cell Biology*, vol. 23, no. 6, pp. 744–755, 2011.

[26] D. Celebi-Birand, N. I. Ardic, E. T. Karoglu-Eravsar, G. F. Sengul, H. Kafaligonul, and M. M. Adams, "Dietary and pharmacological interventions that inhibit mammalian target of rapamycin activity alter the brain expression levels of neurogenic and glial markers in an age-and treatment-dependent manner," *Rejuvenation Research*, vol. 23, no. 6, pp. 485–497, 2020.

[27] A. Arslan-Ergul, B. Erbaba, E. T. Karoglu, D. O. Halim, and M. M. Adams, "Short-term dietary restriction in old zebrafish changes cell senescence mechanisms," *Neuroscience*, vol. 334, pp. 64–75, 2016.

[28] D. ROSSI, D. BRYDER, and I. WEISSMAN, "Hematopoietic stem cell aging: Mechanism and consequence," *Experimental Gerontology*, vol. 42, no. 5, pp. 385–390, 2007.

[29] E. Mejia-Ramirez and M. C. Florian, "Understanding intrinsic hematopoietic stem cell aging," *Haematologica*, vol. 105, no. 1, pp. 22–37, 2019.

[30] D. J. Rossi, D. Bryder, J. M. Zahn, H. Ahlenius, R. Sonu, A. J. Wagers, and I. L. Weissman, "Cell intrinsic alterations underlie hematopoietic stem cell aging," *Proceedings of the National Academy of Sciences*, vol. 102, no. 26, pp. 9194–9199, 2005.

[31] A. F. Kramer, L. Bherer, S. J. Colcombe, W. Dong, and W. T. Greenough, "Environmental influences on cognitive and brain plasticity during aging," *The Journals of Gerontology Series A: Biological Sciences and Medical Sciences*, vol. 59, no. 9, 2004.

[32] E. L. L. Glisky, “Chapter 1 Changes in Cognitive Function in Human Aging,” in Brain aging: Models, methods, and Mechanisms, *CRC Press*, 2019.

[33] M. K. Johnson, S. Hashtroudi, and D. S. Lindsay, “Source monitoring.,” *Psychological Bulletin*, vol. 114, no. 1, pp. 3–28, 1993.

[34] Raz N. Aging of the brain and its impact on cognitive performance: integration of structural and functional findings. In: Craik FIM, Salthouse TA, editors. *The Handbook of Aging and Cognition*. 2. Erlbaum; Mahwah, NJ: 2000. p. 1.

[35] K. M. Trewartha, A. Garcia, D. M. Wolpert, and J. R. Flanagan, “Fast but fleeting: Adaptive motor learning processes associated with aging and cognitive decline,” *Journal of Neuroscience*, vol. 34, no. 40, pp. 13411–13421, 2014.

[36] R. Hullinger and L. Puglielli, “Molecular and cellular aspects of age-related cognitive decline and alzheimer’s disease,” *Behavioural Brain Research*, vol. 322, pp. 191–205, 2017.

[37] M. M. Esiri, “Ageing and the brain,” *The Journal of Pathology*, vol. 211, no. 2, pp. 181–187, 2007.

[38] P. R. Rapp and M. Gallagher, “Preserved neuron number in the hippocampus of aged rats with spatial learning deficits.,” *Proceedings of the National Academy of Sciences*, vol. 93, no. 18, pp. 9926–9930, 1996.

[39] E. B. Petcu, V. Sfredel, D. Platt, J. G. Herndon, C. Kessler, and A. Popa-Wagner, “Cellular and molecular events underlying the dysregulated response of the aged brain to stroke: A mini-review,” *Gerontology*, vol. 54, no. 1, pp. 6–17, 2008.

[40] T. C. Foster and A. Kumar, “Calcium dysregulation in the aging brain,” *The Neuroscientist*, vol. 8, no. 4, pp. 297–301, 2002.

[41] B. H. Anderton, “Changes in the ageing brain in health and disease,” *Philosophical Transactions of the Royal Society of London. Series B: Biological Sciences*, vol. 352, no. 1363, pp. 1781–1792, 1997.

[42] G. Pasqualetti, D. J. Brooks, and P. Edison, “The role of neuroinflammation in Dementias,” *Current Neurology and Neuroscience Reports*, vol. 15, no. 4, 2015.

[43] C. K. Glass, K. Saijo, B. Winner, M. C. Marchetto, and F. H. Gage, “Mechanisms underlying inflammation in neurodegeneration,” *Cell*, vol. 140, no. 6, pp. 918–934, 2010.

[44] V. H. Perry, “The influence of systemic inflammation on inflammation in the brain: Implications for chronic neurodegenerative disease,” *Brain, Behavior, and Immunity*, vol. 18, no. 5, pp. 407–413, 2004.

[45] Y. Tang and W. Le, “Differential roles of M1 and M2 microglia in Neurodegenerative Diseases,” *Molecular Neurobiology*, vol. 53, no. 2, pp. 1181–1194, 2015.

[46] J. I. Odegaard, R. R. Ricardo-Gonzalez, M. H. Goforth, C. R. Morel, V. Subramanian, L. Mukundan, A. R. Eagle, D. Vats, F. Brombacher, A. W. Ferrante, and A. Chawla, “Macrophage-specific PPARΓ controls alternative activation and improves insulin resistance,” *Nature*, vol. 447, no. 7148, pp. 1116–1120, 2007.

[47] C. A. Colton and D. M. Wilcock, “Assessing activation states in Microglia,” *CNS & Neurological Disorders - Drug Targets*, vol. 9, no. 2, pp. 174–191, 2010.

[48] K. Saijo and C. K. Glass, "Microglial cell origin and phenotypes in health and disease," *Nature Reviwes Immunology*, vol. 11, pp. 775–786, 2011.

[49] C. A. Colton, "Heterogeneity of microglial activation in the innate immune response in the brain," *Journal of Neuroimmune Pharmacology*, vol. 4, no. 4, pp. 399–418, 2009.

[50] V. Rothhammer, D. M. Borucki, E. C. Tjon, M. C. Takenaka, C.-C. Chao, A. Ardura-Fabregat, K. A. de Lima, C. Gutiérrez-Vázquez, P. Hewson, O. Staszewski, M. Blain, L. Healy, T. Neziraj, M. Borio, M. Wheeler, L. L. Dragin, D. A. Laplaud, J. Antel, J. I. Alvarez, M. Prinz, and F. J. Quintana, "Microglial control of astrocytes in response to microbial metabolites," *Nature*, vol. 557, no. 7707, pp. 724–728, 2018.

[51] F. Giovannoni and F. J. Quintana, "The role of astrocytes in CNS inflammation," *Trends in Immunology*, vol. 41, no. 9, pp. 805–819, 2020.

[52] M. V. Sofroniew, "Reactive astrocytes in neural repair and protection," *The Neuroscientist*, vol. 11, no. 5, pp. 400–407, 2005.

[53] S. Kyrkanides, A. H. Moore, J. A. Olschowka, J. A. C. Daeschner, J. P. Williams, J. T. Hansen, and M. Kerry O'Banion, "Cyclooxygenase-2 modulates brain inflammation-related gene expression in central nervous system radiation injury," *Molecular Brain Research*, vol. 104, no. 2, pp. 159–169, 2002.

[54] G. E. Caughey, M. Pouliot, L.G. Cleland, M.J. James, "Regulation of tumor necrosis factor-alpha and IL-1 beta synthesis by thromboxane A2 in nonadherent human monocytes," *J Immunology*, vol. 158, no. 1, pp. 351–358, 1997.

[55] H. J. Murray and J. J. O'Connor, "A role for cox-2 and p38 mitogen activated protein kinase in long-term depression in the rat dentate gyrus *in vitro*," *Neuropharmacology*, vol. 44, no. 3, pp. 374–380, 2003.

[56] K. I. Andreasson, A. Savonenko, S. Vidensky, J. J. Goellner, Y. Zhang, A. Shaffer, W. E. Kaufmann, P. F. Worley, P. Isakson, and A. L. Markowska, "Age-dependent cognitive deficits and neuronal apoptosis in cyclooxygenase-2 transgenic mice," *The Journal of Neuroscience*, vol. 21, no. 20, pp. 8198–8209, 2001.

[57] S. J. Hewett, S. C. Bell, and J. A. Hewett, "Contributions of cyclooxygenase-2 to neuroplasticity and neuropathology of the Central Nervous System," *Pharmacology & Therapeutics*, vol. 112, no. 2, pp. 335–357, 2006.

[58] K. A. Kelley, L. Ho, D. Winger, J. Freire-Moar, C. B. Borelli, P. S. Aisen, and G. M. Pasinetti, "Potentiation of excitotoxicity in transgenic mice overexpressing neuronal cyclooxygenase-2," *The American Journal of Pathology*, vol. 155, no. 3, pp. 995–1004, 1999.

[59] P. Rockwell, "Redox regulates COX-2 upregulation and cell death in the neuronal response to cadmium," *Cellular Signalling*, vol. 16, no. 3, pp. 343–353, 2004.

[60] J. J. Hoozemans, A. J. Rozemuller, I. Janssen, C. J. De Groot, R. Veerhuis, and P. Eikelenboom, "Cyclooxygenase expression in microglia and neurons in alzheimer's disease and Control Brain," *Acta Neuropathologica*, vol. 101, no. 1, pp. 2–8, 2001.

[61] P. Teismann, K. Tieu, D.-K. Choi, D.-C. Wu, A. Naini, S. Hunot, M. Vila, V. Jackson-Lewis, and S. Przedborski, "Cyclooxygenase-2 is instrumental in parkinson's disease neurodegeneration," *Proceedings of the National Academy of Sciences*, vol. 100, no. 9, pp. 5473–5478, 2003.

[62] K. Yasojima, W. W. Tourtellotte, E. G. McGeer, and P. L. McGeer, "Marked increase in cyclooxygenase-2 in ALS spinal cord: Implications for therapy," *Neurology*, vol. 57, no. 6, pp. 952–956, 2001.

[63] J. S. Tilstra, C. L. Clauson, L. J. Niedernhofer, and P. D. Robbins, "NF-KB in Aging and Disease," *Aging and Disease*, vol. 2, no. 6, pp. 449–465, 2011.

[64] Y. Ogura, N. Inohara, A. Benito, F. F. Chen, S. Yamaoka, and G. Núñez, "Nod2, a NOD1/APAF-1 family member that is restricted to monocytes and activates NF-KB," *Journal of Biological Chemistry*, vol. 276, no. 7, pp. 4812–4818, 2001.

[65] V. F.-S. Shih, R. Tsui, A. Caldwell, and A. Hoffmann, "A single NFKB system for both canonical and non-canonical signaling," *Cell Research*, vol. 21, no. 1, pp. 86–102, 2010.

[66] L. A. J. O'Neill and C. Kaltschmidt, "NF-KB: A crucial transcription factor for glial and neuronal cell function," *Trends in Neurosciences*, vol. 20, no. 6, pp. 252–258, 1997.

[67] P. N. Moynagh, D. C. Williams, and L. A. O'Neill, "Interleukin-1 activates transcription factor nfκ B in glial cells," *Biochemical Journal*, vol. 294, no. 2, pp. 343–347, 1993.

[68] K. Yamagata, K. I. Andreasson, W. E. Kaufmann, C. A. Barnes, and P. F. Worley, "Expression of a mitogen-inducible cyclooxygenase in brain neurons: Regulation by synaptic activity and glucocorticoids," *Neuron*, vol. 11, no. 2, pp. 371–386, 1993.

[69] T. H. Nguyen, H. D. Le, T. Nguyen Thi Kim, H. Pham The, T. M. Nguyen, V. Cornet, J. Lambert, and P. Kestemont, "Anti–inflammatory and antioxidant properties of the ethanol extract of Clerodendrum Cyrtophyllum Turcz in copper sulfate-induced inflammation in zebrafish," *Antioxidants*, vol. 9, no. 3, p. 192, 2020.

[70] L. Eckmann, M. F. Kagnoff, and J. Fierer, “Epithelial cells secrete the chemokine interleukin-8 in response to bacterial entry,” *Infection and Immunity*, vol. 61, no. 11, pp. 4569–4574, 1993.

[71] M. Cota, A. Kleinschmidt, F. Ceccherini-Silberstein, F. Aloisi, M. Mengozzi, A. Mantovani, R. Brack-Werner, and G. Poli, “Upregulated expression of interleukin-8, rantes and chemokine receptors in human astrocytic cells infected with HIV-1,” *Journal of Neurovirology*, vol. 6, no. 1, pp. 75–83, 2000.

[72] S.-H. Du, W. Zhang, X. Yue, X.-Q. Luo, X.-H. Tan, C. Liu, D.-F. Qiao, and H. Wang, “Role of CXCR1 and interleukin-8 in methamphetamine-induced neuronal apoptosis,” *Frontiers in Cellular Neuroscience*, vol. 12, 2018.

[73] D. J. J. Waugh and C. Wilson, “The interleukin-8 pathway in cancer,” *Clinical Cancer Research*, vol. 14, no. 21, pp. 6735–6741, 2008.

[74] K. A. Roebuck, “Regulation of interleukin-8 gene expression,” *Journal of Interferon & Cytokine Research*, vol. 19, no. 5, pp. 429–438, 1999.

[75] J. G. McLarnon, “Chemokine interleukin-8 (IL-8) in alzheimer’s and other neurodegenerative diseases,” *Journal of Alzheimer’s Disease & Parkinsonism*, vol. 6, no. 5, 2016.

[76] S. S. Shaftel, W. S. Griffin, and M. K. O'Banion, “The role of interleukin-1 in neuroinflammation and alzheimer disease: An evolving perspective,” *Journal of Neuroinflammation*, vol. 5, no. 1, 2008.

[77] A. Silva-Gotay, J. Davis, E. R. Tavares, and H. N. Richardson, “Alcohol drinking during early adolescence activates microglial cells and increases frontolimbic interleukin-1 beta and toll-like receptor 4 gene expression, with heightened sensitivity in male rats compared to females,” *Neuropharmacology*, vol. 197, p. 108698, 2021.

[78] O. Sheppard, M. P. Coleman, and C. S. Durrant, "Lipopolysaccharide-induced neuroinflammation induces presynaptic disruption through a direct action on brain tissue involving microglia-derived interleukin 1 beta," *Journal of Neuroinflammation*, vol. 16, no. 1, 2019.

[79] R. Cacabelos, XA Alvarez, and F. Novoa, "Brain interleukin-1 beta in Alzheimer's disease and vascular dementia," *Methods and Findings in Experimental and Clinical Pharmacology*, vol. 16, no. 2, pp. 141-151, 1994.

[80] G. Olmos and J. Lladó, "Tumor necrosis factor alpha: A link between neuroinflammation and excitotoxicity," *Mediators of Inflammation*, vol. 2014, pp. 1–12, 2014.

[81] S. Biesmans, J. A. Bouwknecht, L. Ver Donck, X. Langlois, P. D. Acton, P. De Haes, N. Davoodi, T. F. Meert, N. Hellings, and R. Nuydens, "Peripheral administration of tumor necrosis factor-alpha induces neuroinflammation and sickness but not depressive-like behavior in mice," *BioMed Research International*, vol. 2015, pp. 1–14, 2015.

[82] D. Tweedie, R. A. Ferguson, K. Fishman, K. A. Frankola, H. Van Praag, H. W. Holloway, W. Luo, Y. Li, L. Caracciolo, I. Russo, S. Barlati, B. Ray, D. K. Lahiri, F. Bosetti, N. H. Greig, and S. Rosi, "Tumor necrosis factor-α synthesis inhibitor 3,6′-dithiothalidomide attenuates markers of inflammation, alzheimer pathology and behavioral deficits in animal models of neuroinflammation and alzheimer's disease," *Journal of Neuroinflammation*, vol. 9, no. 1, 2012.

[83] M. Stampanoni Bassi, F. Mori, F. Buttari, G. A. Marfia, A. Sancesario, D. Centonze, and E. Iezzi, "Neurophysiology of synaptic functioning in multiple sclerosis," *Clinical Neurophysiology*, vol. 128, no. 7, pp. 1148–1157, 2017.

[84] J. Sheng, "Lipopolysaccharide-induced-neuroinflammation increases intracellular accumulation of amyloid precursor protein and amyloid β peptide in appswe transgenic mice," *Neurobiology of Disease*, vol. 14, no. 1, pp. 133–145, 2003.

[85] A. R. Burmeister and I. Marriott, "The interleukin-10 family of cytokines and their role in the CNS," *Frontiers in Cellular Neuroscience*, vol. 12, 2018.

[86] S. S. Iyer and G. Cheng, "Role of interleukin 10 transcriptional regulation in inflammation and autoimmune disease," *Critical Reviews™ in Immunology*, vol. 32, no. 1, pp. 23–63, 2012.

[87] Y. Zhu, Z. Liu, Y.-P. Peng, and Y.-H. Qiu, "Interleukin-10 inhibits neuroinflammation-mediated apoptosis of ventral mesencephalic neurons via JAK-STAT3 pathway," *International Immunopharmacology*, vol. 50, pp. 353–360, 2017.

[88] Y. Zhu, X. Chen, Z. Liu, Y.-P. Peng, and Y.-H. Qiu, "Interleukin-10 protection against lipopolysaccharide-induced neuro-inflammation and neurotoxicity in ventral mesencephalic cultures," *International Journal of Molecular Sciences*, vol. 17, no. 1, p. 25, 2015.

[89] J. M. Garcia, S. A. Stillings, J. L. Leclerc, H. Phillips, N. J. Edwards, S. A. Robicsek, B. L. Hoh, S. Blackburn, and S. Doré, "Role of interleukin-10 in acute brain injuries," *Frontiers in Neurology*, vol. 8, 2017.

[90] A. Liesz, A. Bauer, J. D. Hoheisel, and R. Veltkamp, "Intracerebral interleukin-10 injection modulates post-ischemic neuroinflammation: An experimental microarray study," *Neuroscience Letters*, vol. 579, pp. 18–23, 2014.

[91] K. Bjarnadóttir, M. Benkhoucha, D. Merkler, M. S. Weber, N. L. Payne, C. C. Bernard, N. Molnarfi, and P. H. Lalive, "B cell-derived transforming growth factor-β1 expression limits the induction phase of autoimmune neuroinflammation," *Scientific Reports*, vol. 6, no. 1, 2016.

[92] E. Cekanaviciute, N. Fathali, K. P. Doyle, A. M. Williams, J. Han, and M. S. Buckwalter, "Astrocytic transforming growth factor-beta signaling reduces subacute neuroinflammation after stroke in mice," *Glia*, vol. 62, no. 8, pp. 1227–1240, 2014.

[93] M. Cacquevel, N. Lebeurrier, S. Cheenne, and D. Vivien, "Cytokines in neuroinflammation and alzheimers disease," *Current Drug Targets*, vol. 5, no. 6, pp. 529–534, 2004.

[94] D. O. Hebb, The organization of behavior- A neuropsychological theory. New York, *Ny: John Wiley & Sons*, 1949.

[95] M. Di Filippo, P. Sarchielli, B. Picconi, and P. Calabresi, "Neuroinflammation and synaptic plasticity: Theoretical basis for a novel, immune-centred, therapeutic approach to neurological disorders," *Trends in Pharmacological Sciences*, vol. 29, no. 8, pp. 402–412, 2008.

[96] J. S. Rao, M. Kellom, H.-W. Kim, S. I. Rapoport, and E. A. Reese, "Neuroinflammation and synaptic loss," *Neurochemical Research*, vol. 37, no. 5, pp. 903–910, 2012.

[97] Y. C. Chang, H.-W. Kim, S. I. Rapoport, and J. S. Rao, "Chronic NMDA administration increases neuroinflammatory markers in rat frontal cortex: Cross-talk between excitotoxicity and neuroinflammation," *Neurochemical Research*, vol. 33, no. 11, pp. 2318–2323, 2008.

[98] J. S. Rao, S. I. Rapoport, and H.-W. Kim, "Correction: Altered neuroinflammatory, arachidonic acid cascade and synaptic markers in postmortem alzheimer's disease brain," *Translational Psychiatry*, vol. 7, no. 5, 2017.

[99] O. Sheppard, M. P. Coleman, and C. S. Durrant, "Lipopolysaccharide-induced neuroinflammation induces presynaptic disruption through a direct action on brain tissue involving microglia-derived interleukin 1 beta," *Journal of Neuroinflammation*, vol. 16, no. 1, 2019.

[100] M. Migaud, P. Charlesworth, M. Dempster, L. C. Webster, A. M. Watabe, M. Makhinson, Y. He, M. F. Ramsay, R. G. Morris, J. H. Morrison, T. J. O'Dell, and S. G. Grant, "Enhanced long-term potentiation and impaired learning in mice with mutant postsynaptic density-95 protein," *Nature*, vol. 396, no. 6710, pp. 433–439, 1998.

[101] L. Yang, X. Xin, J. Zhang, L. Zhang, Y. Dong, Y. Zhang, J. Mao, and Z. Xie, "Inflammatory pain may induce cognitive impairment through an interlukin-6-dependent and postsynaptic density-95-associated mechanism," *Anesthesia & Analgesia*, vol. 119, no. 2, pp. 471–480, 2014.

[102] R.-Y. Tsai, K.-Y. Chou, C.-H. Shen, C.-C. Chien, W.-Y. Tsai, Y.-N. , P.-L. Tao, Y.-S. Lin, and C.-S. Wong, "Resveratrol regulates N-methyl-D-aspartate receptor expression and suppresses neuroinflammation in morphine-tolerant rats," *Anesthesia & Analgesia*, vol. 115, no. 4, pp. 944–952, 2012.

[103] D. Chugh, P. Nilsson, S.-A. Afjei, A. Bakochi, and C. T. Ekdahl, "Brain inflammation induces post-synaptic changes during early synapse formation in adult-born hippocampal neurons," *Experimental Neurology*, vol. 250, pp. 176–188, 2013.

[104] Y. Wang, Y. Li, R. Zhao, B. Wu, B. Lanoha, Z. Tong, J. Peer, J. Liu, H. Xiong, Y. Huang, and J. Zheng, "Glutaminase C overexpression in the brain induces learning deficits, synaptic dysfunctions, and neuroinflammation in mice," *Brain, Behavior, and Immunity*, vol. 66, pp. 135–145, 2017.

[105] Z. Li, F. Liu, H. Ma, P. F. White, R. Yumul, Y. Jiang, N. Wang, and X. Cao, "Age exacerbates surgery-induced cognitive impairment and neuroinflammation in Sprague-Dawley rats: The role of IL-4," *Brain Research*, vol. 1665, pp. 65–73, 2017.

[106] S. F. Spampinato, S. Merlo, E. Fagone, M. Fruciano, Y. Sano, T. Kanda, and M. A. Sortino, "Reciprocal interplay between astrocytes and CD4+ cells affects blood-brain barrier and neuronal function in response to β amyloid," *Frontiers in Molecular Neuroscience*, vol. 13, 2020.

[107] S. K. Tyagarajan and J.-M. Fritschy, "Gabaareceptors, Gephyrin and homeostatic synaptic plasticity," *The Journal of Physiology*, vol. 588, no. 1, pp. 101–106, 2010.

[108] F. Fernandez, W. Morishita, E. Zuniga, J. Nguyen, M. Blank, R. C. Malenka, and C. C. Garner, "Pharmacotherapy for cognitive impairment in a mouse model of down syndrome," *Nature Neuroscience*, vol. 10, no. 4, pp. 411–413, 2007.

[109] A. J. Al Omran, A. S. Shao, S. Watanabe, Z. Zhang, J. Zhang, C. Xue, J. Watanabe, D. L. Davies, X. M. Shao, and J. Liang, "Social isolation induces neuroinflammation and microglia overactivation, while dihydromyricetin prevents and improves them," *Journal of Neuroinflammation*, vol. 19, no. 1, 2022.

[110] X. Zhang, M. V. Green, and S. A. Thayer, "HIV gp120-induced neuroinflammation potentiates NMDA receptors to overcome basal suppression of inhibitory synapses by p38 MAPK," *Journal of Neurochemistry*, vol. 148, no. 4, pp. 499–515, 2019.

[111] C.-H. Kim, E. Ueshima, O. Muraoka, H. Tanaka, S.-Y. Yeo, T.-L. Huh, and N. Miki, "Zebrafish Elav/HUC homologue as a very early neuronal marker," *Neuroscience Letters*, vol. 216, no. 2, pp. 109–112, 1996.

[112] H.-C. Park, S.-K. Hong, H.-S. Kim, S.-H. Kim, E.-J. Yoon, C.-H. Kim, N. Miki, and T.-L. Huh, "Structural comparison of zebrafish ELAV/hu and their differential expressions during neurogenesis," *Neuroscience Letters*, vol. 279, no. 2, pp. 81–84, 2000.

[113] C.-H. Kim, Y.-K. Bae, Y. Yamanaka, S. Yamashita, T. Shimizu, R. Fujii, H.-C. Park, S.-Y. Yeo, T.-L. Huh, M. Hibi, and T. Hirano, "Overexpression of neurogenin induces ectopic expression of HUC in zebrafish," *Neuroscience Letters*, vol. 239, no. 2-3, pp. 113–116, 1997.

[114] K. B. Casper and K. D. McCarthy, "GFAP-positive progenitor cells produce neurons and oligodendrocytes throughout the CNS," *Molecular and Cellular Neuroscience*, vol. 31, no. 4, pp. 676–684, 2006.

[115] A. D. Garcia, N. B. Doan, T. Imura, T. G. Bush, and M. V. Sofroniew, "GFAP-expressing progenitors are the principal source of constitutive neurogenesis in adult mouse forebrain," *Nature Neuroscience*, vol. 7, no. 11, pp. 1233–1241, 2004.

[116] F. Azzolini, L. Gilio, L. Pavone, E. Iezzi, E. Dolcetti, A. Bruno, F. Buttari, A. Musella, G. Mandolesi, L. Guadalupi, R. Furlan, A. Finardi, T. Micillo, F. Carbone, G. Matarese, D. Centonze, and M. Stampanoni Bassi, "Neuroinflammation is associated with GFAP and STREM2 levels in multiple sclerosis," *Biomolecules*, vol. 12, no. 2, p. 222, 2022.

[117] V. S. Catts, J. Wong, S. G. Fillman, S. J. Fung, and C. Shannon Weickert, "Increased expression of astrocyte markers in schizophrenia: Association with Neuroinflammation," *Australian & New Zealand Journal of Psychiatry*, vol. 48, no. 8, pp. 722–734, 2014.

[118] R. Niranjan, R. Nagarajan, K. Hanif, C. Nath, and R. Shukla, "LPS induces mediators of neuroinflammation, cell proliferation, and GFAP expression in human astrocytoma cells U373MG: The anti-inflammatory and anti-proliferative effect of Guggulipid," *Neurological Sciences*, vol. 35, no. 3, pp. 409–414, 2013.

[119] E. M. Hol, R. F. Roelofs, E. Moraal, M. A. Sonnemans, J. A. Sluijs, E. A. Proper, P. N. de Graan, D. F. Fischer, and F. W. van Leeuwen, "Neuronal expression of GFAP in patients with

alzheimer pathology and identification of novel GFAP splice forms," *Molecular Psychiatry*, vol. 8, no. 9, pp. 786–796, 2003.

[120] FDA, "RAPAMUNE (sirolimus) ORAL SOLUTION AND TABLETS, " pp. 1-46, 1999.

[121] N.-S. Mengke, B. Hu, Q.-P. Han, Y.-Y. Deng, M. Fang, D. Xie, A. Li, and H.-K. Zeng, "Rapamycin inhibits lipopolysaccharide-induced neuroinflammation *in vitro* and *in vivo*," *Molecular Medicine Reports*, vol. 14, no. 6, pp. 4957–4966, 2016.

[122] J. Huang and B. D. Manning, "The TSC1–TSC2 complex: A molecular switchboard controlling cell growth," *Biochemical Journal*, vol. 412, no. 2, pp. 179–190, 2008.

[123] J. Arowoogun, O. O. Akanni, A. O. Adefisan, S. E. Owumi, A. S. Tijani, and O. A. Adaramoye, "Rutin ameliorates copper sulfate-induced brain damage via Antioxidative and anti-inflammatory activities in rats," *Journal of Biochemical and Molecular Toxicology*, vol. 35, no. 1, 2020.

[124] A. Becaria, D. K. Lahiri, S. C. Bondy, D. M. Chen, A. Hamadeh, H. Li, R. Taylor, and A. Campbell, "Aluminum and copper in drinking water enhance inflammatory or oxidative events specifically in the brain," *Journal of Neuroimmunology*, vol. 176, no. 1-2, pp. 16–23, 2006.

[125] A. Campbell, "The role of aluminum and copper on neuroinflammation and alzheimer's disease," *Journal of Alzheimer's Disease*, vol. 10, no. 2-3, pp. 165–172, 2006.

[126] A. M. Stewart, O. Braubach, J. Spitsbergen, R. Gerlai, and A. V. Kalueff, "Zebrafish models for translational neuroscience research: From Tank to bedside," *Trends in Neurosciences*, vol. 37, no. 5, pp. 264–278, 2014.

[127] N. F. Belyaeva, V. N. Kashirtseva, N. V. Medvedeva, Y. Y. Khudoklinova, O. M. Ipatova, and A. I. Archakov, "Zebrafish as a model system for biomedical studies," *Biochemistry (Moscow) Supplement Series B: Biomedical Chemistry*, vol. 3, no. 4, pp. 343–350, 2009.

[128] J. Jeevanandam, Y. S. Chan, and M. K. Danquah, "Zebrafish as a model organism to study nanomaterial toxicity," *Emerging Science Journal*, vol. 3, no. 3, pp. 195–208, 2019.

[129] A. V. Kalueff, A. M. Stewart, and R. Gerlai, "Zebrafish as an emerging model for studying complex brain disorders," *Trends in Pharmacological Sciences*, vol. 35, no. 2, pp. 63–75, 2014.

[130] T. Mueller, Z. Dong, M. A. Berberoglu, and S. Guo, "The dorsal pallium in zebrafish, danio rerio (Cyprinidae, Teleostei)," *Brain Research*, vol. 1381, pp. 95–105, 2011.

[131] B. Adolf, P. Chapouton, C. S. Lam, S. Topp, B. Tannhäuser, U. Strähle, M. Götz, and L. Bally-Cuif, "Conserved and acquired features of adult neurogenesis in the zebrafish telencephalon," *Developmental Biology*, vol. 295, no. 1, pp. 278–293, 2006.

[132] C. Kizil, J. Kaslin, V. Kroehne, and M. Brand, "Adult neurogenesis and brain regeneration in zebrafish," *Developmental Neurobiology*, vol. 72, no. 3, pp. 429–461, 2012.

[133] M. De la Fuente, "Role of the immune system in aging," *Inmunología*, vol. 27, no. 4, pp. 176–191, 2008.

[134] Y.-X. Sun, X. Ji, X. O. Mao, L. Xie, J. Jia, V. Galvan, D. A. Greenberg, and K. Jin, "Differential activation of mTOR complex 1 signaling in human brain with mild to severe alzheimer's disease," *Journal of Alzheimer's Disease*, vol. 38, no. 2, pp. 437–444, 2013.

[135] I. N. Srivastava, J. Shperdheja, M. Baybis, T. Ferguson, and P. B. Crino, "mTOR pathway inhibition prevents neuroinflammation and neuronal death in a mouse model of Cerebral Palsy," *Neurobiology of Disease*, vol. 85, pp. 144–154, 2016.

[136] C. Scheldeman, J. D. Mills, A. Siekierska, I. Serra, D. Copmans, A. M. Iyer, B. J. Whalley, J. Maes, A. C. Jansen, L. Lagae, E. Aronica, and P. A. M. de Witte, "mTOR-related neuropathology in mutant TSC2 zebrafish: Phenotypic, transcriptomic and pharmacological analysis," *Neurobiology of Disease*, vol. 108, pp. 225–237, 2017.

[137] J.-wei Li, R.-liang Wang, J. Xu, K.-yang Sun, H.-ming Jiang, Z.-ying Sun, Z.-yang Lv, X.-quan Xu, R. Wu, H. Guo, Q. Jiang, and D.-quan Shi, "Methylene blue prevents osteoarthritis progression and relieves pain in rats via upregulation of Nrf2/PRDX1," *Acta Pharmacologica Sinica*, vol. 43, no. 2, pp. 417–428, 2021.

[138] G. M. de Oliveira, L. W. Kist, T. C. Pereira, J. W. Bortolotto, F. L. Paquete, E. M. de Oliveira, C. E. Leite, C. D. Bonan, N. R. de Souza Basso, R. M. Papaleo, and M. R. Bogo, "Transient modulation of acetylcholinesterase activity caused by exposure to dextran-coated iron oxide nanoparticles in brain of adult zebrafish," *Comparative Biochemistry and Physiology Part C*, vol. 162, pp. 77–84, 2014.

[139] N. Rojas-Hernandez, D. Véliz, and C. Vega-Retter, "Selection of suitable reference genes for gene expression analysis in gills and liver of fish under field pollution conditions," *Scientific Reports*, vol. 9, no. 1, 2019.

[140] S.-H. Kim, C. K. Speirs, L. Solnica-Krezel, and K. C. Ess, "Zebrafish model of tuberous sclerosis complex reveals cell-autonomous and non-cell-autonomous functions of mutant tuberin," *Disease Models & Mechanisms*, vol. 4, no. 2, pp. 255–267, 2011.

[141] Y. Ding, X. Sun, W. Huang, T. Hoage, M. Redfield, S. Kushwaha, S. Sivasubbu, X. Lin, S. Ekker, and X. Xu, "Haploinsufficiency of target of rapamycin attenuates cardiomyopathies in adult zebrafish," *Circulation Research*, vol. 109, no. 6, pp. 658–669, 2011.

[142] Z. An, J. Li, J. Yu, X. Wang, H. Gao, W. Zhang, Z. Wei, J. Zhang, Y. Zhang, J. Zhao, and X. Liang, "Neutrophil extracellular traps induced by IL-8 aggravate atherosclerosis via activation NF-KB signaling in macrophages," *Cell Cycle*, vol. 18, no. 21, pp. 2928–2938, 2019.

[143] Y. KIDA, M. KOBAYASHI, T. SUZUKI, A. TAKESHITA, Y. OKAMATSU, S. HANAZAWA, T. YASUI, and K. HASEGAWA, "Interleukin-1 stimulates cytokines, prostaglandin E and matrix metalloproteinase-1 production via activation of MAPK/AP-1 and NF-κB in human gingival fibroblasts," *Cytokine*, vol. 29, no. 4, pp. 159–168, 2005.

[144] H.-K. Song, E.-M. Noh, J.-M. Kim, Y.-O. You, K.-B. Kwon, and Y.-R. Lee, "Reversine inhibits MMP-3, IL-6 and IL-8 expression through suppression of ROS and JNK/AP-1 activation in interleukin-1β-stimulated human gingival fibroblasts," *Archives of Oral Biology*, vol. 108, p. 104530, 2019.

[145] A. Szczepanik, "Il-4, IL-10 and IL-13 modulate aβ(1–42)-induced cytokine and chemokine production in primary murine microglia and a human monocyte cell line," *Journal of Neuroimmunology*, vol. 113, no. 1, pp. 49–62, 2001.

[146] A. M. Szczepanik and G. E. Ringheim, "Il-10 and glucocorticoids inhibit AB(1–42)- and lipopolysaccharide-induced pro-inflammatory cytokine and chemokine induction in the central nervous system," *Journal of Alzheimer's Disease*, vol. 5, no. 2, pp. 105–117, 2003.

[147] G. A. Soliman, H. A. Acosta-Jaquez, E. A. Dunlop, B. Ekim, N. E. Maj, A. R. Tee, and D. C. Fingar, "MTOR ser-2481 autophosphorylation monitors mtorc-specific catalytic activity and

clarifies rapamycin mechanism of action," *Journal of Biological Chemistry*, vol. 285, no. 11, pp. 7866–7879, 2010.

[148] K. Chellappa, J. A. Brinkman, S. Mukherjee, M. Morrison, M. I. Alotaibi, K. A. Carbajal, A. L. Alhadeff, I. J. Perron, R. Yao, C. S. Purdy, D. M. DeFelice, M. H. Wakai, J. Tomasiewicz, A. Lin, E. Meyer, Y. Peng, S. I. Arriola Apelo, L. Puglielli, J. N. Betley, G. K. Paschos, J. A. Baur, and D. W. Lamming, "Hypothalamic mTORC2 is essential for metabolic health and longevity," *Aging Cell*, vol. 18, no. 5, 2019.

[149] Y. Liu, T. Namba, J. Liu, R. Suzuki, S. Shioda, and T. Seki, "Glial fibrillary acidic protein-expressing neural progenitors give rise to immature neurons via early intermediate progenitors expressing both glial fibrillary acidic protein and neuronal markers in the adult hippocampus," *Neuroscience*, vol. 166, no. 1, pp. 241–251, 2010.

[150] J. L. Bizon, H. J. Lee, and M. Gallagher, "Neurogenesis in a rat model of age-related cognitive decline," *Aging Cell*, vol. 3, no. 4, pp. 227–234, 2004.

[151] B. Wang and K. Jin, "Current perspectives on the link between neuroinflammation and neurogenesis," *Metabolic Brain Disease*, vol. 30, no. 2, pp. 355–365, 2014.

[152] B. J. Till, S. H. Reynolds, E. A. Greene, C. A. Codomo, L. C. Enns, J. E. Johnson, C. Burtner, A. R. Odden, K. Young, N. E. Taylor, J. G. Henikoff, L. Comai, and S. Henikoff, "Large-scale discovery of induced point mutations with high-throughput tilling," *Genome Research*, vol. 13, no. 3, pp. 524–530, 2003.

[153] S.-L. Lai, M. R. Mustafa, and P.-F. Wong, "Panduratin a induces protective autophagy in melanoma via the AMPK and mTOR pathway," *Phytomedicine*, vol. 42, pp. 144–151, 2018.

[154] Y.-M. Wei, X. Li, M. Xu, J. M. Abais, Y. Chen, C. R. Riebling, K. M. Boini, P.-L. Li, and Y. Zhang, "Enhancement of autophagy by simvastatin through inhibition of Rac1-mTOR signaling pathway in coronary arterial myocytes," *Cellular Physiology and Biochemistry*, vol. 31, no. 6, pp. 925–937, 2013.

[155] S.-C. Sun, "Non-canonical NF-KB Signaling pathway," *Cell Research*, vol. 21, no. 1, pp. 71–85, 2010.